

博士論文番号 : 0981205
(Doctoral student number)

A single – molecule approach to the speed of DNA replication
forks in *Escherichia coli* cells

Pham Minh Tuan

Nara Institute of Science and Technology
Graduate School of Biological Sciences
Microbial Molecular Genetics

(Prof. Hisaji Maki)

(Submitted on 2013/08/08)

Lab name (Supervisor)	Microbial Molecular Genetics (Prof. Hisaji Maki)		
Name (surname) (given name)	Pham Minh Tuan	Date	2013/08/08
Title	A single-molecule approach to the speed of DNA replication forks in <i>Escherichia coli</i> cells		

Abstract

DNA replication is an important process for cells to accurately copy genomic DNA. Replication of double-stranded DNA is carried out by the replisome, the multi-protein complex formed at a Y-shaped DNA replication fork. *Escherichia coli* have served as the leading model system for clarifying the molecular mechanisms underlying DNA replication. The key components of the *E. coli* replisome are DnaB helicase for DNA unwinding, DnaG primase for initiation of the Okazaki fragments on the lagging strand, and the replicative DNA polymerase III (Pol III) holoenzyme for polymerizing nucleotides into the nascent DNA strand. The replication fork can be reconstituted from purified proteins including the three key components, which is unique in *E. coli*. It has recently been investigated for dynamics of the reconstituted replication fork using single-molecule measurements *in vitro*. In the reconstituted DNA replication system, DNA synthesis is catalyzed on a very homogeneous DNA template without various DNA transactions other than the basic reactions essential for DNA replication. In contrast, the replisome fork on genomic DNA in cells undergoes various stresses including collisions with the transcription machinery and DNA binding proteins, higher-order DNA structures, torsional stress emerged on DNA by the fork movement, and obstructive DNA damage. However, the molecular behavior of the individual replication forks in growing *E. coli* cells remains unknown.

It is challenging to obtain an accurate value of fork speed to assess the fine dynamics of individual replication forks on the *E. coli* genome. Molecular DNA combing is a single-molecule approach used to examine chromosomal DNA that has been pulse-labeled with halogen analogs of thymidine such as 5-Bromo-2'-deoxyuridine during DNA replication. Replication dynamics only in eukaryotic cells have been successfully investigated with DNA combing. Since the analog-labeled DNA is stretched on a glass surface and visualized under a microscope, the field of view restricts the measurable DNA length below 300 kb. Due to this limitation, pulse-labeling for *E. coli* cells with the analogs needs to be done in less than 6 min based on the average rate of DNA synthesis of 900 nt/s that is about 10-fold faster than that in eukaryotes. Despite of a long time history of *E. coli* genetics, there is no strain that meets the criteria. To overcome this

difficulty, we constructed a novel *E. coli* strain, eCOMB (*E. coli* for combing), which incorporates BrdU with a dramatically enhanced efficiency. Analysis of replication fork progression in the eCOMB cells using the DNA combing method revealed that most of the individual replication forks of *E. coli* move rather homogeneously with the estimated average speed of 653 nt/s while there were small subpopulations of forks with lower and faster speed. The single-molecule technique *in vivo* was further used to study how replication fork progression is controlled in *E. coli* cells as follows.

Pol III and DnaB are progressive molecular motors that respectively translocate on single-stranded DNA. Since the DNA unwinding rate of DnaB helicase (35 nt/s) is much slower than the DNA chain elongation rate of Pol III (900 nt/s) and the strand displacement by Pol III is weak, it has been postulated that elongation of the leading strand could act as the pacemaker of replication fork progression such that Pol III pushes DnaB in the replisome. However, no direct evidence for this hypothesis has been provided. The *dnaE* gene encodes the catalytic α -subunit of Pol III holoenzyme. The rate of DNA chain elongation by the *dnaE173* Pol III holoenzyme is greatly reduced to 300 nt/s, one-third of that observed with the wild-type Pol III holoenzyme *in vitro*. The single-molecule technique *in vivo* revealed that the fork speed of *dnaE173*-eCOMB cells was slowed down to the extent at which the chain-elongation rate of *dnaE173*-Pol III is decreased, demonstrating clearly that the velocity of DNA chain elongation by Pol III contributes to the majority of the fork speed in *E. coli* cells.

Genomic DNA is always damaged by various environmental factors, such as endogenous reactive oxygen species and exogenous UV light. Inhibition of DNA replication by DNA damage triggers a complex cellular tolerance mechanism termed the SOS response in bacteria and checkpoint in eukaryotes. In the checkpoint, a rate of bulk DNA synthesis is reduced on a damaged template by slowing down unperturbed replication fork progression by unknown mechanisms. Although the SOS response in *E. coli* was discovered about 40 years ago, it has not been known if replication fork speed reduced in bacterial SOS as well as in eukaryotic checkpoint. When the SOS response was induced in eCOMB cells by genetically eliminating the negative regulator of the response, the fork speed was reduced to about a half of that in the SOS-uninduced cells. Moreover, the fork speed reduction in SOS was mediated independently by *recA* encoding DNA recombinase and *dinB* encoding a specialized DNA polymerase.

In this study, I developed for the first time a single-molecule technique to measure replication fork speed *in vivo* with a novel *E. coli* strain, eCOMB, and obtained the following findings that have never been yielded by previous measurements of DNA replication in the cells. The speed of individual forks was relatively uniform although minor populations of forks move with higher and lower rates. In addition, I showed that that Pol III but not the replicative DnaB helicase is the molecular engine that provides a major driving force for fork movement in the cells, and discovered that RecA recombinase and DinB DNA polymerase are the molecular brakes that slow down fork progression in the SOS damage response. These findings in the leading model of DNA replication will provide a general insight into molecular mechanisms that control replication fork progression.

List of contents

	Page
1. Introduction	1
1.1. Mechanisms for DNA synthesis at a DNA replication fork in <i>E. coli</i>	1
1.2. Bulk rate of DNA synthesis in <i>E. coli</i> cells	4
1.3. A single molecular analysis of replication fork speed <i>in vitro</i>	5
1.4. A possible difference between replication fork progression <i>in vitro</i> and <i>in vivo</i>	6
1.5. A DNA combing method that enables visualization of individual DNA molecules	8
1.6. A determinant of replication fork speed in <i>E. coli</i> cells	9
1.7. Fork speed in the DNA damage response of <i>E. coli</i> cells	10
1.8. Objectives of this research	11
2. Materials and Methods	15
2.1. Reagents and chemicals	15
2.2. List of bacterial strains	15
2.3. List of plasmids	17
2.4. List of oligonucleotides	17
2.5. Construction of bacterial strains	18
2.5.1. P1(<i>vir</i>) – mediated transduction	18
2.5.2. One-step gene disruption by Red recombinase	19
2.5.3. Construction of eCOMB	19
2.5.4. Construction of derivative strains of eCOMB	20
2.6. Bacterial growth conditions	21
2.7. Establishment of DNA combing with λ phage DNA	22
2.8. DNA combing with chromosomal DNA of eCOMB cells	23
2.8.1. Labeling of eCOMB cells with thymidine analogs	23
2.8.2. Preparation and treatment of agarose plugs	24
2.8.3. Detection of the labeled DNA on glass surface	24
2.8.4. Observation of individual DNA molecules with a fluorescent microscope	25
2.9. Analyses of physiological characteristics of eCOMB cells	26
2.9.1. Analyses of cell growth rate	26
2.9.2. Observation of cell shape and nucleoid structures	26
2.10. Detection of the SOS response by Western blotting	26

2.11.	Determination of efficiency for BrdU incorporation into cells	27
2.12.	Determination of DNA synthesis rate with radioactive thymidine	28
2.13.	Determination of <i>oriC/ter</i> ratio by quantitative real-time PCR	28
3.	Results	30
3.1.	Construction of the novel thymidine-requiring eCOMB strain for DNA combing	30
3.2.	High efficiency of thymidine-analogs incorporation into eCOMB cells	32
3.3.	A rate of DNA synthesis in the presence of BrdU	34
3.4.	Physiological characteristics of eCOMB cells	34
3.5.	Calibration of DNA length with λ DNA as a standard for DNA combing	36
3.6.	DNA combing with the chromosomal DNA extracted from eCOMB cells	38
3.7.	Determination of replication fork speed in asynchronous eCOMB cells	40
3.8.	Accurate determination of the replication fork speed in <i>E. coli</i>	44
3.9.	Replication fork speed in synchronized eCOMB cells	48
3.10.	A reduced rate of replication fork progression in <i>dnaE173</i> cells	50
3.11.	An increased number of the replication fork sin the <i>dnaE173</i> cells	53
3.12.	Induction of the SOS response in the absence of DNA damage	56
3.13.	Reduced speed of replication fork progression in the SOS response	59
3.14.	Din B functions in slowdown of the fork speed in the SOS response	63
3.15.	RecA recombinase functions in slowdown of the fork speed in the SOS response	64
3.16.	RuvA and UvrD are not responsible for the slow fork speed in the SOS response	64
3.17.	DinB and RecA independently slow down fork progression in the SOS response	67
3.18.	RecA controls fork progression in recFOR-independent manner	69
4.	Discussions	71
4.1.	High efficiency of thymidine-analogs incorporation and the application of molecular combing in eCOMB cells	71
4.2.	The unimodal accurate speed and sub-population in speed distribution	

of individual replication forks in <i>E. coli</i> cells	73
4.3. DNA Pol III provides a major driving force for the replisome progression	74
4.4. Speed of replication fork may modulate initiation timing of DNA replication	75
4.5. The reduction of replication fork speed under SOS response without DNA damage	77
4.6. Translesion DNA polymerase (DinB) and recombinase (RecA) individually control fork progression under SOS response	78
4.7. Conclusions	83
5. Acknowledgements	84
6. References	85

1. Introduction

1.1. Mechanisms for DNA synthesis at a DNA replication fork in *E. coli*

DNA replication is a biological process in which cells accurately copy their entire genomic DNA. During DNA replication, the replisome catalyzes DNA synthesis at a replication fork that is a Y-shaped DNA region where the two parental strands are separated. Because of the antiparallel structure of genomic DNA and the unidirectional chain elongation by DNA polymerase, DNA synthesis of the nascent DNA strands at the replication fork are continuous on the leading strand and discontinuous on the lagging strand. The short DNA segments produced in the discontinuous synthesis are called Okazaki fragments (Watson *et al.*, 2008). In *E. coli* cells, the circular genomic DNA is replicated in a bidirectional manner from *oriC* (the replication origin) toward *ter* (the chromosomal terminus region) by the replisome. The key components of the *E. coli* replisome are DnaB, DnaG, and a dimeric (or trimeric) complex of DNA polymerase III (Pol III) holoenzyme (Maki, 2004). The molecular functions of these components are DNA unwinding of double-stranded DNA, synthesis of RNA primer on the lagging strand, and polymerization of nucleotides into the nascent DNA strand, respectively (O'Donnell, 2006; McHenry, 2011). The concurrent DNA synthesis of the leading and lagging strands by the dimeric Pol III complex can be explained by a "Trombone" model as shown in Fig. 1. In addition to the basic components of the replisome, single-strand DNA binding proteins (SSB) are required to stabilize the single-stranded DNA (ssDNA) formed on the lagging strand DNA at the replication fork. Furthermore, the supercoils that accumulated ahead during the unwinding process and elongation is released by topoisomerases to avoid the inhibition of replication fork progression.

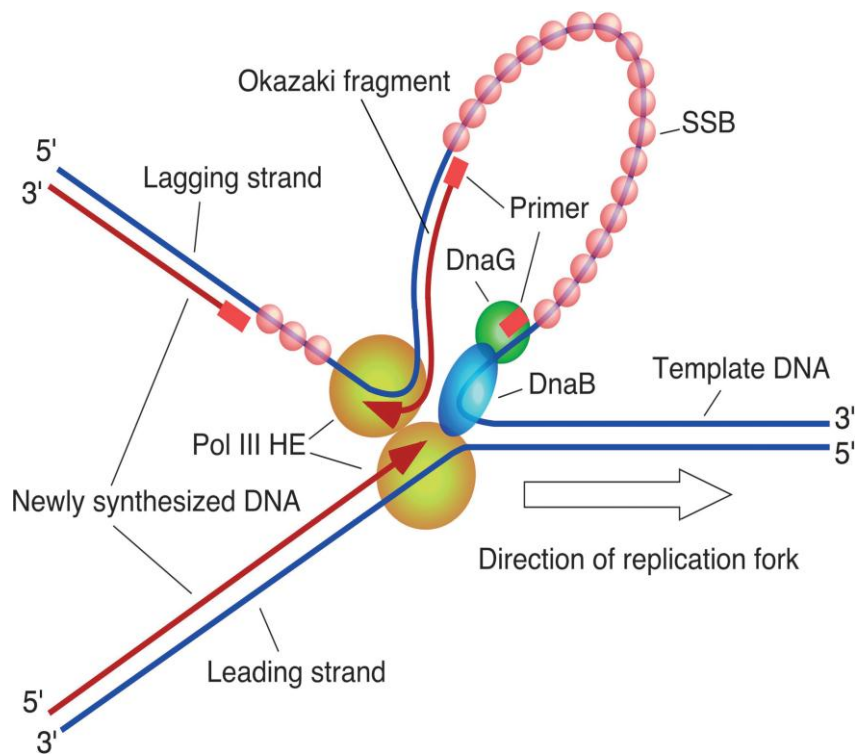


Figure 1. DNA synthesis at DNA replication fork in *E. coli* with basic components of replicative apparatus (Maki, 2004). At the replication fork, the DnaB helicase interacts with the Pol III holoenzyme and travels along the template in a 5' – 3' direction to unwind DNA. The Pol III holoenzyme polymerizes nucleotides in a continuous manner on the leading strand and a discontinuous manner by forming Okazaki fragments on the lagging strand. On ssDNA of the lagging strand coated by the SSB, the DnaG primase synthesizes new RNA primers for the synthesis of each Okazaki fragment. After completing the synthesis of each Okazaki fragment, the primase is released, and DNA ligase seals a gap between the Okazaki fragments.

DNA polymerase III holoenzyme of *E. coli* is the replicative enzyme and is composed of 10 subunits including the β subunit, the sliding clamp (Table 1, Fig. 2). The Pol III holoenzyme synthesizes DNA at a fast speed of 1000 nucleotides/second (nt/s) (Chandler *et al.*, 1975) and with very high fidelity (1 mistake in 10^{10} base pairs (bp)) (Watson *et al.*, 2008; Drake *et al.*, 1969). The α , ϵ , and θ subunits forms the Pol III core complex that has a very low processivity of about 10 nucleotides (nt) due to a low affinity of the core subassembly for template- primer DNA (Maki, 2004; Fay *et al.*,

1981). The processivity increases remarkably when the α subunit of Pol III core binds to the β sliding clamp and form a complex with template-primer DNA. The Pol III holoenzyme that contains the β subunit but not Pol III* that lacks the β subunit travels on DNA at high processivity; it can extend several thousand nucleotides of a DNA chain or even entire *E. coli* genomic DNA (4.6 Mb) without dissociating from the template DNA (McHenry, 1988; Kelman & O'Donnell, 1995). Thus, the β clamp is the primary determinant for the very high processivity of chain elongation in *E. coli* DNA replication (LaDuca *et al.*, 1986; Kong *et al.*, 1992).

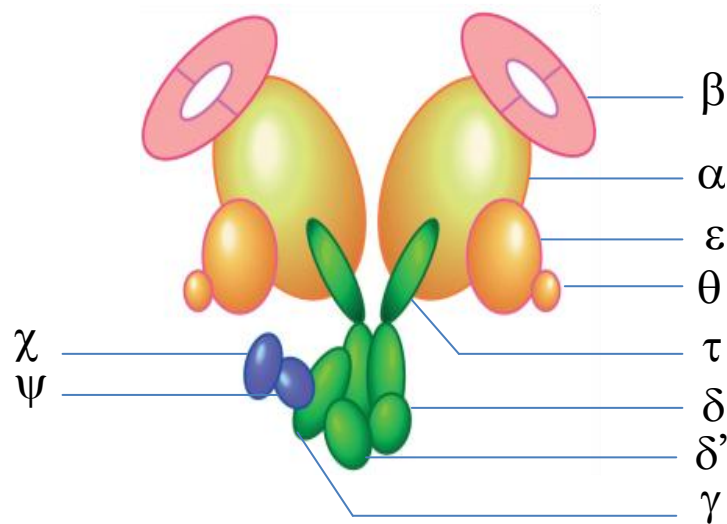


Figure 2. DNA polymerase III holoenzyme with 10 subunits (Maki, 2004). This complex is quite stable in the replisome. Pol III core is the complex of the α , ϵ , and θ subunits which functions in catalyzing the DNA chain elongation, proofreading by 3'-5' exonuclease and stimulation of the proofreading exonuclease, respectively. Two Pol III cores are connected by the τ subunit. The γ -complex consists of the γ , δ , δ' , χ , and ψ subunits functions in the β clamp loading that support the high processivity and the high speed of DNA chain elongation in *E. coli* cells.

Table 1: The subunits and the subassemblies of DNA polymerase III holoenzyme

(Zvi Kelman and Mike O'Donnell, 1995; Sugaya *et al.*, 2002)

Subunit	Gene	Mass (kDa)	Function	Subassembly
α	<i>dnaE</i>	129.9	Catalyze elongation of the DNA chain	Core

ϵ	<i>dnaQ</i> (<i>mutD</i>)	27.5	Proofreading 3'-5' exonuclease	Core
θ	<i>holE</i>	8.6	Stimulates ϵ exonuclease	Core
τ	<i>dnaX</i>	71.1	Demerizes core, DNA-dependent ATP	
γ	<i>dnaX</i>	47.5	Binds ATP	γ - complex
δ	<i>holA</i>	38.7	Bind to β	γ - complex
δ'	<i>holB</i>	36.9	Cofactor for γ ATPase and stimulates clamp loading	γ - complex
χ	<i>holC</i>	16.6	Binds SSB	γ - complex
ψ	<i>holD</i>	15.2	Bridge between χ and γ	γ - complex
β	<i>dnaN</i>	40.6	Sliding clamp on DNA	

Because of the significant concept in the central dogma of molecular biology, DNA replication has attracted many attentions in biological sciences. In the study of DNA replication, *E. coli* has been a leading model to uncover the molecular mechanisms of DNA replication due to the simple biological system with basic molecular mechanisms that are highly conserved from bacteria to human. In the case of the replication apparatus, the functions of Pol III, the β clamp and the clamp loader (γ -complex) in bacteria are functionally homologous to DNA polymerase δ (and/or ϵ), the proliferating cell nuclear antigen (PCNA) and the replication factor C in eukaryotes, respectively (McHenry, 2011). Thus, the new findings in *E. coli* replication have always provided a general insight into the mechanisms of DNA replication. In this sense, the progression of replication fork or the rate of DNA synthesis in *E. coli* cells has also been studied both *in vivo* and *in vitro* for several decades.

1.2. Bulk rate of DNA synthesis in *E. coli* cells

The replication fork of *E. coli* cells was firstly analyzed in 1963 by ^3H -thymidine labeling experiments in which newly synthesized DNA was directly

visualized by fiber-autoradiography (Cairns, 1963). Later, the bulk rate of DNA synthesis and the average speed of replication fork were estimated by various other methods. Using genomic microarray, Cozzarelli's group determined the fork speed to be 600-750 nt/s at 30°C (Khodursky *et al.*, 2000; Breier *et al.*, 2005). Waldminghaus *et al* determined translocation speed of the SeqA-covered hemimethylated DNA by using the genome-wide ChIP on Chip analysis and found that speed of a SeqA track was approximately 600 nt/s at 30°C, which coincides to the average rate of DNA synthesis (Waldminghaus *et al.*, 2012). To detect the position of replication fork by measuring a gene dosage in these two studies, it was crucial to synchronize the cell cycle of the *E. coli* cells with the temperature-sensitive *dnaC2* gene that prevents the initiation of DNA replication but not chain elongation at the restrictive temperature. In other study, using flow cytometry for analysis of DNA contents and the temperature-sensitive *dnaA46* allele for the cell cycle synchronization, McGlynn's group showed that it takes 40-50 min for the *E. coli* cells to complete one round of DNA replication of the 4.6 Mb chromosome at 42°C, indicating that the rate of DNA synthesis is about 760-950 nt/s (Atkinson *et al.*, 2011). Based on these reports, the replication fork speed in *E. coli* cells is in a range of 600-950 nt/s that is consistent with the known rate of DNA chain elongation by Pol III *in vitro*, 1000 nt/s (Chandler *et al.*, 1975). However, these values are the mean speed obtained by bulk analysis of many replication forks that averages over a large ensemble of molecules and obscures variations of individual replication fork progression.

1.3. A single molecular analysis of replication fork speed *in vitro*

Using the *oriC* plasmid (Funnell *et al.*, 1986, Higuchi *et al.*, 2003) and the rolling-circle DNA replication systems (Wu *et al.*, 1992, McInerney & O'Donnell, 2004), the functional replisome can be reconstituted from purified proteins including the three key components, SSB, and DNA gyrase. The replisome moves at approximately 500-700 nt/s in these experimental systems. Recently, the real-time observation of a

single molecule has been applied to study the dynamic behavior of individual *E. coli* replisomes reconstituted in the rolling-circle DNA replication systems *in vitro* (van Oijen & Loparo, 2010). Tanner *et al.* has successfully developed the rolling-circle DNA replication system for real-time observations of the replication fork progression. In this method, the Y-shaped template DNA was prepared by annealing a M13 ssDNA template and a tailed primer having 5'-biotinylation (Tanner *et al.*, 2008, Tanner *et al.*, 2009). The biotinylated template DNA was attached on streptavidin-coated glass surface of a flow chamber by the high affinity interaction between biotin and streptavidin. The replisome was reconstituted on the template by flowing the all required replicative proteins for the replication reaction into the chamber. DNA replication catalyzed at 37°C converts ssDNA to dsDNA in a rolling-circle manner. The rolling-circle dsDNA was stretched by the flowing force in the chamber, detected SYTOX dsDNA intercalating dye, and individually visualized under a fluorescent microscope. This study demonstrated that the fork speed ranged from 200 to 1,000 nt/s with a mean speed of 535 nt/s with processivity of 85.3 kb at 37°C (Tanner *et al.*, 2009). The real-time measurements of many individual replisomes assembled on a synthetic fork substrate revealed action properties of the replisome and the speed distributes in a Gaussian curve. Another study at 23°C suggested that the varying speeds for 112 replisomes fitted to a single Gaussian function with a mean rate of 246 nt/s (Yao *et al.*, 2009).

1.4. A possible difference between replication fork progression *in vitro* and *in vivo*

Although these single-molecule approaches seem to be ideal to study the dynamic of the replication fork progression, replications forks in cells move on genomic DNA that differs from the template DNA used in the reconstituted experiments *in vitro*. The reconstituted rolling-circle DNA replication systems used a very homogeneous DNA template and catalyzed DNA synthesis without various DNA transactions other than the basic reactions essential for DNA replication. In contrast, the replisome

working in cells replicates a more complex template of chromosomal DNA undergoing various biological reactions.

In growing *E. coli* cells, the replisome must travel half of the 4.6-Mb chromosome and it encounters numerous natural obstacles on the chromosome: transcription, DNA binding proteins and unusual DNA structures (Mirkin & Mirkin, 2007). Many non-essential factors help the replisome to overcome pausing or collapse of the replication fork due to collisions with transcribing RNA polymerases so called the replication-transcription conflict (Soulтанas, 2011). DNA replication and transcription are simultaneously operated in the rapidly growing *E. coli* cells unlike the temporal separation of those in the cell cycle of eukaryotic cells. An accessory DNA replicative helicase, Rep interacts with the replicative DnaB helicase of the replisome (Atkinson *et al.*, 2011a), and together with UvrD and DinG helicases promotes replication across highly transcribed regions (Guy *et al.*, 2009, Boubakri *et al.*, 2010). Absence of Rep indeed reduces two folds in chromosomal replication speed (Atkinson *et al.*, 2011b). The transcription factor DskA also prevents transcription from interfering with replication upon nutrient stress (Tehranchi *et al.*, 2010). Abundant nucleoid (bacterial chromosome structure) proteins associate with DNA participate in chromosomal organization and transcriptional regulation (Rimsky & Travers, 2011), and form a compact cluster on genome (Wang *et al.*, 2011), at which fork progression could be interfered. Spontaneous DNA lesions and their repair enzymes are also potential obstacles for the progressing replisome. Even in the absence of exogenous DNA damage, replication is disrupted in more than 15% of *E. coli* cells (Renzette *et al.*, 2005). In fact, a few percent of the cells experiences one or more spontaneous double-strand breaks (Pennington & Rosenberg, 2007). Chromosomal DNA contains several non-B DNA structures, including cruciforms, slipped structures, triplexes, G-quadruplexes, and Z-DNA have been shown to cause mutations (Zhao *et al.*, 2010). A more serious and unavoidable problem for the replisome is topological barriers on

DNA. Torsional stress inhibits replication fork movement unless promptly resolved by topoisomerases that remove positive supercoils that can accumulate ahead of the replication fork (Khodursky *et al.*, 2000). However, the extent to which the fork speed varies during DNA replication under those environments on the chromosomal DNA in *E. coli* cells remains unknown because of difficulty in speed determination of individual replication forks with the cells.

1.5. A DNA combing method that enables visualization of individual DNA molecules

DNA combing is a newly developed technique to stretch individual DNA molecules by receding air-water interface and bound on a positively charged glass surface (a coverslip). The individual DNA molecules on glass are detected by an intercalating fluorescent dye, antibodies to react incorporated nucleotide analogs or *in situ* hybridization (FISH) method with a fluorescently-labeled probe, and visualized the fluorescent signals with a fluorescent microscope (Bensimon *et al.*, 1994; Herrick & Bensimon, 1999). Initially, the DNA combing method was used to map a specific region on DNA in eukaryotes. The eukaryotic cells were labeled with biotin-dUTP and 5-bromo-2'-deoxyuridine (BrdU) to monitor entire genomic DNA and replicated DNA, respectively and subjected to measurements of the frequency of replication origin activation by DNA combing (Herrick & Bensimon, 1999). Recently, replication fork dynamics in eukaryotic cells has been successfully investigated at the single-molecular level with DNA combing. In the approach, the nascent DNA of the eukaryotic cells is sequentially labeled with halogen analogs of thymidine, 5-Chloro-2'-deoxyuridine (CldU) and 5-Iodo-2'-deoxyuridine (IdU). The double-labeled DNA molecules are extracted, stretched and irreversibly attached on a positively charged glass surface by the DNA combing procedure. The stretched DNA molecules are reacted with antibodies specific to each analog. The first labeling with CldU serves to mark on-going replication forks, while the second labeling with IdU is to monitor the chain

elongation rate that coincides with the fork speed. By measuring the length of the IdU tracks on the dual DNA molecules, the speed of individual replication forks was accurately determined in eukaryotic cells (Sugimura *et al.*, 2008; Petermann *et al.*, 2006; Pertermann *et al.*, 2010). As the case of *in vitro* reconstituted replisomes, the single-molecule approach with DNA combing is powerful to investigate the replication-fork movement in living cells. However, in the case of *E. coli* cells, the technique was impracticable for determination of the fork speed because of poor incorporation of thymidine analogs into the cells. In an earlier report, Breier *et al.* stated that thymidine-auxotroph derivatives of the wild-type K12 strains were not satisfactory for BrdU incorporation. They only used the DNA combing method to map the replication origin region by the FISH method and detect the newly synthesized DNA only near the origin region by immune detection of incorporated BrdU (Breier *et al.*, 2005).

1.6. A determinant of replication fork speed in *E. coli* cells

As shown in the Figure 2, Pol III and DnaB are the replicative DNA polymerase and the replicative DNA helicase, respectively, functioning in DNA synthesis at the replication fork. Coordinated functions of the replisome components including Pol III and DnaB determine replication fork speed in *E. coli* cells, which is estimated to be 600-950 nt/s in bulk-phase analysis (see the section 1.2). Pol III and DnaB are progressive molecular motors that respectively translocate on single-stranded DNA (ssDNA). Coupling of these motors is mediated by the τ subunit of the DnaX complex (Table 1) and enhances both the DNA unwinding rate and processivity of DNA synthesis compared with those of each motor alone in the rolling circle system. Studwell and O'Donnell analyzed the synchronous DNA synthesis by incorporation of radioactive dTTP at 30°C and found that the reconstituted Pol III core synthesizes DNA at the average rate of about 500 nt/s, which is approximately the same speed as the naturally purified Pol III holoenzyme (Studwell and O'Donnell, 1990). In our

laboratory, the velocity of the chain elongation by the naturally purified Pol III holoenzyme was determined to be about 900 nt/s by the burst DNA synthesis with single-stranded circular DNA at 30°C (Sugaya *et al.*, 2002). In contrast, the DNA unwinding rate of DnaB helicase (35 nt/s) is much slower than the DNA chain elongation rate of Pol III (about 900 nt/s) (Kim *et al.*, 1996; Sugaya *et al.*, 2002). Since the strand displacement by Pol III is weak, it has been postulated that elongation of the leading strand could act as the pacemaker of replication fork progression such that Pol III pushes DnaB in the replisome (Patel *et al.*, 2011). However, no direct evidence for this hypothesis has been provided.

1.7. Fork speed in the DNA damage response of *E. coli* cells

The chromosomal DNA is frequently damaged by various factors such as endogenous reactive oxygen species (ROS) and exogenous UV light in cells. Therefore, the replicative DNA polymerase often encounters various kinds of obstructive DNA lesions and is blocked due to the high fidelity of the DNA synthesis activity. The stalled replication forks result in instability of genome and threaten viability of cells. Therefore, inhibition of DNA replication by DNA damage induces a complex cellular tolerance mechanism termed the SOS response in bacteria and the S-phase checkpoint in eukaryotes (Fig. 3). When DNA replication is blocked in *E. coli* cells, the RecA protein is activated and then triggers autodigestion of the LexA protein, the negative regulator of the SOS-controlled genes, which results in induction of the SOS response. In the S-phase checkpoint, speed of unperturbed replication forks is decreased although the mechanisms for the slowdown are unknown due to the highly complex response pathway operated by an enormous number of genes. The slowdown of the fork speed may delay the unblocked replication forks to further encounter DNA lesions that potentially exist ahead in the cells suffered from DNA damage. Thereby, the checkpoint activation may help the eukaryotic cells preserve enough time to repair the damaged DNA before it is replicated (Petermann *et al.*, 2006; Syljuasen *et al.*,

2005).

Evelyn Witkin hypothesized in 1967 that bacterial cell division is controlled by a repressor and is inactivated by a complex process that starts with the presence of replication-blocking lesions in DNA. Mirokov Radman proposed in 1970 the SOS hypothesis that there exists an inducible system which is responsible for UV-irradiation induced mutations in bacteria (Bridges, 2005). Subsequently, it became clear that there are many SOS genes controlled by the LexA repressor, leading to the current concept of the SOS response. In *E. coli* cells, the LexA repressor protein negatively regulates more than 40 genes (SOS genes) by binding to a 20 bp consensus sequence (SOS box) in the operator region of the genes (Little *et al.*, 1981; Brent & Ptashne, 1981). The replication forks stalled by DNA damage trigger uncoupling of the leading and lagging strand synthesis, and lead to accumulation of ssDNA. In the presence of ssDNA at the stalled replication forks, the RecA protein binds to the ssDNA region to form the nucleo-protein filament and induces autocleavage of the LexA repressor. The degradation of the LexA repressor results in upregulation of the SOS genes. The expression level of the SOS genes varies from gene to gene because of the different affinity of the LexA repressor to the SOS boxes in each gene (Little *et al.*, 1980; Courcelle *et al.*, 2001; Goodman, 2002). To protect the bacterial cells from replication stress, the upregulated SOS genes function in various pathways such as DNA repair (*uvrABCD* in nucleotide excision repair, *recA* in recombination repair), control of cell division (*sula*), or translesion DNA synthesis and damage-induced mutagenesis (*polB*, *polIV*, and *umuDC*). Although the SOS response was discovered more than 40 years ago, because of difficulty in fork speed determination with *E. coli* cells, no one knows if replication fork speed is reduced in the SOS response.

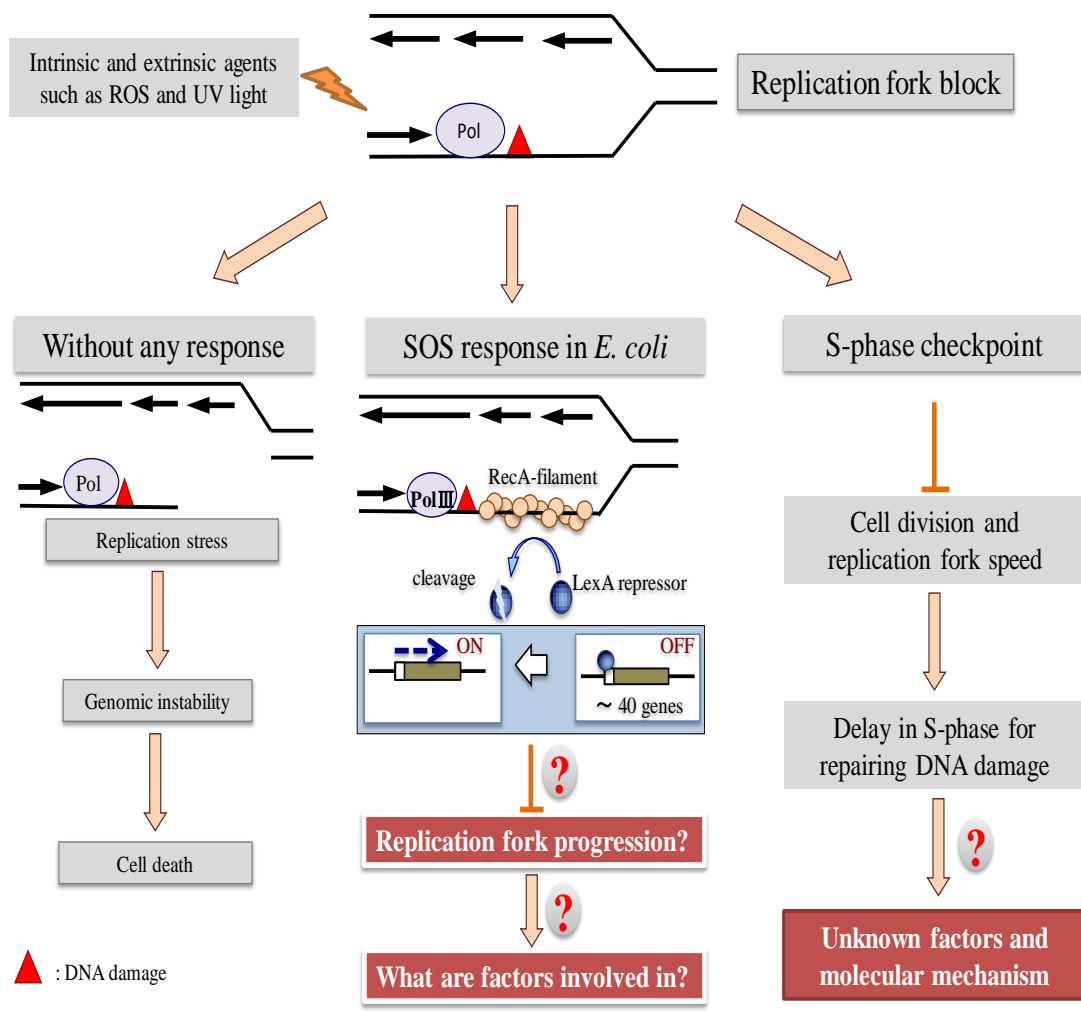


Figure 3: DNA damage induces the SOS response in *E. coli* and the S-phase checkpoint in eukaryotes. The replication fork is blocked when it encounters the DNA damage (red triangle). Activation of the SOS response and the S-phase checkpoint protect *E. coli* and eukaryotic cells, respectively from genomic instability and ultimately cell death. In the S-phase checkpoint, the fork speed is slowed down with unknown mechanism and unknown factors. In the SOS response, about 40 SOS genes are upregulated by autocleavage of the LexA repressors in the activated RecA-dependent manner.

1.8. Objectives of this research

It is challenging to obtain an accurate value of fork speed to assess the fine dynamics of individual replisomes on the *E. coli* chromosome. Dynamics of replication fork progression remains unknown with *E. coli* cells, the leading model of DNA replication. It has not been directly demonstrated that the replicative Pol III of *E. coli* provides a major driving force for the replication fork progression. Moreover, it has not been shown for about 40 years that the fork speed is slowed down in the SOS response as well as the eukaryotic checkpoint.

To obtain a more precise view of replisome dynamics in the cell and approach to these unanswered questions in *E. coli* DNA replication, I planed to use the DNA combing method with *E. coli* cells. Since the labeled DNA is stretched on a glass surface and visualized under a microscope in the DNA combing method, the field of view restricts the measurable DNA length below 300 kb. Due to this limitation, pulse-labeling for *E. coli* cells with the analogs needs to be done in less than 6 min based on the average rate of DNA synthesis (800 nt/s). However, there is no such a strain that meet the criteria despite of a long time history of *E. coli* genetics. To overcome this difficulty, I planed first to construct a novel *E. coli* strain, which incorporates BrdU with a dramatically enhanced efficiency. Using the strain with the DNA combing, the extent to which the fork speed varies during chromosomal DNA replication in the cell could be determined for the first time in *E. coli* cells.

Furthermore, I planed to use the strain with the DNA combing to approach two questions in DNA replication; what is a major determinant of replication fork speed and if fork speed is reduced in the SOS response. The *dnaE* gene encodes the catalytic α -subunit of Pol III holoenzyme (Maki *et al.*, 1985). Maki and his colleagues previously isolated a *dnaE173* mutant strain that produces an altered Pol III with remarkable enzymatic characteristics (Maki *et al.*, 1991). Among those, the most

striking feature is that the rate of DNA chain elongation by the *dnaE173* Pol III holoenzyme is greatly reduced to 300 nt/s, one-third of that observed with the wild-type Pol III holoenzyme *in vitro* (Sugaya *et al.*, 2002). If the Pol III holoenzyme is a major determinant of the replication fork to move, the fork speed in the *dnaE173* cells should be close to one-third of that in the control cells.

The SOS response is the cellular network activated by DNA damage and much simpler than the eukaryotic checkpoint. The mediator of the response is RecA, and the target of the mediator is well known to be LexA repressor. It is easy to obtain the SOS-induced cells in which *lexA* gene encoding the repressor protein is disrupted by simple genetic manipulation. If the SOS response slows down the replication fork progression, the fork speed in the $\Delta lexA$ cells should be reduced compared with that in the *lexA*⁺ cells. When the speed is showed down in the SOS response, there is a good chance to find the gene(s) responsible the slow down because the number of the SOS-induced genes is limited.

2. Materials and Methods

2.1. Reagents and chemicals

Reagents for LB and 56/2 media were purchased from Wako Pure Chemical Industries, Japan and Becton Dickinson, USA. Rabbit anti-RecA antibodies and HRP-conjugated anti-rabbit IgG were purchased from Bio Academia, Japan and GE Healthcare, USA, respectively. Fluorescent dyes, YOYO-1 and FM4-64, were purchased from Life Technologies, USA, and DAPI (4',6-diamidino-2-phenylindole) was from Dojindo Laboratories, Japan. BrdU (5-bromo-2'-deoxyuridine), IdU (5-Idodo-2'-deoxyuridine), and DL-serine hydroxamate were purchased from Sigma-Aldrich, USA. CldU (5-chloro-2'-deoxyuridine) were purchased from MP Biomedicals, USA. Mouse and rat anti-BrdU monoclonal antibodies were purchased from Becton Dickinson, USA and Abcam, USA, respectively. Alexa Fluor 555-conjugated anti-rat IgG and Alexa Fluor 488-conjugated anti-mouse IgG were purchased from Life Technologies, USA. [¹⁴C] thymidine (> 50 mCi/mmol) and [³H] thymidine (70-90 Ci/mmol) were purchased from PerkinElmer, USA. Silane-coated coverslips were purchased from Matsunami Glass Industry, Japan. Vectashield mounting medium H-1000 was purchased from Vector Laboratories, USA.

2.2. List of bacterial strains

All *E. coli* strains used in this study are listed in Table 2.

Table 2: Bacterial strains used in this study

Name	Bacterial genotype	Reference or source
MG1655	Sequenced wild-type <i>E. coli</i> K-12	Guyer <i>et al.</i> , 1981 ^a
BW25113	<i>lacI^f rrnB_{T14} ΔlacZ_{WJ16} hsdR514</i> <i>ΔaraBAD_{AH33} ΔrhaBAD_{LD78}</i>	Datsenko & Wanner, 2000
15T ⁻	<i>thyA42 deoB20</i>	Roepke <i>et al.</i> , 1944 (Not a K-12 strain)
eCOMB	MG1655 except <i>ΔthyA Δ(yjg-deoB)</i>	this work ^d

JWK2795	BW25113 except $\Delta thyA::kan$	Baba <i>et al.</i> , 2006: Keio Collection ^b
JWK4336	BW25113 except $\Delta yjgG::kan$	Baba <i>et al.</i> , 2006: Keio Collection ^b
JWK4346	BW25113 except $\Delta deoB::kan$	Baba <i>et al.</i> , 2006: Keio Collection ^b
JWK0059	BW25113 except $\Delta polB::kan$	Baba <i>et al.</i> , 2006: Keio Collection ^b
JWK0221	BW25113 except $\Delta dinB::kan$	Baba <i>et al.</i> , 2006: Keio Collection ^b
JWK0941	BW25113 except $\Delta sulA::kan$	Baba <i>et al.</i> , 2006: Keio Collection ^b
JWK1850	BW25113 except $\Delta ruvA::kan$	Baba <i>et al.</i> , 2006: Keio Collection ^b
JWK2669	BW25113 except $\Delta recA::kan$	Baba <i>et al.</i> , 2006: Keio Collection ^b
JWK3786	BW25113 except $\Delta uvrD::kan$	Baba <i>et al.</i> , 2006: Keio Collection ^b
JWK7004	BW25113 except $\Delta umuDC::kan$	Baba <i>et al.</i> , 2006: Keio Collection ^b
JWK2549	BW25113 except $\Delta recO::kan$	Baba <i>et al.</i> , 2006: Keio Collection ^b
MK7158	MG1655 except $\Delta thyA$	this work ^d
MK7167	MG1655 except $\Delta thyA \Delta deoB$	this work ^d
MK7426	MG1655 except $\Delta thyA \Delta deoB \Delta yjgG::kan$	this work ^d
MK7453	eCOMB except $\Delta sulA$	this work ^d
MK7456	eCOMB except $\Delta sulA \Delta lexA::kan$	this work ^d
MK7460	eCOMB except $\Delta sulA \Delta dinB \Delta lexA::kan$	this work ^c
MK7463	eCOMB except $\Delta sulA \Delta polB \Delta lexA::kan$	this work ^c
MK7466	eCOMB except $\Delta sulA \Delta umuDC \Delta lexA::kan$	this work ^c
MK7486	eCOMB except $\Delta sulA \Delta recA \Delta lexA::kan$	this work ^c
MK7489	eCOMB except $\Delta sulA \Delta uvrD \Delta lexA::kan$	this work ^c
MK7498	eCOMB except $\Delta sulA \Delta dinB \Delta recA \Delta lexA::kan$	this work ^e
MK7916	eCOMB except $\Delta sulA \Delta ruvA \Delta lexA::kan$	this work ^c
MK7954	eCOMB except $\Delta sulA \Delta recO \Delta lexA::kan$	this work ^c
SMR7467	MG1655 except $lexA3(\text{Ind}^+) malB::Tn9$ $\Delta att\lambda::P_{sulA}\Omega gfp-mut2$	Pennington & Rosenberg, 2007
SMR7623	MG1655 except $lexA51(\text{Def}) malB::Tn9$ $\Delta att\lambda::P_{sulA}\Omega gfp-mut2 sulA211$	Pennington & Rosenberg, 2007
MK935	MG1655 except $dnaE173 zae-502::Tn10$	Laboratory stock
MK7927	MG1655 except $zae-502::Tn10$	this work ^f
MK7928	MG1655 except $dnaE173 zae::Tn10$	this work ^f

All strains in this study are derivatives of *E. coli* K-12, excepting 15T⁻. ^a MG1655 is a *E. coli* K12 strain that were purchased from The Coli Genetic Stock Center at Yale University, USA. ^b Keio Collection strains were obtained from the National BioResource Project: *E. coli* (National Institute of Genetics, Japan). ^c The strains were constructed in this study by P1 transduction as a strain of the Keio collection as a donor. ^d *yjgG* or *lexA* genes were deleted by the one-step gene disruption method (Datsenko & Wanner, 2000). ^e The temperature-sensitive plasmid pRECA1 was introduced into eCOMB $\Delta sulA$ to delete *recA* and *lexA* by P1 transduction, and then eliminated by

incubating the cells at 42°C. ^f The strains were constructed by transferring the *dnaE173* mutator mutation together with tetracycline-resistant gene from MK935 to eCOMB strain by P1 transduction. *kan*; kanamycin resistant gene.

2.3. List of plasmids

All plasmids used in this study are shown in Table 3.

Table 3: Plasmids were used in this study

Name	Plasmid properties	Reference
pCP20	flippase helper plasmid (<i>amp</i>)	Datsenko & Wanner, 2000
pKD13	template plasmid with FRT-flanked <i>kan</i>	Datsenko & Wanner, 2000
pKD46	Red recombinase plasmid (<i>amp</i>)	Datsenko & Wanner, 2000
pNTR- <i>thrA</i>	Mobile plasmid clone with P _{tac} - <i>thrA</i> (<i>amp</i>)	Saka <i>et al.</i> , 2005 ^a
pNTR- <i>lexA</i>	Mobile plasmid clone with P _{tac} - <i>lexA</i> (<i>amp</i>)	Saka <i>et al.</i> , 2005 ^a
pKO3	a temperature-sensitive pSC101 vector (<i>cam</i>)	Link <i>et al.</i> , 1997
pRECA1	pKO3 carrying <i>recA</i> ⁺ (<i>cam</i>)	Laboratory stock

^a Mobile plasmids were obtained from National BioResource Project: *E. coli* (National Institute of Genetics, Japan). Abbreviations are: *amp*, ampicillin resistant gene; *kan*, kanamycin resistant gene; *cam*, chloramphenicol resistant gene; FRT, Flippase Recognition Target; P_{tac}, Tac promoter. Antibiotics markers used for transformation are shown in parentheses.

2.4. List of oligonucleotides

The oligonucleotides shown in Table 4 were used to disrupt chromosomal genes (see the section 2.5) and to evaluate a ratio of *oriC* relative to *ter* by real time PCR (see the section 2.13). The primers used for verification of gene disruption are not listed here.

Table 4: Oligonucleotides were used in this study

Name	DNA sequences of oligonucleotides (5' - 3')	Purpose
yjg-F	CCGCCATTGCCCTGTACGAAAG	this work ^a
yjg-R	CTTCTTGAGTAAGCGGCATCGC	this work ^a
JW4003-KC	TGCTGTATATACTCACAGCATAACTGTATATACACCCAG GGGGCGGAATG <u>ATTCCGGGGATCCGTCGACC</u>	this work ^b
JW4003-KN	CCAGGCGGCATCGCGGTCTCAGAGATATGTTACAGCC AGTCGCCGTTGCG <u>TGTAGGCTGGAGCTGCTTCG</u>	this work ^b

mioC-rF1	TTGAGTAAATTAACCCACGATCC	this work ^c
mioC-rR1	AACATTCTTGATCACGACATTCC	this work ^c
tus-rF1	TGAAATCACCACGCAGTGTC	this work ^c
tus-rR1	TCCTGATACTCTCGCTCCAGT	this work ^c

^a For amplification of $\Delta yjg::kan$ of JW4336. ^b For amplification of FRT-franked *kan* fragment of plasmid pKD13 to disrupt *lexA*. Nucleotides complementary to genomic target sequences are shown without underline, whereas the underlined nucleotides are complementary sequence to pKD13. ^c For amplification of *mioC* and *tus* regions in quantitative real time PCR experiments.

2.5. Construction of bacterial strains

P1(*vir*)-mediated transduction (Miller, 1972) were used to construct a thymidine-requiring eCOMB strain (MG1655 $\Delta thyA \Delta (deoB-yjg)$) and derivatives of the eCOMB cell with an appropriate donor strain. The one-step gene disruption procedure (Datsenko & Wanner, 2000) was also used to construct eCOMB and MK7456 (MG1655 $\Delta thyA \Delta deoB \Delta yjg::kan$). DNA manipulation and transformation were carried out with standard procedures as described (Sambrook & Russell, 2001).

2.5.1. P1(*vir*)-mediated transduction

Genetic markers of a donor strain were transferred to a recipient strain by P1-phage transduction. Overnight culture of a donor strain was subcultured in 5 ml of LB medium containing 5 mM CaCl₂ to obtain OD₆₀₀ of 0.4 - 0.5, and then 10⁶ pfu (plaque forming units) of P1 phage solution was added to 1 ml of the cell culture followed by incubation at 37°C for 20 min for infection. Next, 2 ml of R-top agar at 55°C was mixed with the phage-infected cells, and the mixture was poured on each R-plate. After the plates were incubated for 8 hours at 37°C, the R-top agar of each plate was scraped and transferred to a centrifuge tube. To each tube, 0.1 ml of chloroform was added to kill the donor cells. The P1 phage lysate was recovered by centrifugation of the tube at 8,500 x g for 20 min at 4°C, and 0.04 ml of chloroform was added to the lysate supernatant for storage.

For transduction, 1 ml of the overnight culture of a recipient strain was

collected by centrifugation and suspended in 1 ml of MC buffer. To 1 ml of the cell-suspension, 0.1 ml of the 10- and 100-fold diluted phage solution was added respectively. After infection of phage at 37°C for 20 min, 0.2 ml of 1 M Sodium citrate was added to the cell suspension to stop further phage infection. The phage-infected cells were incubated at 37°C for 2 hours and plated on LB plates containing an appropriate antibiotic to select transductants. When a strain of the Keio Collection (Table 2; Baba *et al.*, 2006) was used as a donor, the transductants were transformed with plasmid pCP20 to eliminate the FRT-flanked *kan* by flippase recombinase unless otherwise noted (Datsenko & Wanner, 2000; Doublet *et al.*, 2008).

2.5.2. One-step gene disruption by Red recombinase

A DNA fragment containing the FRT-flanked *kan* gene was amplified by PCR with appropriate primers (Table 4). *E. coli* cells carrying the temperature sensitive pKD46 plasmid (Table 3) were transformed with the DNA fragment; the pKD46 plasmid has three red genes that function in Red-mediated recombination. A chromosomal gene of the resulting transformant was replaced with the FRT-flanked *kan* gene by Red-mediated recombination as described (Datsenko & Wanner, 2000). The gene disruption was verified by PCR with two primers that are complementary to upstream and downstream regions of the targeted gene, respectively. The pKD46 plasmid was removed by incubating the transformants at 42°C to use the transductants for each experiment.

2.5.3. Construction of eCOMB

A new *E. coli* strain, eCOMB (*E. coli* for combing), that efficiently incorporates thymidine analogs was constructed in this study. Both *thyA* and *deoB* of the wild-type MG1655 (Guyer *et al.*, 1981; Lee *et al.*, 2009) were deleted by P1 transduction with JWK2795 and JWK4346 (Table 2) as donors, respectively, and MK7167 was obtained. The chromosomal *yjjG* gene of MK7167 was replaced with

the $\Delta yjg::FRT-kan$ by the one-step gene disruption method (Weiss, 2006; Titz *et al.*, 2007) as follows. The $\Delta yjg::FRT-kan$ DNA fragment of JWK4336 was amplified with *yjg*-F and *yjg*-R oligonucleotides as primers (Table 4) by PCR. MK7167 carrying pKD46 (Table 3) was transformed with the amplified DNA fragment, resulting in MK7456 (MG1655 $\Delta thyA \Delta deoB \Delta yjg::kan$). When the *kan* gene of the strain was eliminated by flippase, seven genes between *yjg* and *deoB* was deleted, and the resulting strain was named eCOMB. The eCOMB cell lacks the 5 genes involved in the *de novo* synthesis and the salvage pathways of thymidine as shown in Fig. 5, and the other seven genes (*prfC*, *osmY*, and five hypothetical genes).

2.5.4. Construction of derivative strains of eCOMB

A constitutively SOS-induced MK7456 cell was constructed from eCOMB (Table 2). The *sulA* gene was deleted by P1 transduction with JWK0941 as a donor, and MK7453 was obtained after eliminating *kan* with the pCP20 plasmid (Table 3). The $\Delta lexA::kan$ fragment was amplified with pKD13 template DNA (Table 3) and primers, JW4003-KC and JW4003-KN (Table 4) by PCR. MK7453 carrying pKD46 was transformed with the DNA fragment to replace the chromosomal *lexA* with the $\Delta lexA::kan$ by one-step gene disruption method. The resulting transformant was MK7456 (eCOMB except $\Delta sulA \Delta lexA::kan$). The *kan* gene of $\Delta lexA::kan$ was not removed by flippase.

The various genes (*dinB*, *polB*, *umuDC*, *uvrD*, *ruvA*, *recA*, and *recO*) were respectively disrupted in the SOS-constitutive eCOMB (MK7456). Each gene was deleted from MK7453 (eCOMB except $\Delta sulA$) by P1 transduction with an appropriate Keio collection cell as a donor. After eliminating *kan*, the $\Delta lexA::kan$ was introduced to the resulting strains by P1 transduction or the one-gene disruption method. The FRT-flanked *kan* gene was not pop out from $\Delta lexA::kan$ by flippase. When $\Delta recA$ strains were used as a recipient in P1 transduction experiments, the cells were transformed with the temperature-sensitive pRECA1 plasmid (Table 3). After deleting

chromosomal genes, the pRECA1 plasmid was eliminated by incubation of the cells at 42°C.

The *dnaE173* mutator mutation of MK935 was cotransferred with the tetracycline-resistant gene of *zea-502::Tn10* into the recipient eCOMB strain by P1 phage transduction. Among the tetracycline-resistant transductants, mutator and non-mutator colonies were selected on LB plates containing rifampicin. The mutator MK7928 (eCOMB *dnaE173 zae-502::Tn10*) and the control MK7927 (eCOMB *zea-502::Tn10*) cells were obtained.

2.6. Bacterial growth conditions

The 56/2 minimal medium was prepared without streptomycin as described (Willetts *et al.*, 1969). For amino acids, the medium was supplemented with 0.2% casamino acids and 20 µg/ml tryptophan. When $\Delta lexA$ was complemented with the Mobile plasmid (Table 3), IPTG was included in the 56/2 medium at a final concentration of 0.5 mM. LB medium and M9 salts were prepared as described (Sambrook & Russell, 2001). All medium include 2 µg/ml thymidine. The cells were grown in LB containing 2 µg /ml thymidine at 37°C for 14-16 h. The overnight culture was rinsed with five-time volume of M9 salts, harvested by centrifuge at 8,500 x g for 10 min at room temperature and suspended in an original volume of M9 salts. The suspended cells were added to 15-20 ml of pre-warmed 56/2 medium containing 2 µg/ml thymidine to give an OD₆₀₀ of 0.02 in a 50-ml bioreactor tube (TPP, Switzerland), and the tube was shaken at 125 rpm in a water bath at 37°C until OD₆₀₀ reaches 0.3. The exponentially growing cells were treated in each experiment as indicated.

To synchronize the cell cycle of eCOMB, the exponentially growing cells were incubated in 56/2 medium containing 1 mg/ml of a seryl-tRNA synthetase inhibitor, DL-serine hydroxamate (Sigma-Aldrich, USA) at 37°C for 90 min. The cells cannot initiate DNA replication due to amino acids starvation in the presence of the drug (Ferullo *et al.*, 2009). In pulse-labeling experiments, the cell cycle block was released

by transferring the cells into 56/2 medium with thymidine analog but without the inhibitor.

2.7. Establishment of DNA combing with λ phage DNA

A DNA combing procedure was established with λ DNA in this study. λ DNA (2 μ g; Life Technologies, USA) was added to 200 μ l of TE buffer (pH8.0). The cos site of λ DNA was denatured by heating the DNA solution at 60°C for 10 min and immediately cooling down on ice for 10 min (Wu & Taylor, 1971). Next, the linearized λ DNA was mixed with 0.6 μ l of 1 mM YOYO-1 and placed on ice for 60 min. The stained DNA solution mixed with 8 ml of 0.5 M MES buffer (pH 5.5) was poured into a 10-ml PTFE (Polytetrafluoroethylene) plastic beaker. A positively charged coverslip was soaked into the DNA solution for 5 min and then slowly pulled up at a constant speed of 300 μ m/s (Fig. 4). DNA molecules were uniformly stretched on glass surface by force of water meniscus. The coverslip was baked at 60 °C in the dark for overnight (12-16 hours) to fix the DNA on glass surface. Next day, the coverslip was placed on a slide glass plate with 5 μ l of the mounting medium, Vectashield H-1000. Finally, the YOYO-1 stained λ DNA was visualized using a fluorescent microscope, Axiovert 200M (Zeiss, Germany) with 63X objective and GFP filter, and lengths of the individual DNA molecules were measured with the AxioVision 4.5 software (Zeiss, Germany). The measured length in pixel was converted to μ m by the following equation: $\mu\text{m} = \text{pixel} \times 0.0992$. An unit scale (kb/ μ m) to convert μ m into kb was calculated by dividing the size of λ DNA (48.5 kb) by the peak value of the combed DNA length (21 μ m) experimentally determined in this study (Fig. 8A).

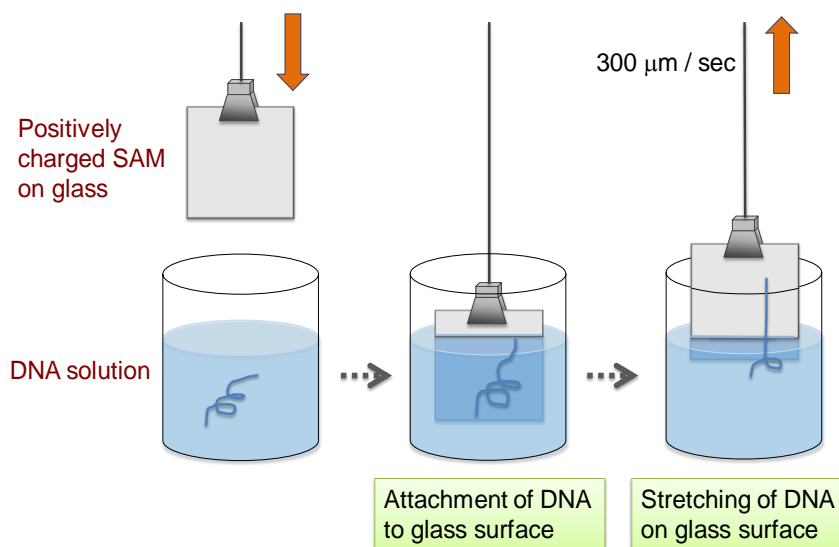


Figure 4. The schematic view of molecular combing to stretch DNA molecules on glass surface. The positively charged glass were soaked into DNA solution for 5 min followed by pulling up at constant speed $300 \mu\text{m}/\text{s}$ to stretch DNA molecules on glass surface.

2.8. DNA combing with chromosomal DNA of eCOMB cells

2.8.1 Labeling of eCOMB cells with thymidine analogs

Asynchronously growing eCOMB cells were generally used for pulse-labeling of chromosomal DNA with thymidine analogs. Because the cells that had been synchronized with DL-serine hydroxamate did not simultaneously start DNA replication, the synchronized cells were only used in the very early stage of this study. During pulse-labeling, the cells were incubated in a 50-ml bioreactor tube in the dark.

The exponentially growing cells were harvested by centrifugation at $8,500 \times g$ for 10 min at 20°C . The cells equivalent to 1 ml of a suspension at $\text{OD}_{600} = 4.0$ were transferred into 20 ml of pre-warmed 56/2 medium containing $50 \mu\text{g}/\text{ml}$ CldU to obtain final OD_{600} of 0.2 and inoculated at 37°C for 2 min in a water bath with shaking at 125 rpm. The CldU-labeled cells were collected by vacuum filtration with $0.22\text{-}\mu\text{m}$

MF-Millipore membrane filter (Merck Millipore, USA) and suspended in 40 ml of pre-warmed flesh 56/2 medium containing 50 µg/ml IdU. The cell suspension was divided into four bioreactor tubes (10 ml/tube). The tubes were continued to incubate at 37°C with shaking. To determine the distribution of fork velocities, cells were pulse-labeled with IdU for 2 min. To estimate fork speed with a slope value on the IdU-labeled DNA length over an IdU-labeling time, cell growth was sequentially terminated in 1-min intervals for 4 min. Cell growth was stopped by addition of 1.1 ml of ice-cold 20% sodium azide (final concentration 2%). After the tubes were kept on an ice water bath for 5 min, the labeled cells were harvested by centrifugation at 8,500 x g for 10 min at 4°C, rinsed with 500 µl of ice-cold TNE buffer (10 mM Tris-HCl (pH 8.0), 20 mM NaCl, 50 mM EDTA) containing 2% sodium azide and suspended in 100µl of TNE buffer.

2.8.2. Preparation and treatment of agarose plugs

The labeled cell suspension (100µl) was warmed at 37 °C and mixed with 100 µl of molten 2% GTG low melting agarose that had been heated at 55°C. The mixture was poured in two plug molds (100 µl/plug) (Bio-Rad, USA). The molds were kept at 4°C for 30 min to solidify agarose. The agarose plugs were taken out of the molds and treated gently to extract the chromosomal DNA as described (Rayssiguier *et al.*, 1989). The plugs were treated with 10 mg/ml lysozyme and 0.2 mg/ml RNase at 37 °C for overnight followed by incubation with 2 mg/ml protease K at 50°C for overnight. The plugs were washed with 0.5 M EDTA followed by TE (pH8.0) and stained with YOYO-1 at room temperature for 1 hour. After melting the plugs at 68°C for 20 min, agarose of the DNA solution was digested with β-agarase I at 40°C for overnight. The DNA solution was gently mixed to 8 ml of 0.5 M MES buffer (pH 5.5), and the mixture was poured into a 10-ml PTPE plastic beaker.

2.8.3. Detection of the labeled DNA on glass surface

The chromosomal DNA molecules were stretched on glass surface and fixed by baking the cover glass at 60°C as described in the section 2.7. For immune detection of thymidine analogs, the labeled DNA was denatured by soaking the cover slip in the denature solution (50% formamide and 2x SSC) at 72°C for 12 min and then immediately in ice-cold 70% ethanol. The rat anti-BrdU antibody binds to CldU but with very low affinity for IdU, while the mouse anti-BrdU antibody binds to both CldU and IdU (Sugimura *et al.*, 2008; Breier *et al.*, 2005). The antibodies were diluted in 25 µl of detection buffer (0.05% Tween and 1% Roche blocking reagent in 1x PBS buffer pH 7.4). Denatured DNA molecules on the coverslips were incubated first with the former antibody (25 fold dilution) to saturate CldU sites, and then with the latter antibody (5 fold dilution) to selectively react with IdU. Both immune-complexes were detected with Alexa Fluor 555-conjugated anti-rat IgG (25 fold dilution) and Alexa Fluor 488-conjugated anti-mouse IgG (25 fold dilution), respectively. The immune reactions above were carried out at 37°C for 1 hour, excepting for Alexa Fluor-conjugated antibodies with which incubation was done only for 30 min. After each immune reaction, the coverslips were washed 3 times for 5 min each in 1x PBS buffer (pH 7.4) containing 0.05% Tween.

2.8.4. Observation of individual DNA molecules with a fluorescent microscope

After the immune reactions, the coverslips were mounted with Vectashield-1000 on glass plates. The immune-complexes were visualized using a fluorescent microscope Axiovert 200M (Zeiss, Germany) with a 63X objective, and GFP and Cy3 filters. The double-labeled molecules were selected to measure the length of IdU-labeled tracts for analyzing fork progression, whereas the CldU-labeled tracts specify ongoing forks. The measured length of IdU-labeled tracts in pixel was converted to kb as described in the section 2.7. The length of the IdU-tracks at each time point in time course experiments was the median value of more than 100

measurements. The values were used to calculate the slope as a function of the IdU-labeling time. Fork speed of each strain was determined by three independent labeling experiments.

2.9. Analyses of physiological characteristics of eCOMB cells

2.9.1. Analyses of cell growth rate

Growth rate of cells was determined in the log phase by measurements of both OD₆₀₀ and CFU (colony forming units). The exponentially growing cells in 56/2 medium were withdrawn every 30 min for 6 h. In each time point, the density of the cell cultures was measured at OD₆₀₀. An aliquot of each sample was plated on LB plate containing 2 µg/ml thymidine, and the plate was incubated at 37°C to count numbers of viable cells (CFU). The average generation time was determined from three independent experiments based on the OD₆₀₀ and CFU.

2.9.2. Observation of cell shape and nucleoid structures

When cells were exponentially grown to OD₆₀₀ of 0.3, 1 ml of the culture was taken and mixed with 3 ml of ice cold 4% paraformaldehyde in PBS (Nacalai Chemicals, Japan). After incubation on ice for 1 h, the cells were collected by centrifugation at 4200 x g for 5 min and rinsed with 1 ml of PBS buffer, and suspended in 0.1 ml of PBS. To the cell suspension, 2 µl of 1 mg/ml DAPI and 5 µl of 1 mg/ml FM4-64 were added; nucleoids and membrane of the cells were stained by DAPI and FM4-64, respectively. Cell shape and nucleoid structures were visualized using a fluorescent microscope Axiovert 200M (Zeiss, Germany) with 100x objective and appropriate filters (DAPI and Cy3). The size of the cells were measured in pixel and converted to µm according to the instruction of AxioVision 4.5 (Zeiss, Germany).

2.10. Detection of the SOS response by Western blotting

The SOS response was monitored by the cellular amounts of RecA. The

amounts of the RecA protein were measured by Western blotting with anti-RecA antibodies. The strains, SMR7623 (*lexA51(Def)*) and SMR7467 (non-cleavable *lexA3(Ind⁻)*), were used as controls for full and no induction of the SOS response, respectively (Table 2; Pennington & Rosenberg, 2007).

SDS-PAGE and Western Blotting were carried out as previously described (Sambrook & Russel, 2001). The exponentially growing cells equivalent to 1 ml of a suspension at $OD_{600} = 0.25$ were harvested by centrifugation, suspended in 50 μ l of SDS sample buffer and heated at 99°C for 5 min. The total cellular proteins from the cells were appropriately diluted, loaded on 12.5% SDS-polyacrylamide gel and separated by electrophoresis. The resolved proteins were transferred to nitrocellulose membranes (Schleicher & Schuell, Germany) and probed with rabbit anti-RecA antibodies followed by HRP-conjugated anti-rabbit IgG antibodies. Immunoblots were developed with ECL reagents (GE Healthcare, USA), and visualized by LAS4000 Mini luminescence image analyzer (GE Healthcare, USA). The signals were quantified by using Multi Gauge software (Fujifilm, Japan). The linear range for the RecA signals from the SOS-constitutive SMR7623 (*lexA51(Def)*) cells was established by serial dilution, and relative amounts of cellular RecA were determined by comparison with the SOS-induced level in three independent experiments.

2.11. Determination of efficiency for BrdU incorporation into cells

The exponentially growing cells were harvested and suspended in 56/2 medium containing 50 μ g/ml BrdU to obtain OD_{600} of 0.1. The culture was incubated at 37°C, and aliquots were withdrawn in time intervals as indicated in each experiment. Cell growth was terminated by addition of ice-cold 20% sodium azide at a final concentration of 2%. Chromosomal DNA of the cells was extracted with DNeasy Blood & Tissue kit (Qiagen, USA). The purified DNA was quantified with Quan-iT PicoGreen kit using λ DNA as a standard (Invitrogen, USA). DNA was denatured at 99°C for 5 min, chilled on ice for 5 min, and loaded on a positively charged nylon

membrane (Roche, Germany) with the Bio-Dot SF blotting apparatus (Bio-Rad) in duplicate. The amount of BrdU-labeled DNA loaded in each well was 10 ng for eCOMB and 100 ng for 15T⁻; for eCOMB, total DNA amounts at each sample were adjusted to 100 ng with non-labeled chromosomal DNA as the carrier. The membrane filter was incubated with blocking reagent (Roche), and BrdU was detected with the mouse anti-BrdU monoclonal antibody followed by incubation with the HRP-conjugated anti-mouse IgG secondary antibody. Immunoblots were developed with ECL reagents (GE Healthcare) to visualize BrdU-labeled DNA by the LAS-4000 Mini luminescence image analyzer (GE Healthcare). The average BrdU amount in each sample was measured on the same membrane and expressed in arbitrary units (AU), which is a unit to measure the emission amount of chemiluminescence material read using LAS4000 Mini.

2.12. Determination of DNA synthesis rate with radioactive thymidine

Cells were grown from an OD₆₀₀ of 0.02 to 0.3 at 37°C in 56/2 medium with 2 µg/ml thymidine and [¹⁴C] thymidine (0.1 µCi/ml). After rinsing with M9 salts, the cells were added to prewarmed 56/2 medium supplemented with 2 µg/ml thymidine and [³H] thymidine (1.0 µCi/ml) to obtain an OD₆₀₀ of 0.1, and incubation was continued at 37°C. Aliquots (2 ml each) of the culture were taken and quenched at the indicated times by adding 0.4 ml of ice-cold 50% trichloroacetic acid, 0.25 M sodium pyrophosphate. Acid-insoluble materials were collected on GF/C glass-fiber discs (Whatman, UK) by filtration. The discs were washed with 1 M HCl, 0.1 M sodium pyrophosphate followed by an ethanol wash, and then air-dried. Filter-retained radioactivity was measured in an Emulsifier Scintillator Plus (PerkinElmer). Incorporation of [³H] thymidine was normalized to [¹⁴C] thymidine that is indicative of the amount of DNA.

2.13. Determination of *oriC/ter* ratio by quantitative real-time PCR

Chromosomal DNA were extracted from exponentially growing *dnaE*⁺ and *dnaE173* eCOMB cells with DNeasy Blood & Tissue kit (Qiagen, USA) and quantified with Quant-iT PicoGreen kit (Invitrogen, USA). SYBR Green I Master kit was used to amplify and quantify the Cp values of the *mioC* and *tus* regions adjacent to *oriC* and *ter*, respectively with the LightCycler 480 system (Roche). The PCR reaction mixtures (10 μ l) contained chromosomal DNA (5 ng) and a pair of oligonucleotides (5 pmol each): *mioC*-rF1 and *mioC*-rR1 for *mioC*, and *tus*-rF1 and *tus*-rR1 for *tus* (Table 4). The crossing point Cp value of each sample was analyzed with Light Cycler 480 Software (Roche, USA). The resultant Cp ratio of *oriC* and *ter* in *dnaE173* cells was normalized by dividing it by the ratio in the control *dnaE*⁺ cells. Quantification of the *oriC/ter* ratio was carried out for each sample in triplicate. Quantitative PCR was performed as shown below.

Program	Target (°C)	Acquisition Mode	Time	Ramp Rate (°C/s)
Step 1 (pre-incubation)	95	None	5 min	4.40
Step 2 (Amplification with 45 cycles)	95	None	10 sec	4.40
	60	None	10 sec	2.20
	72	Single	10 sec	4.40
Step 3 (Melting curves)	95	None	5 sec	4.40
	65	None	1 min	2.20
	97	Continuous		0.11
Step 4 (Cooling)	40	None	30 sec	2.20

3. Results

3.1. Construction of the novel thymidine-requiring eCOMB strain for DNA combing

The molecular combing has been known as a powerful technique to investigate dynamics of replication forks *in vivo*. Since the labeled DNA is stretched on a glass surface and visualized under a microscope in the method, the field of view restricts the measurable DNA length below 300 kb. Due to this limitation, pulse-labeling for *E. coli* cells with the analogs needs to be done in less than 6 min based on the average rate of DNA synthesis of 800 nt/s. In an earlier report, thymidine-auxotroph derivatives of the wild-type K12 strains were not satisfactory for BrdU incorporation (Breier *et al.*, 2005). Thus, The DNA combing has not been successfully applied to DNA replication of *E. coli* due to the low efficiency of thymidine-analogs incorporation into the cells. To overcome this difficulty, I constructed a novel *E. coli* strain, eCOMB (*E. coli* for combing), which incorporates BrdU with a dramatically enhanced efficiency.

In *E. coli* cells, dTMP (deoxythymidine monophosphate) is synthesized *de novo* by the conversion of dUMP (deoxyuridine monophosphate) to dTMP that catalyzed by thymidylate synthetase (encoded by *thyA*). An *E. coli* cell lacking thymidylate synthase (Δ *thyA*) loses the *de novo* synthesis of dTMP but converts thymidine supplied in a medium to dTMP by thymidine kinase (encoded by *tdk*) using the pyrimidine salvage pathway (Kornberg & Baker, 1992; Ahmad *et al.*, 1998). The halogen analogs of thymidine follow the same salvage route as thymidine for incorporation. I anticipated that two genetic determinants, *deoCAB* and *yjjG*, would affect incorporation of the analog in *thyA*-deleted MG1655 (MK7158; Table 2). *deoCAB* functions in thymidine catabolism (Ahmad *et al.*, 1998) and *yjjG* prevents incorporation of non-canonical pyrimidine nucleosides (Titz *et al.*, 2007) (Fig. 5). Thymidine supplied in the medium is converted to thymine that catalyzed by thymidine phosphorylase (encoded by *deoA*) (Ahmad *et al.*, 1998). The *yjjG* gene was known as a

3.2. High efficiency of thymidine-analogs incorporation into eCOMB cells

The 15T⁻ strain (*E. coli thyA42 deoB20*) was a thymidine-requiring strain that showed an efficient incorporation of thymidine-analogs and has been used to study in DNA synthesis for several decades (Roepke *et al.*, 1944). However, it was not an *E. coli* K-12 strain. Even with the strain, BrdU-labeled DNA was only observed with the DNA combing method in cells incubated in medium containing BrdU in 10-15 min (Breier *et al.*, 2005). The efficiency of thymidine-analogs incorporation was compared between 15T⁻ and eCOMB cells. Both exponentially growing cells were incubated at 37 °C in 56/2 medium containing 50 µg/ml BrdU and collected in 5-min intervals for 15 min. The BrdU signals (AU; arbitrary unit) were normalized to the loaded DNA samples (ng) and plotted at the indicated labeling times. The slope value of linear regression of the eCOMB and the 15T⁻ cells were 2.50 and 0.14, respectively (Fig. 6A). From these slope values, the eCOMB cells showed a much higher ability of BrdU incorporation (17.4 folds) than the 15T⁻ strain (Fig. 6B). These results indicate that eCOMB incorporated thymidine as well as thymidine-analogs with a sharply enhanced efficiency compared to 15T⁻. The dramatically increased efficiency of the thymidine-analog enabled us to successfully apply the DNA combing method to *E. coli* as described below.

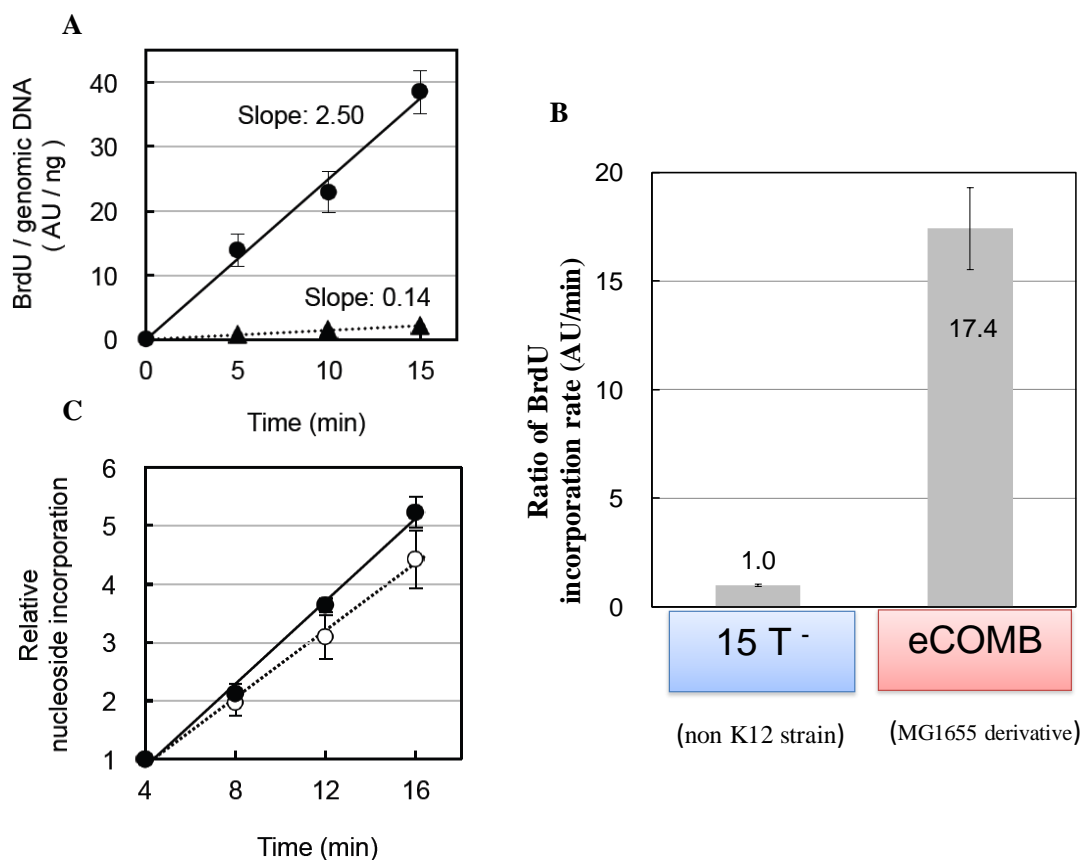


Figure 6. The efficient incorporation of thymidine-analogs into eCOMB cells.

(A) BrdU incorporation into genomic DNA. BrdU signals in genomic DNA at each time point were determined as described in Materials and Methods. The slope values of the eCOMB (close circles) and 15T⁻ strains (open circles) were respectively estimated with the linear regressions. (B) The BrdU incorporation rate. A ratio of BrdU incorporation between two strains was calculated from the slope value of the linear regression line of (A). (C) Comparable incorporation of BrdU and thymidine into eCOMB cells. The eCOMB cells were grown in 56/2 medium containing either BrdU (close circles) or [³H] thymidine (open circles). In the case of [³H] thymidine, the cells were pre-labeled with [¹⁴C] thymidine. BrdU signals and radioactivities of ³H and ¹⁴C were measured as in Materials and Methods. The values at the indicated time points were plotted on the graph. The mean values and the standard error of the mean (SEM) were collected from three independent experiments.

3.3. A rate of DNA synthesis in the presence of BrdU.

Although it is known that halogenated thymidine analogs are toxic to living cells, BrdU or the other modified nucleotides has been used in both prokaryotes and eukaryotes to visualize the newly synthesized DNA without knowing its effects on DNA chain elongation. To examine if thymidine analogs affects DNA replication of eCOMB cells, I compared the initial rate of BrdU incorporation with that of [³H] thymidine into eCOMB cells. In the Fig. 6B, the exponentially growing eCOMB cells were incubated in the medium containing either 50 µg/ml BrdU or 1.0 µCi/ml [³H] thymidine, and then the labeled cells were collected in 4 min intervals up to 16 min. Since the slope of the linear regression line for BrdU was almost the same as that for [³H] thymidine, the initial rate of BrdU did not show any significant inhibition to a rate of DNA replication of eCOMB cells (Fig. 6C). Moreover, the cells were not elongated for up to 30 min incubation under this condition (data not shown). These data indicate that there are neither obvious stresses on cell growth nor an apparent inhibitory effect on DNA chain elongation when eCOMB cells were growth with the halogen thymidine analogs at least for 16 min. Together with measurements of the physiology of eCOMB cells below, I concluded that the normal replication fork speed could be measured with the eCOMB cells grown in the presence of thymidine analogs.

3.4. Physiological characteristics of eCOMB cells

The eCOMB cells lacks 7 genes having unknown functions by deletion of the 12-kb chromosomal region in addition to *thyA*, *yjjG* and *deoCAB*. It is not clear if the deletion affect cell growth. Thus, the physiological characteristics of eCOMB were carefully analyzed for further applications. The eCOMB cells can grow in the minimal 56/2 medium containing thymidine at a low concentration (2 µg/ml) at 37°C. As shown in Fig. 7A, B and C, the cell shapes, nucleoid structures and generation times of eCOMB cells in the medium containing 2µg/ml of thymidine were similar to those of the wild-type MG1655 cells. Furthermore, eCOMB cells did not show induction of

the SOS response in the 56/2 medium containing 50 $\mu\text{g/ml}$ of IdU at 37°C for 6 min (Fig. 7D). These results indicate that the novel eCOMB cells showed no significant difference in physiological characteristics as compared with those of the wild-type MG1655 cells.

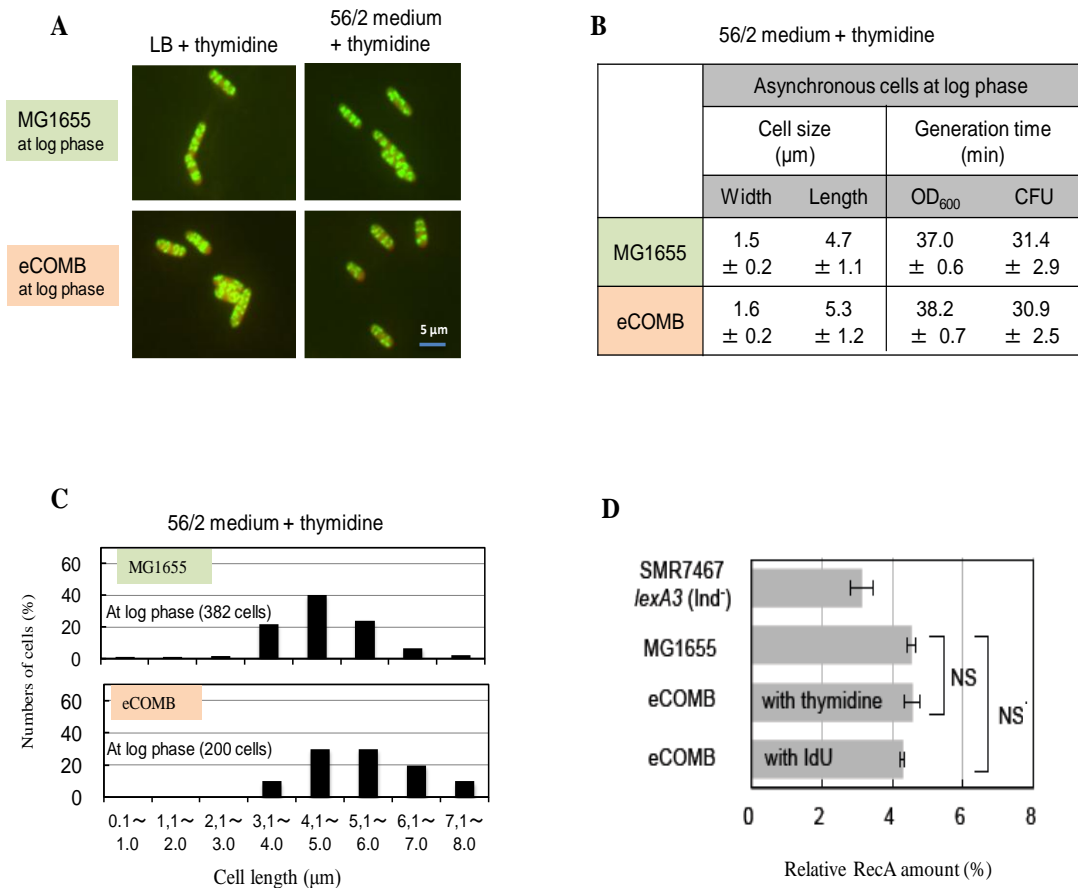


Figure 7. Comparison of physiological characteristics between MG1655 and eCOMB cells. MG1655 and eCOMB cells were exponentially grown in the 56/2 or LB medium containing 2 $\mu\text{g/ml}$ thymidine at 37°C. The mean values and their SEM are determined by three independent experiments. (A-C) The cells were fixed with paraformaldehyde, stained with FM4-64 (for staining membrane), DAPI (for staining nucleoid) and observed under a fluorescent microscope. (A) Cell shape and nucleoid structures. Cells were observed under a fluorescent microscope with 100x objectives, and the representative images of the stained cells are shown. Membrane and nucleoids were stained in red and green, respectively. The bar represents 5 μm . (B) Cell sizes and the generation

time. Width and length of MG1655 and eCOMB were measured with 382 and 200 cells, respectively. The average generation time was determined with OD₆₀₀ values and colony forming units (CFU) from 3 independent experiments. For CFU values, the cells were grown on LB agar plates containing 2µg/ml thymidine at 37°C for overnight. The average value and the standard deviation are shown for the cell sizes and the generation time. (C) The size distributions of the cell length. The length of exponentially growing cells was measured with 382 cells of MG1655 (upper) and 200 cells of eCOMB (lower). (D) Determination of the SOS response. The cells were grown in 56/2 medium containing 50µg/ml thymidine or IdU for 6 min. The bar graph shows the amount of RecA protein relative to that of the fully SOS-induced SMR7623 (*lexA51*) as described in Materials and Methods. The mean values and SEM were determined from three independent experiments. NS; not significant by p values (>0.05) of the two-tailed Student's t-test.

3.5. Calibration of DNA length with λ DNA as a standard for DNA combing.

To establish the coefficient value to convert the actual size of DNA in µm to kb, I measured length of 48.5-kb λ DNA with the DNA combing. Fig. 8A shows the representative picture of combed λ DNA on glass. In this experiment, 2 µg of λ DNA was stained by YOYO-1 and added to 0.5 M MES buffer (pH 5.5). The DNA was stretched on a glass surface by the DNA combing procedure and visualized under a fluorescent microscope with 63x objective and appropriate filters. The pixel length of individual λ DNA molecules was measured and converted to µm according to the manual of the microscope (Zeiss). A histogram was created with frequency of the DNA length in µm for 214 DNA molecules (Fig. 8B). Using the combing condition, the actual length of λ DNA (48.5 kb) was determined to be 21 µm from the mode value of the histogram. Thus, the coefficient value was 2.3 kb/µm. According to the known cryptographic length of one base pair, 3.4 Å (Saenger, 1984), the length of λ DNA is 16.5 µm. This shows that λ DNA was extended by 1.3 fold on a glass surface under our combing conditions. These values were close to those in the original report of the DNA combing method (Herrick & Bensimon, 1999) in which λ DNA were straightened by 1.5 fold, and the coefficient value was 2 kb/µm.

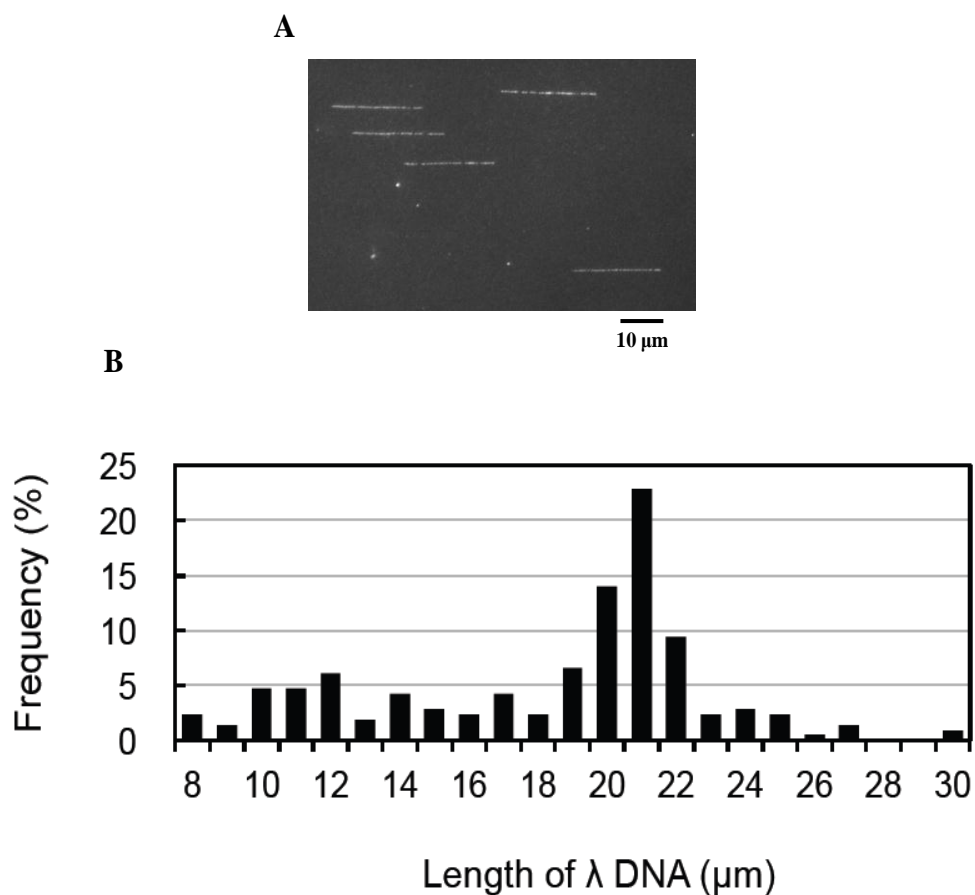


Figure 8. DNA combing with λ DNA. (A) A typical image of λ DNA on glass surface. DNA was stretched on the glass surface, attained with YOYO1 and visualized using a fluorescent microscope with 63X objectives. The black bar represents 10 μm . (B) Distribution of combed λ DNA length (Size distribution of 48.5-kb λ DNA). The relative numbers of DNA molecules (%) are presented as a histogram of lengths. Under our experimental conditions, the length of λ DNA was 21 μm from the peak value among 214 observed molecules.

3.6. DNA combing with the chromosomal DNA extracted from eCOMB cells

For the DNA combing method, chromosomal DNA is extracted from cells, and purity of the extracted DNA is also critical (Herrick & Bensimon, 1999). Moreover, the size of the extracted DNA should be as long as possible, since the DNA length synthesized in *E. coli* cells is about 100-250 kb in 4 min based on the very high rate of *E. coli* DNA synthesis (500–900 nt/s) (Chandler *et al.*, 1975; Khodursky *et al.*, 2000; Breier *et al.*, 2005; Waldminghaus *et al.*, 2012; Atkinson *et al.*, 2011). To achieve these, the chromosomal DNA of the labeled cells was carefully extracted from the cells embedded in an agarose plug by a step-by-step manner as described in Materials and Methods. The chromosomal DNA were extracted from eCOMB cells and stretched on a glass surface as shown in Fig. 9A. The density of the DNA molecules on the glass was very high. In addition, the combed DNA molecules were almost uniformly aligned on the glass surface. However, the DNA solution should be diluted and used for DNA combing to get a good resolution of individual molecules for measurement of DNA length. Using the diluted chromosomal DNA solution, the percentage of molecules having DNA length larger than 300 kb (over the vision of microscope with 63x objectives) were about 20% (Fig. 9B) whereas the length of the shorter molecules evenly distributed in a range from 50 to 300 kb without obvious bias (Fig. 9C). Moreover, there are no significant differences in length between DNA molecules labeled in 2 min (green bars) and 3 min (red bars) with IdU. These results indicate that a large size of the chromosomal DNA of eCOMB cells was successfully observed with the DNA combing method, and that labeling of the cells with the thymidine analog did not affect on the quality of the combed DNA.

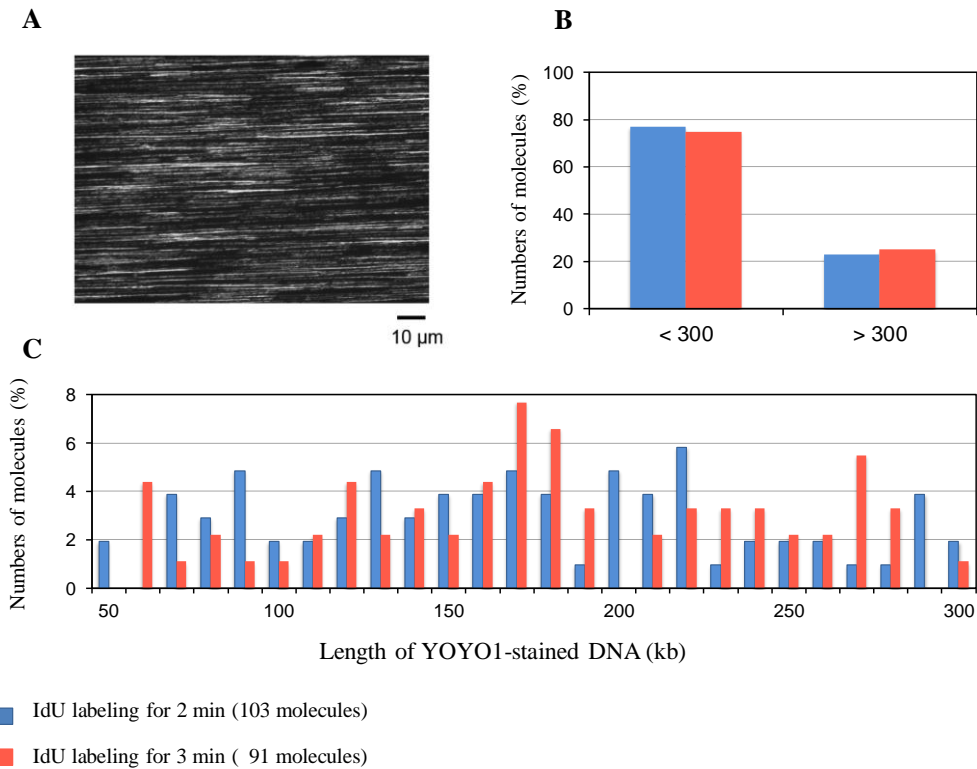


Figure 9. DNA combing with the chromosomal DNA extracted from eCOMB cells. (A) A representative image of the combed chromosomal DNA. The chromosomal DNA were extracted from eCOMB cells, stained with YOYO-1, stretched on a glass surface and visualized under a fluorescent microscope with 63x objectives. (B, C) The length of the chromosomal DNA on a glass surface. The length of the DNA molecules were measured in pixel and converted to kb. The length distribution of the DNA molecules is presented in a histogram. The blue and red bars represent the chromosomal DNA that were extracted from the cells labeled with IdU in 2 min (103 molecules) and 3 min (91 molecules), respectively. DNA molecules larger than the field of view under a fluorescent microscope were showed as the molecules larger than 300 kb in (B). The size distribution of DNA molecules smaller than 300 kb was shown in (C).

3.7. Determination of replication fork speed in asynchronous eCOMB cells

In my combing experiments, the exponentially growing eCOMB cells were sequentially pulse-labeled with CldU for 2 min followed by IdU for 2 min. The schematic outline of the experiments is shown in Fig. 10A. The first labeling with CldU serves to mark the ongoing forks, while the second labeling with IdU to analyze the replication fork speed. The labeled chromosomal DNA was extracted from eCOMB cells, stretched on a glass surface, and then detected by specific antibodies followed by observation under a fluorescent microscope (Fig. 10B). About one-thirds of the DNA fibers were the dual-labeled molecules. For determination of the fork speed, I selected the molecules having an IdU track lined up with a CldU track end-to-end among the dual-labeled DNA fibers, which ensures that the IdU-labeled DNA chain is synthesized at the single replication fork underway throughout the labeling time with IdU. The labeling patterns of both CldU and IdU were sparse probably due to incomplete denaturation of dsDNA; the antibodies react with the thymidine analogs on ssDNA. To estimate the speed of individual replication forks with the IdU tracks adjacent to the CldU tracks, a distance (μm) between the first and the last green dots adjacent to the red track was measured for each DNA fiber. The measured lengths in pixel were converted to kb using the coefficient value established with λ DNA (2.3 kb/ μm), and then divided by the indicated labeling time to determine the fork speed.

Figure 11A shows a speed histogram constructed with 667 individual replication forks collected from three independent labeling experiments. The measured DNA lengths of the IdU tracks were in a range between 30 and 180 kb with mean of about 77 kb. There was no such distribution in DNA length of entire DNA molecules stained with YOYO-1 on glass slides (Fig. 9C). The distribution profile of individual replication forks displayed a single peak with a mean of 644 nt/s (Fig. 11A); the 95% confident interval of the mean was 632-656 nt/s by bootstrap analysis (Fig. 11B and D). In this combing system, the eCOMB strain has shown no significant

difference in physiological characteristics compare to wild type MG1655 strain (Fig. 6). In addition, the thymidine analogs did not obviously affect to the DNA elongation up to 16 min (Fig. 7C), and the eCOMB cells were not induced SOS response in 6 min labeling (Fig. 6D) or elongated cell shape up to 30 min of incubation (data not shown). These results indicated that the estimated replication fork speed in eCOMB cells with this DNA combing system represents the normal speed of individual replication forks in *E. coli* cells.

Two-thirds of the replication forks moved within a relatively narrow speed range, 550-750 nt/s, indicating a rather uniform nature of fork speed *in vivo* (Fig. 11A). These observations are consistent with the fork speed previously estimated by analyses of bulk DNA synthesis in *E. coli* cells, although such bulk analyses provided only an average speed of replication forks. However, our single-molecule analysis revealed the presence of replication forks moving much slower or faster than the major population. The frequency of those replication forks was 14% and 12% within a speed range of 250-450 and 850-1250 nt/s, respectively. Assuming that the speed distribution of a homogeneous replisome population follows a single Gaussian curve (Tanner *et al.*, 2008; Yao *et al.*, 2009), the distribution of total molecules in Figure 11A fits to a mixture of three Gaussian curves that are purple, brown, and green lines with means of 553, 638 and 782 nt/s and mixing proportion of 34%, 42% and 24% respectively (Fig. 11C), suggesting multiple sub-populations of replication forks in the cell.

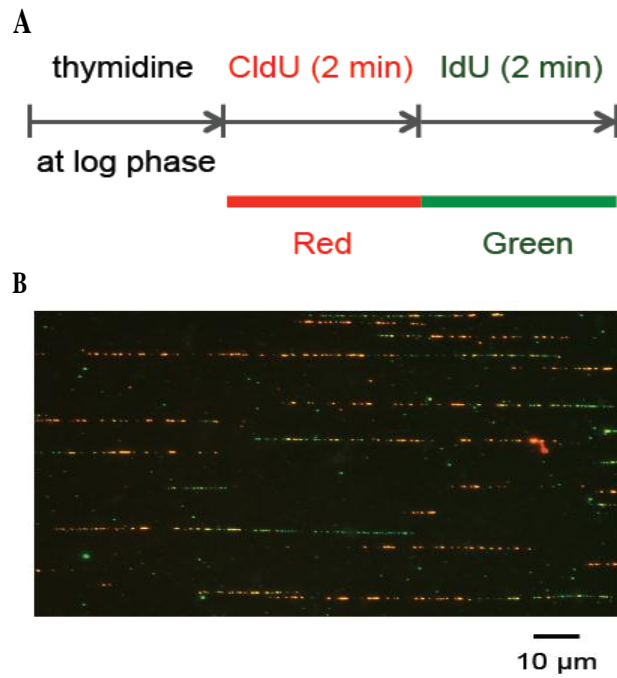


Figure 10. DNA combing with the chromosomal DNA extracted pulse-labeled eCOMB cells for fork speed determination. (A) The experimental diagram of DNA double-labeling. The eCOMB cells were pulse-labeled with CldU (red) for 2 min and sequentially labeled with IdU (green) for 2 min. (B) A representative image of combed DNA fibers. The representative picture of double labeled DNA. CldU and IdU on the labeled DNA were detected with anti-BrdU antibodies followed by fluorescent dye-conjugated secondary antibodies, and observed under a fluorescent microscope with 63X objectives. The black bar represents 10 μ m.

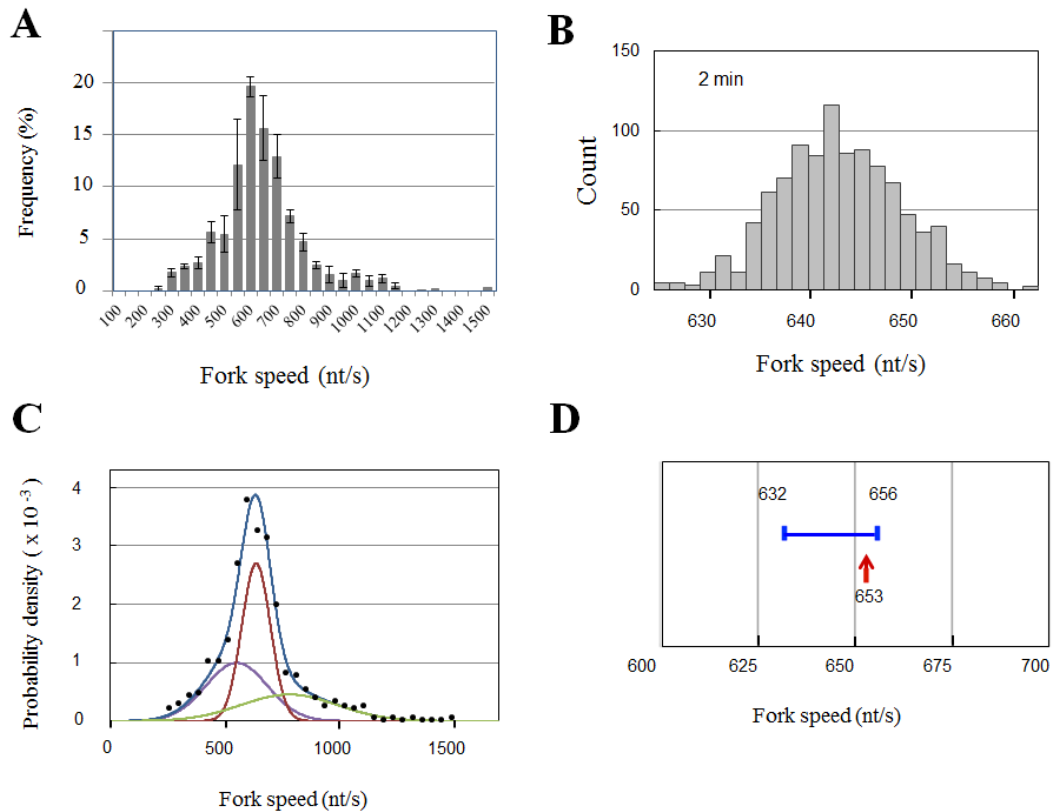


Figure 11. Distribution of replication fork speed in eCOMB cells. (A) Distribution of fork speed. Fork speed was calculated from the length of IdU tracks in combed CldU-IdU DNA. Error bars are the SEM from three independent experiments used to plot the histogram. The total DNA fibers analyzed were 667 molecules. The frequency of the replication fork at speeds ranging from 550 to 750 nt/s was 58.9%. (B) Histogram of bootstrap samples of the average fork speed. The samples were computed from the data in Fig. 11C by the bootstrap algorithm ($n=1000$) to determine the confidence interval for the average fork speed. (C) Fitting of the mixed Gaussian curve to the fork speed distribution. The fork speed distribution in (A) was converted to probability density (closed circles), and then the number of Gaussians was determined by using Akaike's Information Criteria. The data were fit best to the mixed Gaussian distribution (blue line) consisting of three Gaussian curves that are purple, brown, and green lines with means of 553, 638 and 782 nt/s and mixing proportion of 34%, 42% and 24% respectively. (D) Comparison of the average fork speed. The confidence interval for the average fork speed shown in Fig. 11C was determined from the distribution in (A). The blue line represents the confidence value (632-656 nt/s) in (D). The red arrow represents the accurate fork speed (653 nt/s) determined by the time-course experiments shown in Figure 13.

3.8. Accurate determination of the replication fork speed in *E. coli*

In the labeling experiments for DNA replication in eukaryotes (Petermann *et al.*, 2006; Sugimura *et al.*, 2008), the delay of nucleotide incorporation in to cells does not significantly affect on analysis of the slow fork speed (about 50 nt/s) since the cells are pulse-labeled with the thymidine analogs for 15-30 min. However, the time delay could be a significant fraction of the labeling time in determining the fast fork speed (about 800 nt/s) in *E. coli* because the cells must be pulse-labeled only for a few minutes. To verify the fork speed determined by the DNA-combing method shown in Figure 11A, we examined two types of time delays that could affect the value due to the very short labeling time: lag in import of IdU (including the time lag during medium change in the sequential labeling) and conversion of IdU to IdUTP that could underestimate the fork speed.

To obtain better time resolution, newly synthesized DNA in eCOMB cells was labeled in 1-min intervals for 4 min after CldU-labeling for 2 min to achieve higher time resolution (Fig. 12A), and the lengths of IdU-labeled DNA molecules recovered at each time point were measured (Fig. 12B). A net increase in the DNA length was proportional to the pulse-labeling time (Fig. 12C). To remove negative effects of outliers in the dataset, the median length at each time point was plotted as a function of time and analyzed by linear regression in three independent experiments (Fig. 13). The straight lines through the origin clearly indicate that the time delay in import and conversion of IdU was negligible. The chain elongation rate was determined from three slope values to eliminate the possibility of underestimation due to degradation of IdU-labeled DNA during DNA preparation in the DNA-combing procedures. The coefficients of the linear regression indicated a very high reliability in each slope determination. The three slope values were very close, and an accurate average fork speed in *E. coli* cells growing at 37°C was accurately calculated to be 653 ± 9 nt/s (\pm standard error of the mean) (Fig. 13D). The fork speed fell within the 95% confidence interval of the average fork speed shown in Fig. 11B. These show that in the

measurement of the fork speed, the time delay in IdU incorporation and degradation of IdU-labeled DNA during DNA preparation were negligible

The distributions of fork speed at each time point were shown in Fig. 12D. The median speed values were 660, 654, 660, and 667 nt/s at 1, 2, 3 and 4 min of labeling with IdU, respectively. In addition, the histogram also showed that about two-thirds (about 60%) of the replication forks were in the range of 550-750 nt/s in all time point samples (blue bars). This data was consistent with the analysis of replication fork distribution in Fig. 11A. Although the distributions of fork speed in 3 and 4 min IdU – labeling samples were a little wider than 1 and 2 min with a slight increase of the slower sub-population, overall profiles of the distribution at each time point were almost the same. Therefore, it seems likely that individual replication forks continued to proceed with a constant fork speed at least within 200-kb DNA segments replicated in 4 min.

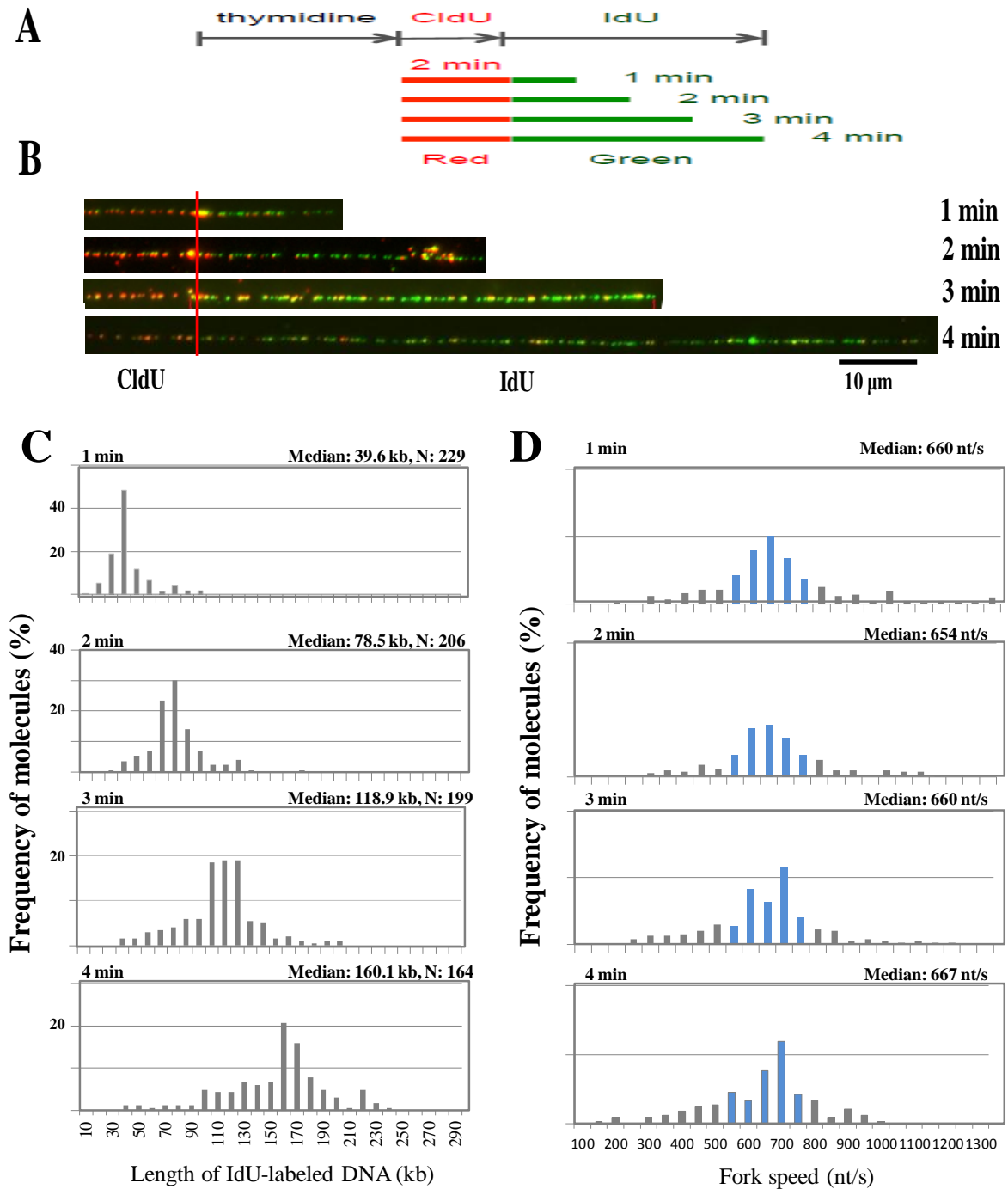


Figure 12. Time-dependent progression of the replication fork in eCOMB cells. (A) Diagram of DNA labeling in a time-course manner. The eCOMB cells were pulse-labeled with CldU (red) for 2 min followed by labeling with IdU (green) for 1-4 min. (B) A representative images of the DNA molecules at each time point. The black bar represents 10 μm . (C) Distribution of IdU-labeled chromosomal DNA length in a time-course experiment. The double-labeled DNA was extracted from cells collected at each time point and was subjected to DNA combing. The IdU-track lengths in the CldU-IdU labeled molecules were measured and shown in a histogram. Median values and number of DNA molecules observed (N) are shown above each panel. (D) Distribution of fork speed. Fork speeds were calculated from the DNA length at each time point in (C), and the median values are shown above each panel. Replication forks at speed within the range of 550 to 750 nt/s (blue bars) were about 66, 68, 67, and 64% at 1, 2, 3, and 4 min, respectively.

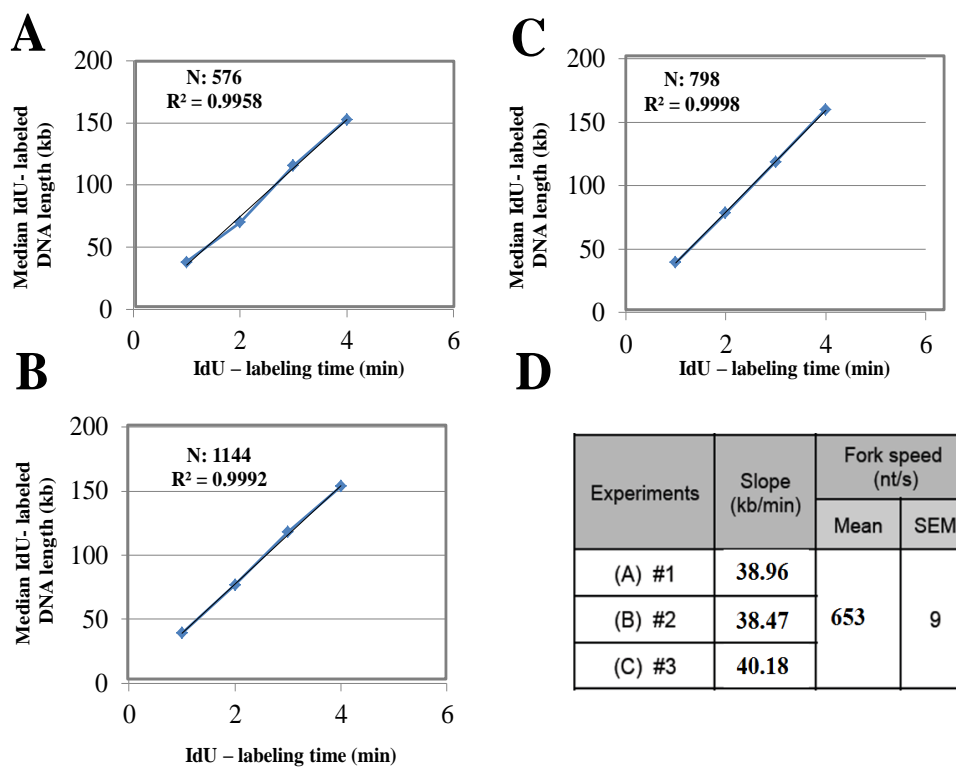


Figure 13. Accurate determination of replication fork speed. The eCOMB cells were pulse-labeled with CldU for 2 min followed by labeling with IdU for 1-min intervals up to 4 min in triplicate. The results of experiments #1, #2, and #3 were shown in (A), (B), and (C) respectively. Median value of IdU-labeled chromosomal DNA length is plotted at each time point. The numbers (N) represent the total DNA fibers observed in each experiment. The broken lines and R^2 values are the linear regression lines by the least square method and their correlation coefficient of determination, respectively. (D) Determination of fork speed. The mean speed and SEM were calculated from the three slope values of (A), (B), and (C). The total DNA fibers observed were 2518 molecules.

3.9. Replication fork speed in synchronized eCOMB cells

The speed of the fork progressing on a random location of the chromosome was accurately determined with asynchronous eCOMB cells above. Next, I show the determination of the fork speed with the cells synchronized for the cell cycle. DL-serine hydroxamate inhibits the initiation but not chain elongation of DNA replication by amino acid starvation (Ferullo *et al.*, 2009). The eCOMB cells were incubated in the medium containing thymidine and the drug before pulse-labeling with thymidine analogs. After 90 min, the drug was removed from the cell culture by washing the cells with M9 salts buffer, and thereby the cells started the cell cycle. Then, the eCOMB cells were sequentially pulse-labeled with CldU for 2 min and IdU for 2 min and 3 min. The number of the dual labeled molecules was increased in the synchronous cells (about 60%) compared to that in the asynchronous cells (about 30%). The length of IdU-labeled tracks in the dual-labeled molecules was measured as above. As shown in Fig. 14A, the mode lengths of the DNA labeled in 2 min (green bars) and 3 min (red bars) were 70 kb and 110 kb, respectively. Each distribution of the length was unimodal similarly to that with asynchronous cells. To eliminate the time lag during medium change or the delay in IdU incorporation, the mode DNA length of the 2-min samples was subtracted from that of the 3-min samples. The resultant value was used to calculate the fork speed. In this case, the mean fork speed was 560 ± 100 nt/s (\pm SEM) from three independent experiments (Fig. 14B). Thus it seems likely that the fork speed at a region near *oriC* was almost the same as that at a random genomic location (Fig. 13-D, 653 ± 9 nt/s). However, in an experiment to determine the *oriC/ter* ratio (representing the average number of replication forks in the cells) by quantitative real-time PCR, we found that the eCOMB cells were incompletely synchronized with DL-serine hydroxamate since the *oriC/ter* ratios were not significantly changed after releasing the cells (data not shown). Because of this reason, I used the exponentially growing cells in the pulse-labeling step of the DNA combing method for further analysis of the fork speed in *E. coli* cells.

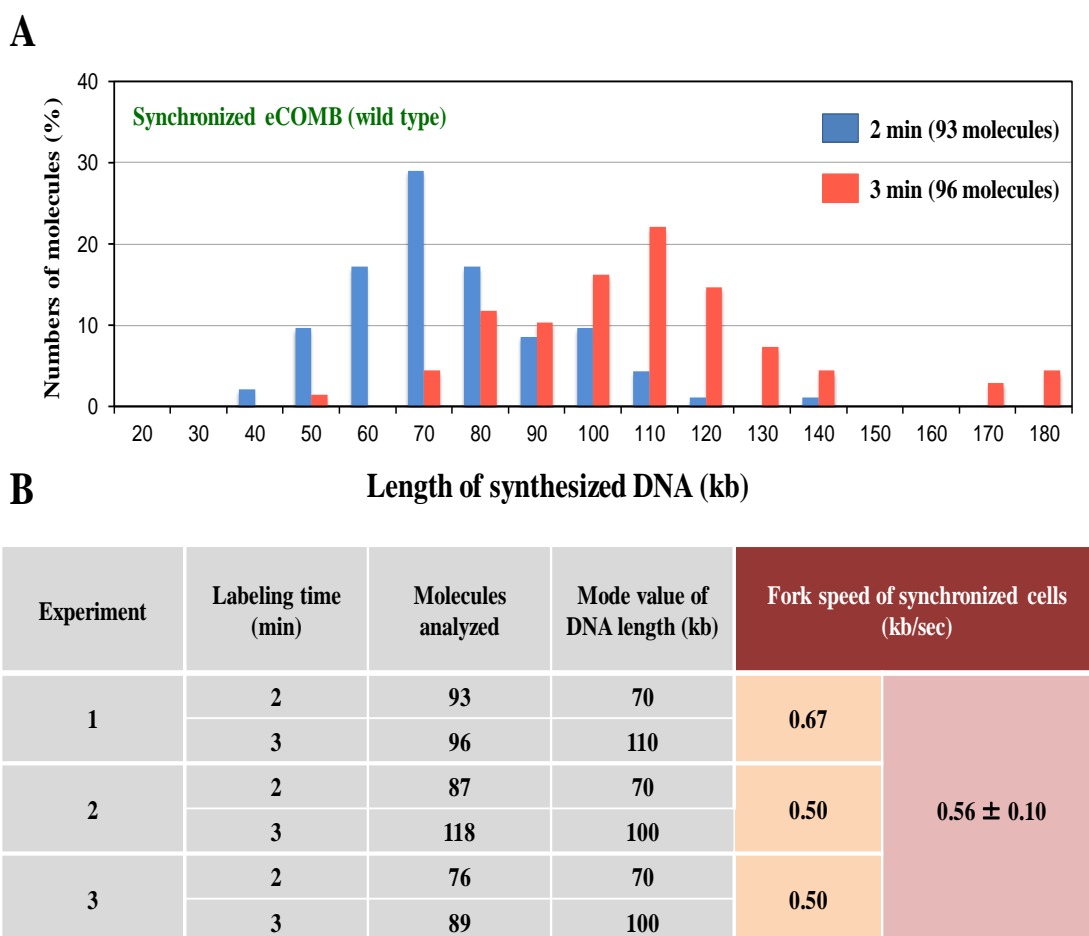


Figure 14. Replication fork speed with the synchronized eCOMB cells. (A) Length distribution of the newly synthesized DNA in 2-min and 3-min labeling with IdU. The exponentially growing eCOMB cells were incubated in 56/2 medium containing DL-serine hydroxamate to final 1 mg/ml at 37°C for 90 min. After releasing from the cell cycle block, the cells were labeled sequentially with CldU for 2 min and IdU for either 2 min or 3 min. The numbers of the observed molecules were 93 for the 2-min sample (green bars) and 96 for the 3-min sample (red bars). The mode value of each time point was used to calculate the fork speed. (B) The fork speed in the synchronized cells. The mode DNA length of the 2-min sample was subtracted from that of the 3-min samples, and the resulted value was divided by 60 seconds. The fork speed of 0.56 ± 0.1 kb/s were a mean and SEM from three independent experiments.

3.10. A reduced rate of replication fork progression in *dnaE173* cells

Since the unwinding rate of DnaB helicase is much slower than the chain elongation rate of Pol III (Kim *et al.*, 1996; Sugaya *et al.*, 2002), it has been postulated that the leading strand synthesis catalyzed by Pol III could be a pacemaker that controls replication fork progression (Patel *et al.*, 2011). However, no direct evidence for this hypothesis has been provided because it was difficult to accurately measure the fork speed in *E. coli* cells. To verify the possibility, the speed of individual replication forks in the *dnaE173* mutant cells were measured with the DNA combing method and compared to that in the wild-type cells as follows.

Pol III is composed of three sub-assemblies: Pol III core (a heterotrimer of α , ϵ , and θ subunits), the DnaX clamp-loading complex, and the sliding β clamp (Maki and Furukohri, 2013). The *dnaE* gene encodes the catalytic α -subunit of Pol III holoenzyme (Maki *et al.*, 1985). Maki and his colleagues previously isolated a *dnaE173* mutant strain that produces an altered Pol III (*dnaE173*-Pol III) with the reduced rate of DNA chain elongation (300 nt/s) compared to the wild-type Pol III holoenzyme *in vitro* (900 nt/s) (Maki *et al.*, 1991; Sugaya *et al.*, 2002; Yanagihara *et al.*, 2007). If the Pol III holoenzyme is a pacemaker for the replication fork to move, the fork speed in the *dnaE173* cells should be close to one-third of that in the control cells. As shown in Figures 15A and B, this is indeed the case.

Two derivatives of the eCOMB strain, *dnaE173 Tn10* eCOMB (MK7928) and *dnaE⁺ Tn10* eCOMB (MK7927) as a control, were constructed by P1 phage transduction (Table 2) and analyzed for their fork speeds at 37°C by the DNA-combing method. The distribution of the fork speed was determined with the eCOMB cells pulse-labeled with IdU for 2 min (Fig. 15A). The fork speed distribution in the control *dnaE⁺*eCOMB cells were the almost same as that shown in Fig. 11A; 73% of forks moved at a rate ranging 550-750 nt/s (blue bars in the upper panel). In contrast, 88% of the replication forks in the *dnaE173* eCOMB cells progressed at a lower range of 200-400 nt/s (blue bars in the lower panel), although the speed distributions in both cells

showed a single peak. These results clearly indicate that the speed of the majority of the forks in the mutant cells was greatly shifted to the slower side compared to that in the control cells. The mean fork speed determined from data obtained by three independent time-course experiments was 264 ± 9 nt/s in the *dnaE173* cells and 657 ± 10 nt/s in the *dnaE*⁺ cells (Fig. 15B) so that the fork in the former cells proceeds at 40% of the speed in the latter cells. The relative reduction in the fork speed is close to the one (33%) expected based on the slow chain-elongation rate of the *dnaE173* Pol III holoenzyme. Therefore, we concluded that the speed of the replication fork in the *dnaE173* cells was reduced almost proportionally to the slow velocity of DNA chain elongation by the *dnaE173*-Pol III holoenzyme. Although there seems to be several other factors affecting fork speed, it becomes clear that the rate of DNA chain elongation by Pol III is a major determinant for the speed of the replication fork in *E. coli* cells.

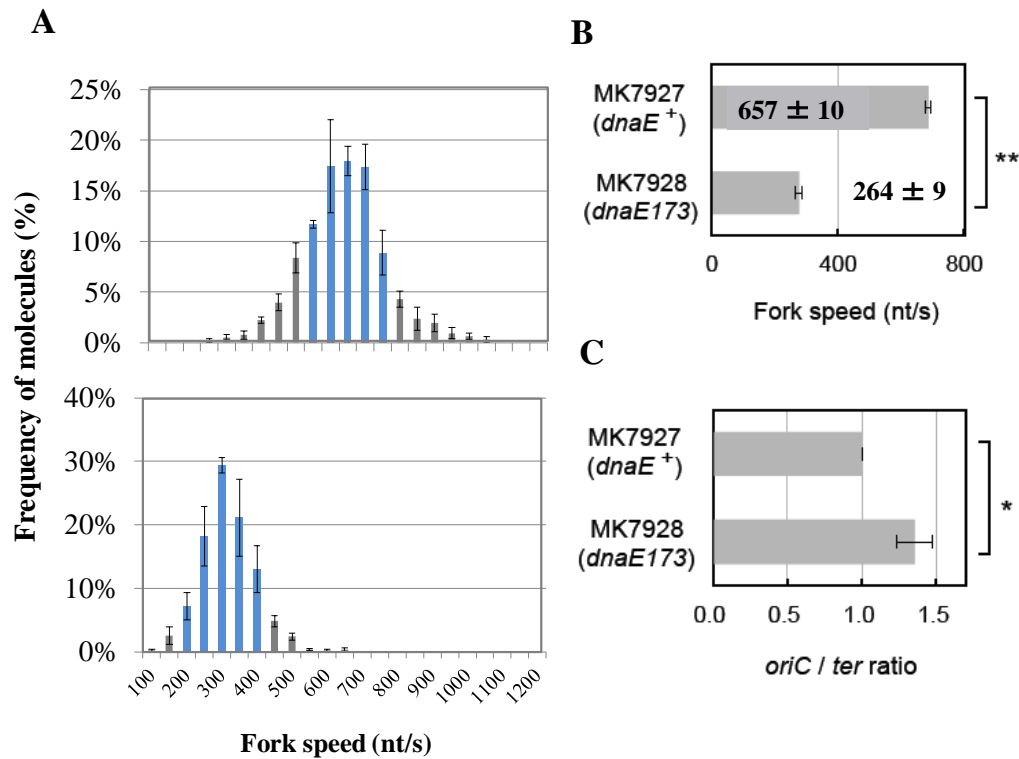


Figure 15. Analysis of DNA replication forks in *dnaE173* eCOMB cells.

(A) The distribution of replication fork speed. The fork speed distribution of MK7927 (eCOMB *zea-502::Tn10*) and MK7928 (eCOMB *dnaE173 zea-502::Tn10*) were determined as described in Fig. 11A, and shown in the upper and lower panels, respectively. The error bars are SEM from three independent experiments. (B) The average fork speed. The fork speed of MK7927 and MK7928 were determined with the time-course experiments as shown in Fig. 13. The mean of fork speed and SEM were collected from three independent experiments. (C) Comparison of *oriC/ter* ratios. The *oriC/ter* ratio of the exponentially growing MK7928 cells were determined by quantitative real-time PCR and normalized to that of MK7927. The ratio represents the average numbers of replication forks on the chromosomal DNA. Error bars are SEM from three independent experiments. The asterisks indicate the *p* values from the Student's *t*-test (one asterisk, <0.05; two asterisks, <0.005).

3.11. An increased number of the replication forks in the *dnaE173* cells

Despite having reduced fork speed, the *dnaE173* eCOMB cells grew normally at 37°C with the same average cell mass and doubling time as the *dnaE*⁺ eCOMB cells (Fig. 16A & B). Moreover, the rate of DNA synthesis measured by incorporation of [³H] thymidine in the *dnaE173* cells was exactly the same as that in the control *dnaE*⁺ cells (Fig. 16C). A similar result was obtained with BrdU (Fig. 16D), which excludes the possibility that the *dnaE173* eCOMB cells exhibited a reduction in fork speed with halogen analogs, but not net DNA synthesis with thymidine. Therefore, *E. coli* cells maintain the rate of bulk DNA synthesis and the resulting cell-division cycle at a certain level when the fork speed is reduced. These results raised a question how the *dnaE173* cells having the slow replication forks maintain the normal rate of the net DNA synthesis.

In a Δrep mutant of *E. coli* cells, the speed of replication fork movement was reduced by about 50%, and the *oriC/ter* ratio of the replication forks was increased to more than 2 folds than that in the wild-type cells (Lane & Denhardt, 1974). The *oriC/ter* ratio is the DNA ratio of *oriC* (the replication origin) relative to *ter* (terminus of chromosomal DNA replication) and represents the number of the replication fork on the chromosome. In eukaryotic cells, the Chk1-deficient cells showed a 30% reduction of fork speed and a 1.4-fold increase in the number of fired origin (Petermann *et al.*, 2010). It seems that there is a causal relationship between speed and number of the replication fork. Therefore, I analyzed the number of the replication fork in the *dnaE173* mutant cells. Using quantitative real-time PCR, I found that the *oriC/ter* ratio in the *dnaE173* cells was enhanced by 1.4-fold compared to that in the *dnaE*⁺ cells (Fig. 15C). Although it is not clear that the 1.4-fold increase in the number of the replication forks can singly complement the 60% reduction of the fork speed to full extent, at least the more multi-forked chromosome contributes to maintain the overall DNA synthesis in *dnaE173* mutant cells.

The higher *oriC/ter* ratio in the *dnaE173* cells than the control *dnaE*⁺ cells

may be caused by an overlap in successive rounds of the cell cycle or by more frequent initiation of DNA replication. In rapidly growing *E. coli* cells, the number of the replication forks increases simply by overlapping replication cycles in which DNA replication initiates before previous round is completed (Cooper & Helmstetter, 1968). Under this circumstance, when the origin fires with a constant timing but independently of the fork speed, the prolonged time necessary to replicate the entire chromosome due to the slow fork progression could produce more forks on the chromosome in the *dnaE173* cell than on the chromosome in the control *dnaE⁺* cell. Another possible explanation is more frequent initiation of the DNA replication in the *dnaE173* cells. The initiation potential of DNA replication in *E. coli* cells is controlled by various feedback mechanisms that repress extra initiation events (Skarstadt & Katayama, 2013). The initiation timing might be modulated by the mechanisms in response to the fork speed in the mutant cells. Further studies are needed to evaluate these possibilities.

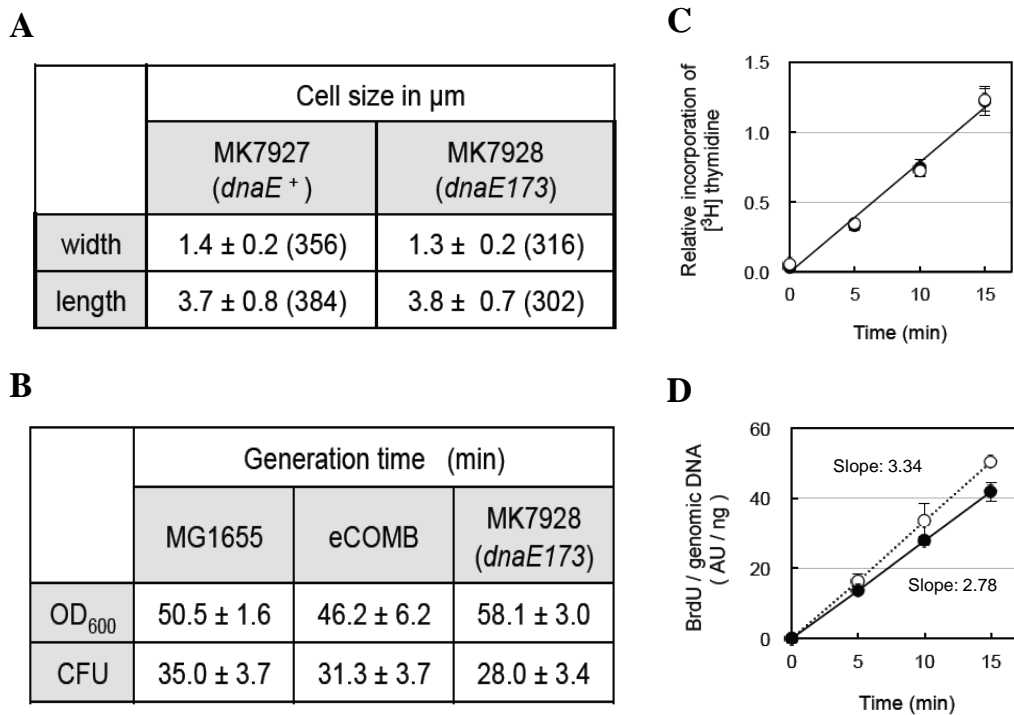


Figure 16. Comparison between the *dnaE173* and wild-type cells.

(A, B) Physiological characteristics of the *dnaE173* and wild-type cells. The *dnaE173* mutant strain MK7928 (eCOMB, *dnaE173*, *zea-502::Tn10*) and its control strain MK7927 (eCOMB, *dnaE*⁺, *zea-502::Tn10*) were constructed by co-transferring *dnaE173* and the tetracycline-resistant gene (*zea-502::Tn10*) into eCOMB strain. (A) The average cellular size (width and length) with standard deviation (SD) was determined from more than 300 measurements. (B) The mean of generation time and SEM were determined for the cells at the log phase from three independent experiments. (C, D) The rate of net DNA synthesis. DNA synthesis was measured with (C) [³H] thymidine and (D) BrdU in MK7927 (open circles) and MK7928 (close circles). The relative incorporation the radioactive thymidine was normalized to radioactivity of [¹⁴C] thymidine (as amount of genomic DNA fully labeled with [¹⁴C] thymidine). The BrdU signals were divided by amount of genomic DNA for normalization. Mean values and SEM from three independent experiments were plotted as a function of the labeling time.

3.12. Induction of the SOS response in the absence of DNA damage

I demonstrated above that the replicative DNA polymerase is the molecular engine that provides major driving force for the replication fork to move on chromosomal DNA. When cells are suffered from DNA damage during DNA replication, the SOS-response in bacteria and the S-phase checkpoint in eukaryotes are activated to protect the cells from deleterious consequences of replication inhibition by the DNA lesions. Since it has been well known that the fork speed is reduced in the S-phase checkpoint (Petermann *et al.*, 2010), it is likely that there are molecular brakes that decelerate speed of replication fork progression. However, any molecular brakes have not been identified in eukaryotes because of the complex gene network functioning in the checkpoint. In contrast to the S-phase checkpoint, nobody knows if the replication fork speed is also reduced in the SOS-response of *E. coli* cells. If it is the case, it may be easier to find genes responsible for slowdown of fork progression since the limited number of the SOS genes (about 40 genes) is up-regulated in the response. Furthermore, investigations of fork speed control with the genes in *E. coli* cells will lead to understand molecular mechanisms underlying slowdown of fork progression in the simple and well studied damage response.

The SOS response is induced by DNA damage that inhibits progression of replication forks. To investigate the fork speed in cells expressing the damage response, DNA damage must be avoided for SOS induction. Genetically manipulating *E. coli* cells constitutively induces the SOS response in the absence of DNA damage. The constitutively SOS-expressing cells were constructed by eliminating the *lexA* gene together with the *sulA* gene from the eCOMB cells (SOS-eCOMB). The former encodes the LexA repressor that negatively regulates the SOS gene expression, and the latter encodes the inhibitor of cell division protein FtsZ in the SOS response. The *sulA* gene was deleted in the SOS-eCOMB strain to grow the cells under constitutive induction of the SOS response.

Beside homologous recombination and recombination repair, RecA protein

functions as a mediator of the SOS induction. Expression of the gene is also enhanced to more than 10 folds at the early stage of the response (5 min post UV irradiation) (Courcelle *et al.*, 2001). Therefore, the RecA amount in cells can be used to monitor onset of the SOS response as shown in Fig. 17. SMR7623 (*lexA51* (Def)) and SMR7623 (*lexA3* (Ind⁻)) were used as controls for full and null induction level of the SOS response, respectively. Comparing the cellular RecA amount that in SMR7623. The induction level of SOS was relatively determined. The eCOMB Δ *sulA* induced the SOS by 6% and 5% in 56/2 medium containing thymidine and IdU, respectively. Those values were close to those of the wild-type MG1655 (5%) and SOS-deficient SMR7467 (3%). Thus, the IdU incorporation into the eCOMB Δ *sulA* cells did not significantly induce the damage response, which is consistent with the result for the eCOMB *sulA*⁺ cells shown in Fig. 7D. In contrast, the SOS-eCOMB cells induced the SOS response to 87% of the full extent, confirming that deletion of the *lexA* genes almost maximally induced SOS in eCOMB. Next, the speed of individual replication forks was measured in the SOS-eCOMB cells by the combing method.

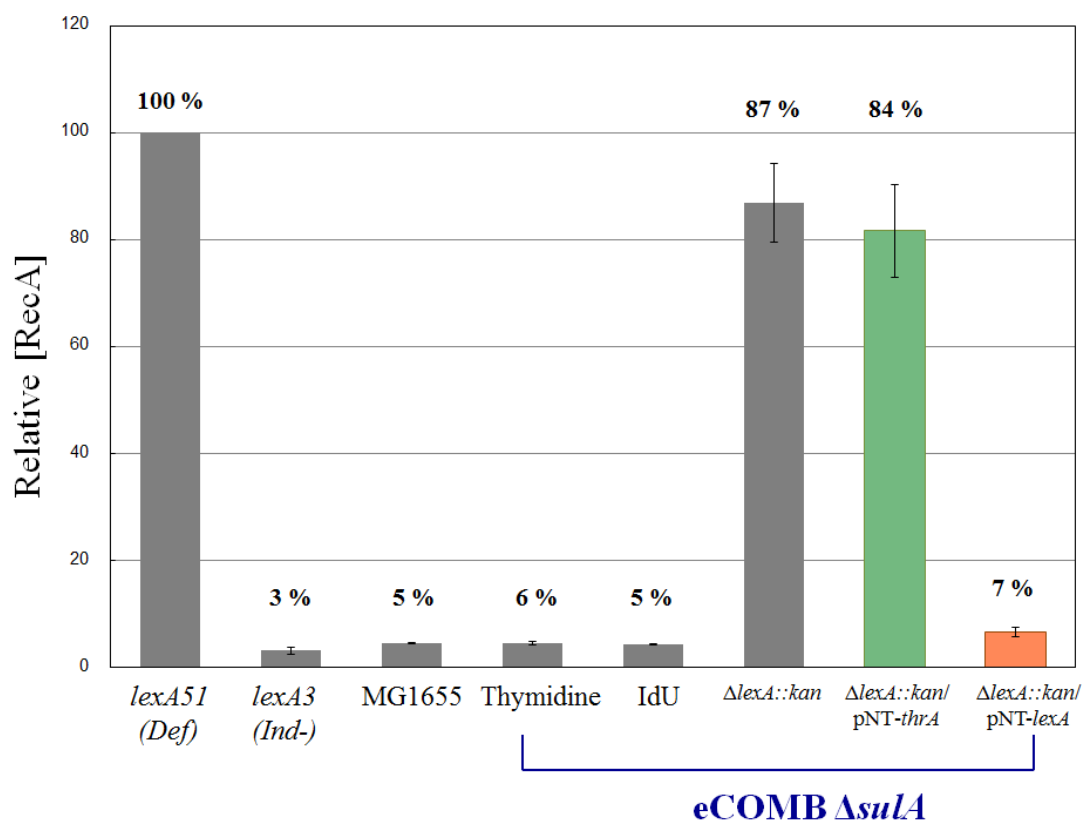


Figure 17. The relative amount of the cellular RecA protein in various cells.

The strains used were and strains were SMR7623 (*lexA51* (Def)), SMR7467 (*lexA3* (Ind⁻)), MG1655 (the wild-type), MK7453 (eCOMB $\Delta sulA$), MK7456 (eCOMB $\Delta sulA \Delta lexA::kan$), MK7456 carrying pNT-*thrA* plasmid and MK7456 carrying pNT-*lexA* plasmid. SMR7623 and SMR7467 were served as the control cells expressing the full and no SOS response, respectively. All strains were exponentially grown in 56/2 medium containing 2 $\mu\text{g/ml}$ thymidine at 37⁰C. For the MK7456 strain carrying either pNT-*thrA* or pNT-*lexA* plasmid, 0.5 mM IPTG was added to medium to induce expression of the genes under the control of Ptac promoter on plasmids. The cells except SMR7467 and SMR7623 were incubated in the medium with 50 $\mu\text{g/ml}$ IdU at 37⁰C for 6 min. Total proteins of the cells were analyzed by Western blotting with anti-RecA antibodies. Chemiluminescent signals of immune blots were measured with a luminescence image analyzer. The mean RecA amount in each strain relative to that in SMR7623 cells were determined from at least three independent experiments. Error bars indicate SEM.

3.13. Reduced speed of replication fork progression in the SOS response

The distribution of the fork speed in SOS-eCOMB cells (eCOMB Δ *sulA* Δ *lexA::kan*) was determined with 2 min IdU labeling samples as in Fig. 11A, and then compared to that of eCOMB cells (Fig. 18A). The results showed the single mode of fork speed in which 66% of the replication forks moved in a range of 300-500 nt/s (blue bars in the lower panel) that lower than that of eCOMB cells (blue bars in the upper panels). It indicates that the fork progression was uniformly slowed down in SOS-eCOMB cells. Furthermore, the accurate fork speed in the SOS-eCOMB cells was determined by the time-course experiments with the DNA combing method as described in Fig. 12. The fork speed of the SOS-eCOMB cells was estimated to be 351 ± 15 nt/s from observation of 2151 DNA molecules in three independent experiments (Fig. 18B). Since the coefficients of the linear regression indicated a very high reliability in each slope determination (data not shown), the average fork speed was accurately determined. This value was 54% of the fork speed in the eCOMB cells (653 ± 9 nt/s; Fig. 13).

To confirm that this reduction of fork speed was resulted from the SOS response induced by deletion of the *lexA* gene in eCOMB, the pNT-*lexA* plasmid, that expresses the wild-type LexA repressor under the control of the Ptac promoter, was introduced into the SOS-eCOMB cells (SOS-eCOMB/pNT-*lexA*). By adding 0.5 mM IPTG to the medium, the high SOS level of SOS-eCOMB was reduced from 87% to 7% of the fully SOS-expressing SMR7623 cells (Fig. 17). The SOS-eCOMB cells harboring the pNT-*thrA* that expresses Aspartate kinase I (Homoserine dehydrogenase I) retained the high level of the SOS response (84%). The pNT-*thrA* plasmid that expresses a non-SOS regulated protein by IPTG addition was chosen as a negative control, since the vector pNT-SD plasmid inhibited cell growth in the presence of IPTG (data not shown). This indicates that the SOS response in the SOS-eCOMB cells was almost suppressed to the wild-type level by complementation of LexA protein rather than the overexpression of other proteins as Aspartate kinase I. The fork speed in

SOS-eCOMB/pNT-*lexA* was determined from cells pulse-labeled with IdU for 2 min and 3 min, instead of 4 time points. The median values of the IdU-labeled DNA length in the 3-min sample was subtracted with that in the 2-min sample to calculate the fork speed. As shown in Fig. 19, the reduced fork speed in the SOS-eCOMB/pNT-*lexA* cells was restored to 602 ± 56 nt/s, while the fork speed of the SOS-eCOMB/pNT-*thrA* were not rescued at all (322 ± 16 nt/s). Thus, the strong SOS induction caused by deletion of the *lexA* gene was responsible for the fork speed reduction. Together with the same physiological characteristics of the constitutively SOS-expressing eCOMB as that of the SOS-unexpressing eCOMB (data not shown), these results indicate that the half reduction of replication rate is caused by the SOS induction but not by the secondary effect of the $\Delta lexA$ and $\Delta sulA$ mutations. I found for the first time that *E. coli* cells slow down fork speed in DNA damage response as well as the S-phase checkpoint of eukaryotic cells.

The rate of net DNA synthesis in the SOS-eCOMB cells was reduced to 47% and 61 % compared to that in the wild-type eCOMB cells when the incorporation rate of nucleoside was measured with BrdU and [³H] thymidine incorporation, respectively (Fig. 18C). The similar incorporation of thymidine and BrdU into the SOS-expressing cells excludes a possibility that the reduced fork speed was apparently observed by a low utilization of thymidine analogs under the cellular response to DNA damage. However, unlike *dnaE173*-eCOMB that also showed the reduced fork speed (Fig. 15A), the constitutively SOS-expressing cells reduced fork speed but did not maintain the normal level of DNA synthesis. This suggests that mechanisms in slowdown of fork speed are probably different between the *dnaE173*-eCOMB and the constitutively SOS-expressing eCOMB. The net DNA synthesis may not be always sustained to the level of the wild-type cells when fork speed is reduced in *E. coli* cells.

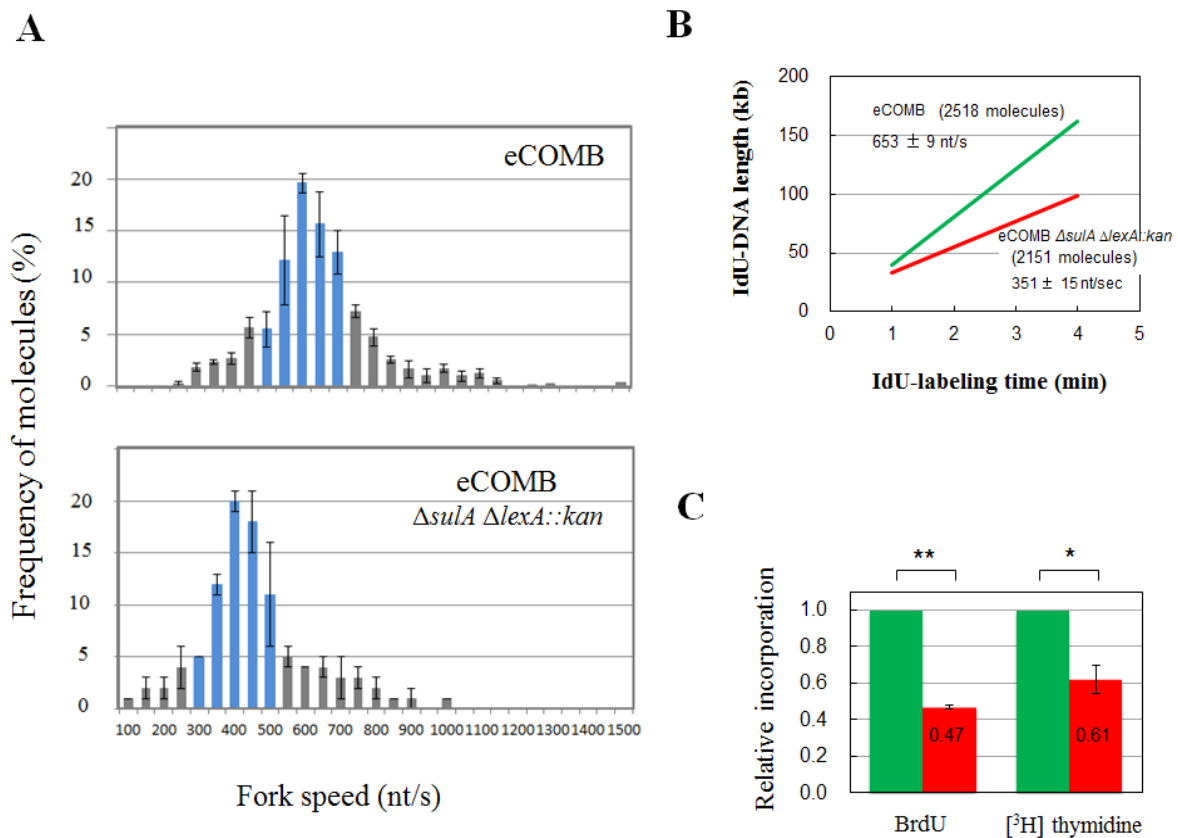


Figure 18. Reduced fork speed in constitutively SOS-expressing cells.

The cells were exponentially grown in 56/2 medium containing 2 μ g/ml thymidine at 37 $^{\circ}$ C and labeled in each experiment as follows. (A) The distribution of replication fork speed. The fork speed distribution of SOS-eCOMB (eCOMB $\Delta sulA \Delta lexA::kan$) was determined as described in Fig. 11A, and shown in lower panel. The data of eCOMB are the same as in Fig. 11A, and shown in the upper panel. The error bars are SEM from three independent experiments. (B) Fork speed determination by time-course experiments. The exponentially growing eCOMB (green line) and SOS-eCOMB (red line) cells were labeled with CldU for 2 min and then IdU for 1-4 min. The average fork speed was determined as in Fig. 13. For SOS-eCOMB, 2151 DNA molecules were measured. The data for eCOMB are the same as that in Fig. 13. (C) Reduced rate of net DNA synthesis in the SOS-eCOMB cells. The relative incorporation of nucleotides into the exponentially growing eCOMB (green bars) and SOS-eCOMB (red bars) cells were analyzed with BrdU and [3 H] thymidine as in Fig. 16C and D. Error bars were SEM from three independent experiments. The asterisks were the p values from the Student's t -test (one asterisk, <0.05 ; two asterisks, <0.005).

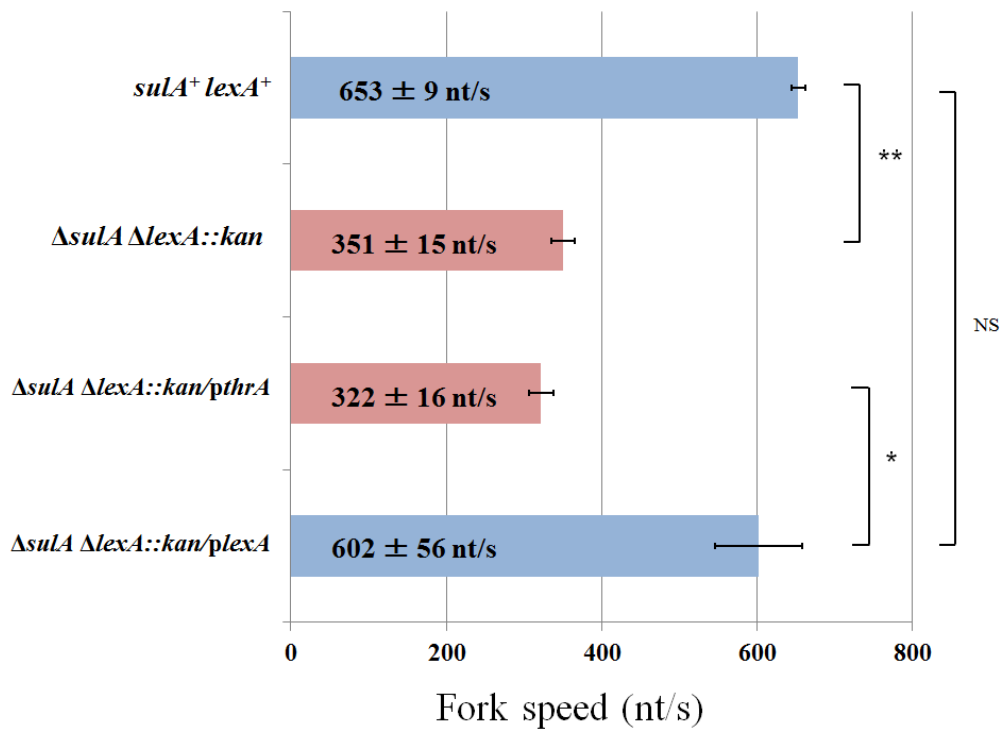


Figure 19. Recovery of the reduced fork speed by suppressing the SOS response.

The SOS-eCOMB/pNT-*lexA* (Δ *sulA* Δ *lexA::kan/plexA*) and SOS-eCOMB/pNT-*thrA* (Δ *sulA* Δ *lexA::kan/pthrA*) cells were exponentially grown in the 56/2 medium containing 2 μ g/ml thymidine and 0.5 mM IPTG at 37°C. The length of the IdU track were only determined in cells labeled at 2 time points (2 min and 3 min). The mean fork speed and SEM were collected from three independent experiments. For eCOMB (*sulA*⁺ *lexA*⁺) and SOS-eCOMB (Δ *sulA* Δ *lexA::kan*) strains, the same data in Figs. 13 and 18A were used, respectively. The asterisks indicate the *p* values from the Student's *t*-test (one asterisk, <0.05; two asterisks, <0.005). NS; not significant.

3.14. DinB functions in slowdown of the fork speed in the SOS response

The reduced fork speed was found in the SOS-eCOMB cells that constitutively express SOS due to the $\Delta lexA$ mutation (Fig. 18). When the SOS response was suppressed by complementing $\Delta lexA$, the fork speed was almost fully restored to the normal level in the wild type, suggesting that the SOS-induced genes play a role in slowdown of the replication fork (Fig. 19). If the genes encode molecular brakes for fork progression, disruption of the genes in the SOS-eCOMB cells will also restore the fork speed to normal. Moreover, it is highly likely that the molecular brakes are proteins that function at replication forks. Thus, I screened the following SOS-induced genes involved in DNA replication of damaged DNA and rescue of stalled forks: *dinB*, *polB*, *umuDC*, *uvrD*, *recA*, and *ruvA*. Each gene was deleted in the SOS-eCOMB cells. The mean fork speed of each mutant strain was determined with the time-course experiment of IdU labeling (in 1 min intervals for 4 min) from 3 independent experiments, excepting the *polB* and *uvrD* mutant.

The *polB*, *dinB*, and *umuDC* genes encode the translesion synthesis (TLS) polymerases Pol II, Pol IV (DinB), and Pol V, respectively, that synthesize damaged DNA over DNA lesion (TLS: translesion DNA synthesis). The Pol II belongs to the family-B DNA polymerase, whereas Pol IV and Pol V are the members of the family-Y DNA polymerases. These TLS DNA polymerases were firstly focused in screening molecular brakes because of their functions in TLS, interactions with the β clamp and formation of the alternative replisomes with the DnaB helicase (Fuji *et al.*, 2004; Indiani *et al.*, 2005; Furukohri *et al.*, 2008; Indiani *et al.*, 2009). As the shown in Fig. 20, the fork speed in the SOS-eCOMB cells lacking one of *polB*, *dinB*, and *umuDC* were 315 nt/s, 424 ± 17 nt/s and 347 ± 13 nt/s, respectively. Thus, only *dinB* was responsible for about 24% of the slowdown in the fork speed, suggesting that the other gene is required to maximally decrease the fork speed in the SOS response. These results also indicate that the TLS polymerases do not necessarily show down the fork speed in the SOS response. In agreement with the fork brake function by *dinB* in SOS,

dinB in *E. coli* cells and its eukaryotic homologue Polk in hamster cells inhibit DNA replication by ectopic overexpression (Bavoux *et al.*, 2005; Uchida *et al.*, 2008; Indiani *et al.*, 2009).

3.15. RecA recombinase functions in slowdown of the fork speed in the SOS response

The *recA* gene, encoding RecA recombinase, has multiple functions in *E. coli* cells: homologous recombination, recombination repair, and stabilization of stalled replication forks (Courcelle & Hanawalt, 2003; Cox, 2007). RecA binds to ssDNA at stalled forks or collapsed forks, and then forms a nucleo-protein filament. The RecA filaments facilitate autodigestion of LexA repressor to induce the SOS response. *recA* is also one of the SOS-induced genes. The molecular number of RecA is largest among the SOS-induced proteins. Because a region of ssDNA is continuously produced on the lagging strand at the replication forks, the increased amount of RecA may inhibit fork progression by forming the filaments at unblocked forks. Therefore, the SOS-eCOMB cells carrying $\Delta recA$ was investigated for the fork speed. The average fork speed was 524 ± 25 nt/s in this strain that is 80% of that in the eCOMB strain (Fig. 20). In the SOS response, the fork speed was reduced to 351 ± 15 nt/s that is 54% of that in the eCOMB cells (653 ± 9 nt/s; Fig. 13). This shows that the RecA protein was responsible for 57% of fork speed reduction in the SOS-eCOMB cells.

Together with results for *dinB* above, I demonstrated for the first time that a specialized TLS polymerase and DNA recombinase are molecular brakes for progression of replication forks in the DNA damage response. In addition to DinB, RecA is functionally conserved from bacteria to human. Those molecular brake functions of these two proteins might also be generally conserved through evolution.

3.16. RuvA and UvrD are not responsible for the slow fork speed in the SOS response

In *E. coli* cells, the replication fork is reversed when fork progression was blocked by DNA lesion. In this reaction, the nascent strands of the leading and lagging strands are re-annealing, and the resulting reversed fork has a Holiday junction structure. New replisome components are recruited to restart the regressed fork in a PriA-dependent manner (Masson *et al.*, 2008; De Septenville *et al.*, 2012). RuvAB are proposed to catalyze this fork regression reaction either through regressed fork stabilization (Seigneur *et al.*, 1998) or by directly catalyzing fork regression (Masson *et al.*, 2008). Although RuvAB rescues the stalled forks in the fork back reaction, it may also result in the regression of unperturbed forks and thereby slow down the speed when expression of the *ruvAB* genes is enhanced in the SOS induction. However, there was no significant change in the fork speed in the SOS-eCOMB cells carrying $\Delta ruvA$ (338 ± 11 nt/s) compare to that in the SOS-eCOMB cells (351 ± 15 nt/s), indicating that the *ruvA* gene is not required in inhibition of fork progression in SOS (Fig. 20).

The *uvrD* gene encodes DNA Helicase II and functions in the nucleotide excision repair pathway that removes the damaged nucleotides such as pyrimidine dimers and bulky adducts (Watson *et al.*, 2008). In addition, UvrD has the second highest protein level among the SOS gene products (Courcelle *et al.*, 2001). The recent data showed that UvrD helicase is involved in maintenance of stable replication fork progression (Boubakri *et al.*, 2010). However, a true function of UvrD in SOS remains unknown. I determined the fork speed in the SOS-eCOMB cells carrying $\Delta uvrD$. The fork speed (291 nt/s) was slower than that of the SOS-constitutive cells (Fig. 20). Although UvrD may be necessary to maintain the stable fork progression, it was not an additional factor to negatively regulate replication fork speed in the damage response.

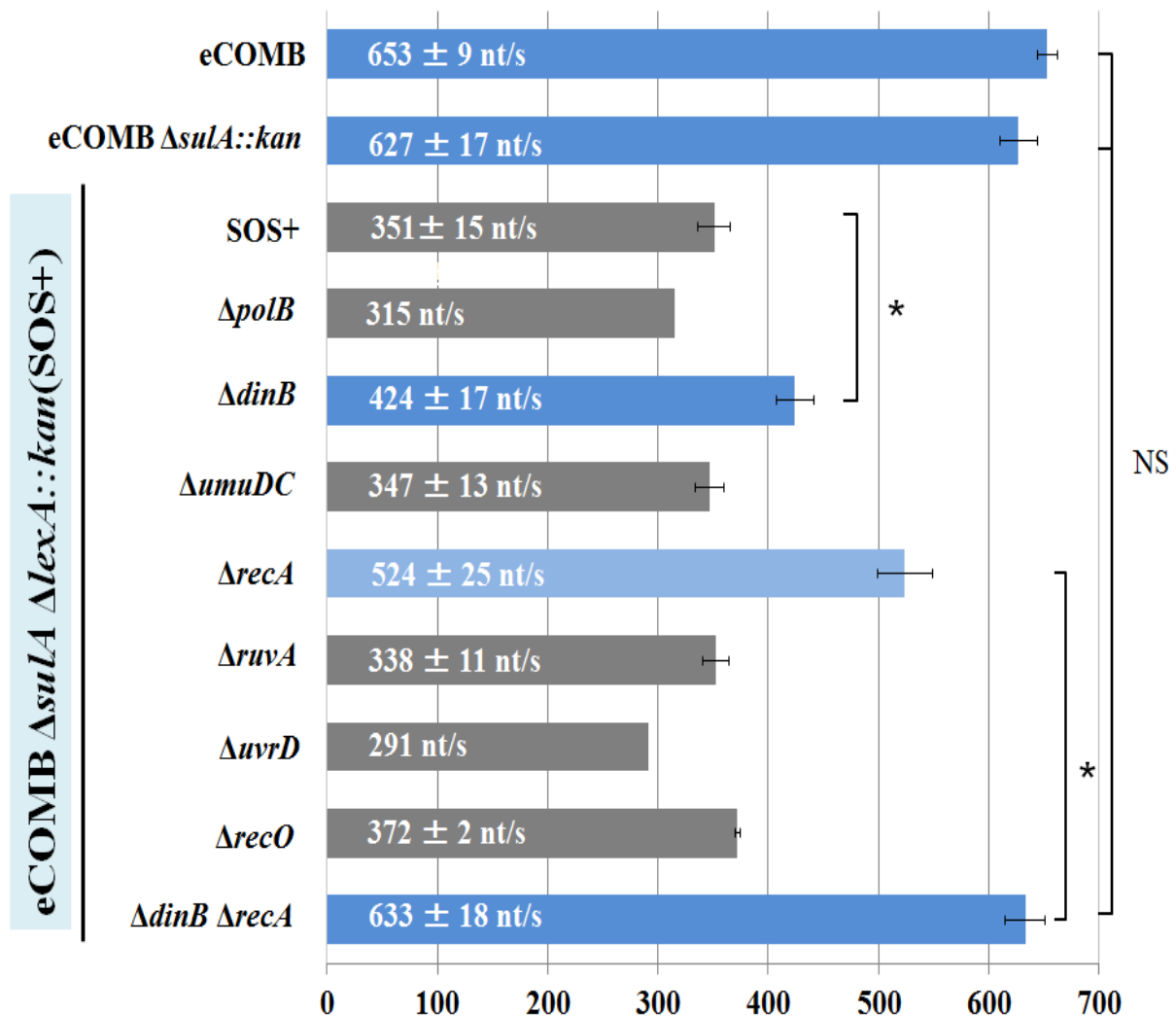


Figure 20. Replication fork speed in the SOS-expressing cells that lack various SOS genes.

The exponentially growing cells were labeled with CldU for 2 min and then IdU for 1-4 min. The average fork speed and SEM was determined from three independent experiments as described in the legend for Figure 13. Excepting eCOMB and eCOMB $\Delta sulA::kan$, all strains are the derivatives of the constitutively SOS-expressing strain (SOS⁺: eCOMB $\Delta sulA \Delta lexA::kan$) with a deletion mutation of the SOS genes. For eCOMB ($sulA^+ lexA^+$), eCOMB $\Delta sulA$, and SOS⁺ (eCOMB $\Delta sulA \Delta lexA::kan$) strains, the same data in Figs. 13 and 18A were used. The asterisks indicate the *p* values from the Student's *t*-test (one asterisk, <0.05), whereas the NS is no significant.

3.17. DinB and RecA independently slow down fork progression in the SOS response

Among the six SOS genes, I found two genes, *dinB* and *recA* were responsible for 24% and 57% of slowdown of the fork speed in the constitutively SOS-expressing cells, respectively. It has been suggested that DinB forms a complex with RecA together with UmuD (Godoy *et al.*, 2007). To know if these two genes work together in the same pathway or separately in two pathways to slow down movements of the replication forks in SOS, I constructed the SOS-eCOMB (eCOMB Δ *sulA* Δ *lexA::kan*) cells carrying both Δ *dinB* and Δ *recA*, resulting in MK7498. Furthermore, analysis of the double mutant could also enable me to know if there are only two genes for the fork brake in the SOS response.

In the cells labeled with IdU for 2 min, the fork speed was determined from three independent experiments with the DNA combing method (Fig. 21A). The speed distribution in the SOS-eCOMB cells (blue bars in Fig. 21A) was shifted to the slower side than eCOMB strain (green bars), which is consistent with the slow fork speed in the cells (Fig. 18A). MK7498 (red bars in Fig. 21A) showed the distribution of fork speed in the same range as eCOMB (green), indicating that elimination of *dinB* and *recA* from the SOS-eCOMB rescued homogeneously the fork progression. The average fork speed in the MK7498 cells was estimated to be 633 ± 18 nt/s by the three time-course experiments, which is almost the same as that in the parental eCOMB Δ *sulA::kan* (627 ± 17 nt/s) (Fig. 20 and 21B). Thus, the slow fork speed of 351 ± 15 nt/s in SOS-eCOMB was fully restored to the wild-type level by the double deletions while the each single deletion of these genes just showed the partly recoveries in fork speed (Fig. 20). Furthermore, the same result was obtained for rates of net DNA synthesis. The MK7498 cells incorporated [³H] thymidine at the same rate as eCOMB (Fig. 21C); the slope values of linear regression lines in Fig. 21C were 0.095 for the former cells (red line) and 0.083 for the latter cells (black line). These results demonstrate the following two conclusions. Firstly, only *dinB* and *recA* genes are

responsible for the reduction of the fork speed in the SOS-constitutive cells. Secondly, the *dinB* and *recA* genes individually control the progression of replication fork under the damage response stress in *E. coli* cells.

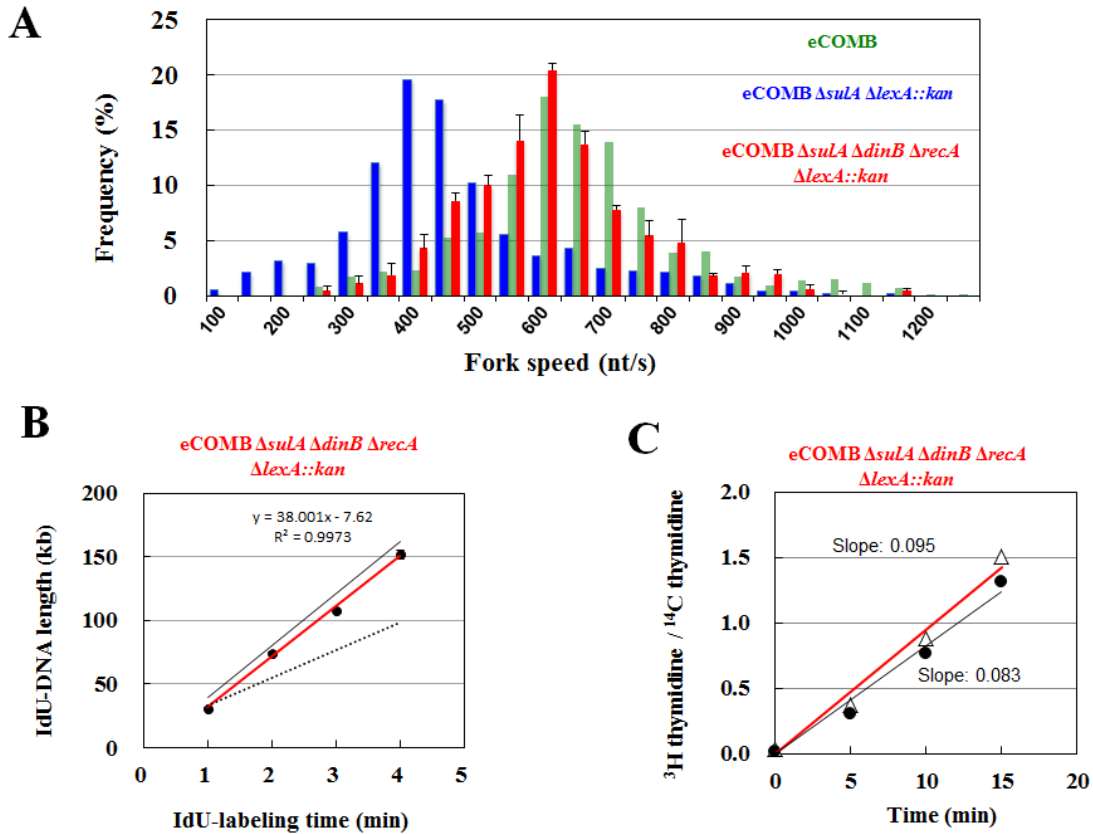


Figure 21. Replication fork speed in the *dinB-recA* double mutant cells.

(A) The distribution of fork speed. The fork speed was determined in cells labeled with IdU for 2 min, and the frequency of the molecules were plotted on histogram of the fork speed. The error bars represent SEM from three independent experiments. The cells analyzed were MK7498 (red bars), eCOMB (green bars), and eCOMB $\Delta sulA \Delta lexA::kan$ (SOS-eCOMB, blue bars). (B) The median values of IdU-labeled DNA length. The median values of IdU-labeled DNA length at each time point were plotted on the graph. The slope of the linear regression line was used to calculate the accurate fork speed as shown in Fig. 20. The red line denotes MK7498, whereas the black and dotted lines are eCOMB and SOS-cCOMB cells, respectively. (C) The rate of net DNA synthesis. DNA synthesis was measured with [3H] thymidine incorporation as in Fig. 13C. The black and red lines were determined by linear regression for eCOMB (closed circles) and MK7498 (opened triangles), respectively.

3.18. RecA controls fork progression in a *recFOR*-independent manner

I found that there are only two independent pathways in which *dinB* and *recA* genes respectively function to reduce the fork speed when *E. coli* cells constitutively induce the SOS response. According to analysis of DinB *in vivo* and *in vitro*, excess DinB in SOS slows down the fork speed probably by displacing the replicative Pol III from replication forks and forming the alternative slow replisome with DnaB helicase in place of Pol III (Uchida *et al.*; 2008; Indiani *et al.*, 2009). Furthermore, the highly purified DinB can dislodge Pol III from the forks *in vitro*, suggesting no additional factor except the replisome components is needed for the molecular brake function. In contrast, it has not been known how RecA inhibits DNA replication. Since SSB rapidly binds to ssDNA in cells, the ssDNA template for RecA assembly is SSB-coated ssDNA. RecA filament formation occurs slowly on SSB-coated DNA in a RecA concentration-dependent manner *in vitro* (Bell *et al.*, 2012). The slow rate of the RecA filament formation is stimulated by the mediator RecFOR complex. I presumed that RecA dominates over SSB for binding to ssDNA of the lagging strand when the RecA protein amounts are enhanced in SOS, and thereby inhibits movements of replication forks. If the RecA slows down the fork speed by the filament formation on SSB-coated ssDNA in a RecFOR-dependent manner, the inactivation of RecFOR in the SOS-eCOMB cells (SOS-eCOMB $\Delta recO$) could show the fork speed comparable to that in SOS-eCOMB $\Delta recA$ cells. However, the fork speed of the SOS-eCOMB $\Delta recO$ cells was 372 ± 2 nt/s (Fig. 20). Thus, the reduced fork speed in the SOS response was only slightly restored by inactivation of the recFOR complex. This result indicates that *recA* gene controls the progression of replication fork mostly in the RecFOR-independent manner under cellular stress in *E. coli* cells. Recently, it has been reported that RecA inhibits the reconstituted replisome in the absence of RecFOR *in vitro* (Indiani *et al.*, 2013), which activity of RecA may represent the RecFOR-independent inhibition of replication fork progression in the SOS response. Further studies are required to clarify the molecular mechanisms underlying the control

of replication fork progression by *recA* in cells.

4. Discussions

4.1. Efficient incorporation of thymidine analogs into eCOMB cells for DNA combing

Since the application of a molecular combing method for visualization of individual replication forks in *E. coli* cells requires a strain that can efficiently incorporate the thymidine-analogs such as BrdU, the novel eCOMB strain has been constructed in this study. In addition to the *thyA* gene, the eCOMB cell lacks 11 genes by deletion of the 12-kb chromosomal region spanning from *yjjG* to *deoCAB*. This strain can grow in minimal medium containing a low concentration of thymidine (2 µg/ml) and showed a much higher ability (17.4 fold) of thymidine-analogs incorporation than the historically used *E. coli* 15T- strain (Fig. 7B). Especially, eCOMB was the first *E. coli* K12 strain that can incorporate the halogenated thymidine analogs as well as [³H] thymidine (Fig. 7C).

To improve the efficiency in labeling cells with thymidine analogs, the bacterial mutant must exclusively use extracellular thymidine as a unique component for DNA synthesis and grow in minimal medium containing a low concentration of thymidine before transferring in medium containing a much higher concentration of a halogenated thymidine (50 µg/ml BrdU). Because the wild-type *E. coli* cells cannot use exogenous thymine, the first deletion for thymine auxotrophy was *thyA* gene encoding thymidylate synthase that catalyze the conversion of dUMP (deoxyuridine monophosphate) to dTMP (deoxythymidine monophosphate) (Fig. 5, reaction 1) (Friedkin & Kornberg, 1957). To construct the thymidine-requiring strain, additional deletion of *deoA* gene that catalyzes the conversion of thymine and thymidine was introduced (Fig. 5, reaction 3). The resulting cells still required a high concentration of thymidine to grow (20 µg/ml – data not shown). The lower thymidine-required strain (2 µg/ml thymidine) was constructed by deletion of both *deoB* and *deoC* genes that catalyze the metabolism of deoxyribose - 1 - phosphate (dR-1-P) (Fig. 5, reaction 4 and 5), since the accumulation

of dR-1-P in the cells leads to the lower requirement for exogenous thymidine (Ahmad & Pritchard, 1969; Bachmann, 1990; Ahmad *et al.*, 1998).

We suspect that the high efficiency of thymidine-analogous incorporation of the novel eCOMB cells were not only from the above reasons, but also from the others as follows. The *deoA* mutant lost ability of breaking down BrdU to bromouracil and dR-1-P, which probably contributed to the sharply enhanced accumulation of BrdU in the cells. Since the YjjG protein (encoded by *yjjG* gene) was known as a house-cleaning nucleoside monophosphate phosphohydrolyase that prevents the incorporation of halogenated nucleotides into DNA, the deletion of *yjjG* gene led to the increase of BrdUTP concentration due to less dephosphorylation of BrdUMP (Fig. 5, reaction 7) (Titz *et al.*, 2007). Thus, the $\Delta yjjG$ cells can efficiently incorporate the halogenated thymidine (BrdU) as well as thymidine. Beside these interpretations, it is not clear if the deletion of the other seven genes (*prfC*, *osmY*, and five hypothetical genes) within *yjjG* and *deoCAB* genes contributes to the greatly improved ability of eCOMB cells to incorporate BrdU.

Although eCOMB cells had a higher ability of BrdU incorporation and provided a much better visualization of newly synthesized DNA than 15T- cells, the CldU and IdU signals were sporadic on DNA fibers. The CldU-IdU labeled tracks were detected and observed under a fluorescent microscope by sequentially applying the anti-BrdU rat antibodies and anti-BrdU mouse antibody followed by the fluorescent dye-conjugated anti-rat and anti-mouse antibodies to DNA on glass surface. Thus, the discontinuous signals may be caused by an incomplete immune detection of the analogs with the antibodies. The other reason for this phenomenon may be the endogenous factors that limit the incorporation of BrdU. For example, the uracil DNA glycosylase (encoded by *ung* gene) that catalyzes the release of free uracil from uracil-containing DNA or DeoR, DNA binding transcriptional repressor (encoded by *deoR* gene), that represses Tsx nucleoside channel (encoded by *tsx* gene) and NupG nucleoside transporter (encoded by *nupG* gene) for thymidine (Makino & Munakata, 1978; Lindahl *et al.*,

1977). As the attempt to improve this system, we constructed COMB lacking either the *ung* or *deoR* genes. However, we detected the same sporadic signals of the analogs in the double-labeled DNA of both eCOMB derivatives as that in genomic DNA of eCOMB (data not shown). In addition to *deoA* gene, the uridine phosphorylase (encoded by *udp* gene) also catalyzes the degradation of BrdU (Fig. 5, reaction 8). Although deletion of *udp* gene may further stabilize intracellular BrdU, we have not studied eCOMB having this mutation to enhance the accumulation of BrdU in the cells.

4.2. The accurate speed and sub-populations in speed distribution of individual replication forks in *E. coli* cells

The eCOMB strain has the similar physiological characteristics to the wild-type *E. coli* K12 strain and grows normally without induction of the SOS response at least for 6 min in the presence of IdU (50 μ g/ml). In measurements of labeled DNA, the bias due to time delay in IdU incorporation and degradation of labeled DNA during DNA preparation were carefully minimized as shown in Figs. 11, 13 and 14. The fork speed is very close to the previously reported average rates of 550–750 nt/s (Khodursky *et al.*, 2000; Breier *et al.*, 2005; Odsbu *et al.*, 2009; Tehranchi *et al.*, 2010; Atkinson *et al.*, 2011). Therefore, the determined fork speed of 653 ± 9 nt/s confidently presents the normal speed of individual replication forks in the growing *E. coli* cells at 37°C (Figs. 6 and 14). The single molecular studies *in vitro* that showed the speed of individual replication fork by the reconstituted replisomes to be 536 ± 39 nt/s at 37°C and 246 ± 10 nt/s at 23°C (Tanner *et al.*, 2009; Yao *et al.*, 2009). When uncertainty of the fork speed is considered based on the standard error of the mean, our fork speed determination in the exponentially growing cells at 37°C is as accurate as that in the single molecular studies *in vitro*. However, the mean speed in the cells is about 20% faster than that of the reconstituted replisomes at 37°C. This suggests that the speed *in vitro* may be slightly underestimated since the reaction conditions do not exactly mimic the cellular environments. The accurate fork speed in the cell may provide a guide to further

optimize the single molecule assays *in vitro*.

Our single molecule studies *in vivo* allow us to analyze the speed distribution and dynamics of individual replication forks in growing *E. coli* cells. The speed distribution of the individual forks showed that two-thirds (about 60%) of replication forks were moving at the relatively uniform speed in a range of 550–750 nt/s (Figs. 11 and 13) while it was significantly varied in the rolling-circle DNA replication systems *in vitro* (Tanner *et al.*, 2008; Tanner *et al.*, 2009; Yao *et al.*, 2009). It should be noted that the distribution pattern of fork speed *in vitro* was flatter than that observed *in vivo* (Fig. 11C). DNA synthesis was performed with homogeneous DNA templates in the rolling-circle DNA replication systems while genomic DNA is heterogeneous in cells, the reason for the observed heterogeneous speeds of replication fork *in vitro* is not attributed to differences in template DNA. In contrast to the rolling-circle DNA replication *in vitro*, the fork movement on chromosome showed slow, moderate and fast subpopulations of fork speed in our single-molecule analysis. This can be interpreted by the natural impediments on genome such as the transcription machinery, unusual DNA structure, spontaneous DNA lesions, and the torsional stress from the accumulation of positive supercoils during DNA chain elongation (Mirkin & Mirkin, 2007). The faster subpopulation of replication forks seem to be the forks moving with the least replication stress and denotes the possible maximum speed of replisomes, whereas the slower sub-population could be subjected to more severe replication obstacles. Furthermore, the main population with medium speed might sustain relatively uniform speed by balancing replication stress with the potential capacity of the replisome and/or with the help of other enzyme.

4.3. Pol III provides a major driving force for the replisome progression

The functional interactions between DNA helicase and DNA polymerase generally increase the speed of DNA synthesis coupled with DNA unwinding *in vitro* (Patel *et al.*, 2011). However, because of difficulties in accurate determination of

replication fork speed, it has never been directly demonstrated that the chain-elongation activity of Pol III holoenzyme drives the replisome in the well-characterized *E. coli* cells. Using the *dnaE173* mutation that showed a slow rate of DNA synthesis *in vitro*, we found the proportional reduction of replication fork speed in the *dnaE173* eCOMB cells *in vivo* and provided an evidence for the above hypothesis.

Since *dnaE173* Pol III* (Pol III lacking the β clamp) showed a much higher processivity (about 10 fold) than wild-type Pol III* in absence of the β clamp, it is unlikely that this slow speed of replication fork was triggered by instability of *dnaE173* Pol III holoenzyme during DNA replication (Maki *et al.*, 1991; Sugaya *et al.*, 2002). Thus, the simple interpretation of the reduced fork speed in the *dnaE173* eCOMB cells is that the slow chain elongation of the Pol III holoenzyme largely dictates the *E. coli* replisome movement *in vivo*. The other DNA polymerase II and IV can synthesize DNA at a much slower rate than Pol III and form an alternative replisome with much slower DNA synthesis rate (Indiani *et al.*, 2009), which supports our conclusion.

4.4. Speed of replication fork may modulate initiation timing of DNA replication.

The cellular DNA replication rate, the average cell mass and doubling time were the same between the *dnaE173* and *dnaE⁺* eCOMB cells (Fig. 15), whereas the replication fork speed of the former cells was much slower than that of the latter (Fig. 16B). Compare with the control cell, the *oriC/ter* ratio was increased in the *dnaE173* cell to contribute to compensate overall DNA replication rate (Fig. 16C). The similar observations were reported not only in *E. coli* such as the *rep* (encodes Rep helicase) mutant cells and the wild-type MG1655 cells that reduced concentrations of dNTP by treatment with hydroxyurea (Lane & Denhardt, 1974; Odsbu *et al.*, 2009), but also in eukaryotes that showed the reduction of fork speed and the increase of origin firing in *chk1* deficient cells (Petermann *et al.*, 2010). However, the molecular mechanism underlying this phenomenon is unknown.

Bipatnath *et al* have mentioned that there is a constant level of cell mass per

replication origin in *E. coli*, indicating that replication is initiated when the cell has reached to a particular mass or amount of protein (Bipatnath *et al.*, 1998). In addition, the previous observations showed increase in origin firing in the rapidly growing cells while the C period (replication time) was not affected (Chandler *et al.*, 1975; Skarstad *et al.*, 1986; Cooper & Helmstetter, 1968). It indicated that the timing of the replication initiation is coupled to the growth rate of *E. coli* cells. Therefore, the above phenomenon may be simply interpreted that when the fork speed is slowed down, the next round of DNA replication is initiated due to the sufficiency of cellular mass before the replicating round is finished and resulted in the increased *oriC/ter* ratio.

In contrast, the frequency of origin firing and progression of replication fork could be balanced in a difference manner. This process should be tightly controlled and does not occur at random time since the initiation of DNA replication is controlled by both positive and negative regulatory mechanisms. The initiator DnaA protein in *E. coli* determines the initiation of DNA replication as the positive regulation. In the active ATP-DnaA form, it binds to DnaA boxes in the origin region (*oriC*) and starts DNA replication by opening dsDNA and recruits the replisome components. There are at least three known systems that negatively regulate the DnaA function that are the SeqA-dependent repression of *dnaA* transcription, Hda-dependent regulatory inactivation of DnaA and *data*-dependent hydrolysis of ATP-DnaA (Katayama *et al.*, 2010). Other than the *oriC* region, the high-affinity DnaA boxes are present in the other chromosomal regions including the *data* gene and the promoter of *dnaA* gene. This leads to the initiator titration model in which DnaA proteins first bind to the high-affinity DnaA boxes and then the remaining DnaA proteins bind to the boxes in the *oriC* region (Roth & Messer, 1998; Ogura *et al.*, 2001). The much slower rate of DNA replication forks in *dnaE173* mutant may result in the less of high-affinity DnaA boxes and more DnaA protein for binding to the *oriC* regions. The other model showed that the initiation is controlled by changes in the balance between positive (DnaA) and negative (SeqA) regulators. The origin sequestration prevents re-initiation through the

binding of multiple hemimethylated GATC sites in *oriC* (containing 11 copies of GATC site) by the SeqA protein (Lu *et al.*, 1994; Fossum *et al.*, 2007). The high affinity of SeqA protein to the hemimethylated GATC sequence allows this protein exactly follows the progression of replication fork until the new DNA strand is methylated by Dam methyltransferase (Waldminghaus *et al.*, 2012). The slower fork movements may cause the longer period of SeqA-hemimethylated sequence and less SeqA for the negative regulation. Although these interpretations were only based on the previous reports, we cannot exclude a possibility that *E. coli* cell has an unknown mechanism to coordinate the initiation timing and fork speed.

4.5. The reduction of replication fork speed under SOS response without DNA damage

The newly established DNA-combing system enabled us to reveal reduction of replication fork speed in the SOS-constitutive *E. coli* cells similarly to the eukaryotic S-phase checkpoint (Fig. 18). While the induction of the S-phase checkpoint was triggered by replication stress (such as formations of ssDNA or double strand breaks) in *chk1*-deficient cells, there was not any the damaged DNA in our SOS-constitutive *E. coli* cells (Syljuasen *et al.*, 2005). In this strain, the SOS response was artificially induced by the genetic manipulation without damaged DNA that differed from the physiological conditions of the SOS induction by UV irradiation. There are several reports about DNA synthesis in the UV irradiated *E. coli* cells that highly induced the SOS response. Since UV irradiation induces formation of the pyrimidine dimers that block replication fork progression and thereby generate ssDNA in the cells. In the presence of ssDNA, the RecA protein is activated by forming the RecA nucleofilament leading to cleavage of LexA repressor followed by upregulation of the SOS genes. When UV was irradiated to *E. coli* cells at 10 J/m^2 , there was about 1 lesion per 10 kb on the chromosome. This high density of damaged DNA frequently blocks replication forks at the lesions and thus sharply decreases DNA synthesis (Khidhir *et al.*, 1985;

Courcelle *et al.*, 2006; Rudolph *et al.*, 2007). The SOS-constitutive cells slowed down the fork speed by the upregulation of SOS genes without stalled replication forks. There are 2-8 replication forks in *E. coli* cells. At a lower dose of UV, DNA lesions are sparsely introduced in genomic DNA in which some of the replication forks are blocked, leading to the SOS induction. Under the condition, unperturbed forks could be slowed down by unregulation of the SOS genes as we observed in the constitutively SOS-expressing cells. Slow speed of replication forks in our SOS-constitutive *E. coli* cells may represent movement of unperturbed forks in this situation.

The common concept about a biological meaning of the reduced fork speed is that fork speed reduction may help cells have extra time for repairing damaged DNA before it is replicated (Petermann *et al.*, 2006; Syljuasen *et al.*, 2005). After UV irradiation, DNA synthesis in *E. coli* cells is inhibited for at least 15-20 min before resuming. Within that time, most of the DNA lesions were repaired, indicating that the cells may likely take the extra time to fix the damaged DNA that generated by UV irradiation (Courcelle *et al.*, 1999). In the natural condition, spontaneous DNA damage is present in a few percent of cells and induces the SOS response once the fork encountered the DNA lesion (Pennington & Rosenberg, 2007). To avoid further production of DNA replication stress due to the blocked forks by DNA lesions, the cell may regulate the progression of unperturbed fork and spare more time to remove the DNA lesions ahead of it. Thus, it is likely that the reduced speed of replication fork may be important to cope with low-density DNA damage that occurs in natural environment.

In addition to the reduced speed of the individual forks, the SOS-constitutive cells showed a proportional reduction in the overall DNA synthesis rate compared to that in the wild-type when DNA replication was examined by BrdU and [³H] thymidine incorporation (Fig. 18C). The data may suggest that the SOS-constitutive cells did not maintain the overall DNA synthesis under cellular stress. However, we cannot explain these results well with the current observation that showed the almost comparable

nucleoid structure, cell shape and generation time between eCOMB and the SOS-constitutive cells (data not shown). Further studies in physiological characteristics of the SOS-constitutive cells are required to verify them.

4.6. Translesion DNA polymerase (DinB) and DNA recombinase (RecA) individually control fork progression in the SOS response

We found that translesion DNA polymerase, DNA polymerase IV (DinB), and DNA recombinase, RecA, individually control fork progression (Figs. 20 and 21). However, the molecular mechanism underlying the regulation of fork progression by these factors is unknown. There were several reports that DinB protein affects on DNA synthesis both *in vivo* and *in vitro*. Overproduction of DinB inhibited the rates of DNA synthesis in the dose-dependent manner without extensive induction of the SOS response in *E. coli* cells (Uchida *et al.*, 2008; Mori *et al.*, 2012). Hydroxyurea (HU) treatment of *E. coli* cells had negative effects on DNA-chain elongation and the initiation of DNA replication since HU inactivates ribonucleotide reductases which catalyze the conversion of ribonucleotides into deoxyribonucleotides. Interestingly, DinB protein also participated in the DNA damage-independent response to the inhibition of replication fork progression in the HU-treated cells (Odsbu *et al.*, 2009; Lopes *et al.*, 2001; Godoy *et al.*, 2006). It indicated that DinB decelerates the fork progression in the dose-dependent manner without the damaged DNA. In the *in vitro* experiments, DinB protein was known to interact with the β clamp that increase its processivity and with DnaB helicase to form an alternative replisome that contributed to the slow fork speed (Wagner *et al.*, 2000; Indiani *et al.*, 2009). The alternative replisome may be slow down by losing the polymerase-helicase coupling that is mediated by the τ subunit of Pol III (Kim *et al.*, 1996; Yuzhakov *et al.*, 1996; Dallmann *et al.*, 2000). According to these results, we suspected that DinB protein seems to put a brake on replication fork progression when it is upregulated in our SOS-constitutive *E. coli* cells without any damaged DNA by forming the alternative

replisome. As the “tool-belt” model was suggested based on the interaction of DinB with the β clamp, the alternative replisome is likely formed by the presence of both DinB and Pol III in one replisome (Pages & Fuchs, 2002).

The recombinase RecA protein is activated when it forms the RecA-filament with ssDNA. The active RecA protein has the role in homologous repair, maintaining the integrity of arrested DNA replication fork or stable DNA replication that initiates DNA replication in DnaA-independent manner (Courcelle *et al.*, 2003; Kogoma, 1997). Since there is not any damaged DNA in our SOS-constitutive *E. coli* cells, it is not known if RecA protein is activated. The RecA protein was showed the localization with the DNA replication factory in the cell centre after UV irradiation in *E. coli* K12 by using RecA-GFP (Renzette *et al.*, 2005). Recently, Bell *et al.* have showed the RecA nucleation on SSB-coated ssDNA. They mentioned that the very short ssDNA (about 3 nt) is transiently unwrapped by sliding of SSB on the lagging strand, creating available sites for RecA to form nucleoprotein filaments. The efficiency of this process depended on the concentration of RecA protein in the reaction *in vitro* (Bell *et al.*, 2012). These results suggested that the RecA protein can be activated without the damaged DNA by replacing the SSB protein from SSB-coated ssDNA on the lagging strand and forming the nucleoprotein filament when it is upregulated in our SOS-constitutive cells. The RecA protein promotes disassembly of stalled replisomes in RecFOR – independent manner when progression of the replisomes is blocked by inactivation of DnaB helicase (Lia *et al.*, 2013). The replisome-replacement activity of RecA may cause slow down of progression of unperturbed forks in a dose-dependent but RecFOR-independent manner. RecA protein also stimulates the action of TLS polymerase replisomes while inhibits the Pol III replisomes, indicating that it can facilitates switching between a TLS polymerase and Pol III under SOS response (Indiani *et al.*, 2013). The slow fork speed may be resulted from the frequent switch of TLS polymerase with Pol III that enhanced by interaction between the RecA protein and the replisome in the RecFOR-independent manner. On the other hand, the

RecA-coated DNA on the lagging strand physically impedes fork progression and slows down fork speed since it is more hardly replicated than SSB-ssDNA during DNA elongation (Indiani *et al.*, 2013). RecA protein has multiple functions in *E. coli* cells such as homologous recombination, DNA repair, SOS induction and stabilization of stalled forks. Expression of various *recA* mutant genes in the SOS-induced $\Delta recA$ cells will verify what functions involved in the reduction of the fork speed in the SOS response. For example, it is interesting to examine *recAS25P* (deficient in stabilization of stalled forks) and *recA423* (deficient in homologous recombinant repair).

We suggest several models for the control of replication fork progression by DinB and RecA proteins in the SOS response in *E. coli* cells (Fig. 22). There are 2-8 replication forks in an exponentially growing cell. When some forks are stalled by DNA damage, the cell quickly upregulates the SOS genes. Among the SOS genes, *dinB* (encode DNA polymerase IV - DinB) and *recA* (encode RecA recombinase) function to slow down the progression of the unperturbed replication forks (Fig. 22A). This brake of fork movement may provide the extra time for DNA repair to remove the DNA lesions ahead of unperturbed forks and avoid production of more replication stress (Fig. 22B). In the SOS response, the fork progression seems to be controlled as follows. The speed of unblocked forks is slowed down by formation of the alternative replisomes in switching Pol III with DinB on the β clamp at the replication forks. The RecA protein promotes this switching reaction. This formation of the alternative replisome allows the forks ready to encounter and to bypass the DNA lesions ahead under cellular stress (Fig. 22C). Alternatively, as the consequence of the RecA upregulation, the abundant amounts of the RecA proteins can form the RecA filament on the lagging strand of undamaged DNA. This presence of RecA-coated ssDNA on the lagging strand may impede or destabilizes the replisome on the replication fork and contributes to the reduced fork speed. Further biochemical studies are required to verify the molecular mechanism underlying these processes by DinB and RecA proteins in *E. coli* cells.

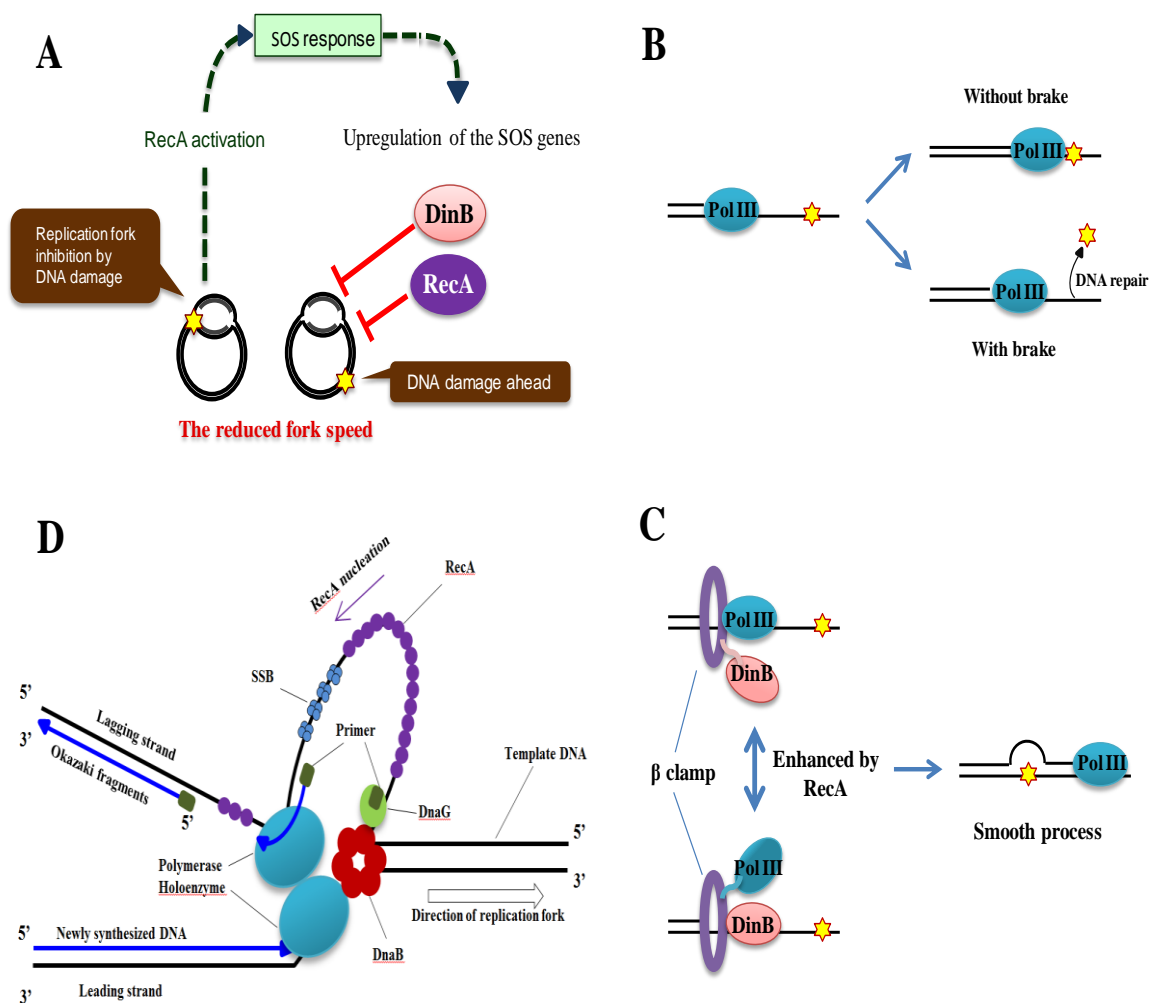


Figure 22. Possible models of replication fork reduction under cellular stress in *E. coli* cells. (A) The reduced fork speed under SOS response. RecA is activated when replication fork inhibited by damaged DNA followed by the induction of SOS response with upregulation of the SOS genes. Among these SOS genes, DinB and RecA protein individually break the progression of unperturbed forks. (B) The possible physiological meaning of fork speed reduction. Since the fast replication fork causes the heavy impact when it rapidly encounters the DNA lesion without break, the slow speed likely provide extra time for DNA repair to move the lesion before the fork reach its. (C) The possible alternative replisome. The “tool-belt” model showed the localization of DinB and Pol III in the same replisome by interacting with β clamp. With this structure of replisome, the cell is always ready to encounter the lesion. However, the frequent translocation between DinB and Pol III that enhanced by RecA protein may result in the slow fork speed. (D) The possible direct effect of RecA protein on fork progression. The presence of extent RecA filament may impede or destabilize the replisome on replication fork and then result in the reduced fork speed.

4.7. Conclusions

In summary, I have successfully constructed a novel thymidine requiring *E. coli* K12 strain, called eCOMB, with the sharply enhanced efficiency of thymidine analogous incorporation into the cells. Using this novel strain, the single molecule combing has been applied to measure speed of individual replication fork in the growing *E. coli* cells and obtained the following findings. The accurate speed of individual replication forks was determined to be 653 ± 9 nt/s and most forks uniformly moved in the range 550 – 750 nt/s. However, there were the minor populations of forks that moved with faster and lower speed. In addition, detecting the slow fork speed in *dnaE173* eCOMB cells compare to its control, I provided the direct evidence to conclude that the rate of DNA chain elongation by Pol III is the major driving force for the fork movement in *E. coli* cells. Finally, I have found the reduced fork speed in SOS-constitutive *E. coli* cells that genetically constructed by deletion of *lexA* gene and discovered that RecA (recombinase) and DinB (Translesion synthesis polymerase) individually control the fork progression under SOS response. Although these findings will possibly lead to the insight into the control of replication fork progression, the further studies are required to verify the molecular mechanism underlying this process by DinB and RecA proteins in *E. coli* cells.

5. Acknowledgements

I am deeply grateful to Prof. Hisaji Maki and Assoc. Prof. Masahiro Tatsumi Akiyama for their continuous guidance, valuable discussions and best supports during this study.

I would like to thank to all former and present members of Prof. Maki's Lab for their valuable comments, continuous supports, helps and friendships when I staying and working in the lab.

I deeply thank to all my advisers in Graduate School of Biological Science for their comments and suggestions to complete this research.

I would like to thank to Prof. Katsuzumi Okumura in Mie University, Tsu, Mie, Japan for his technical instructions in DNA combing method, Dr. Yuichi Sakumura in Aichi Prefectural University, Nagakute, Aichi, Japan for his remarkable mathematical analysis, and all members of Prof. Takagi's lab for their kindness and supports when I have been frequently working in the their lab with the fluorescent microscope.

I also thank to Graduate School of Biological Sciences – Nara Institute of Science and Technology, Japan and Vietnamese Institute of Biotechnology for this education opportunity and the financial support through NAIST Global COE Program.

Finally, I would like to express my highest gratitude to my parents, my wife, my lovely son, my brothers in Vietnam for their everlasting love, continuous encouragements and supports so far.

References

- Ahmad, S.I. & Pritchard, R.H. (1969) A map of four gene specifying enzymes involved in the catabolism of nucleosides and deoxynucleosides in *Escherichia coli*. *Mol. Gen. Genet.* 104:351-359.
- Ahmad, S.I., Kirk, S.H., Eisenstark, A. (1998) Thymine metabolism and thymineless death in prokaryotes and eukaryotes. *Annu. Rev. Microbiol.* 52:591-625.
- Atkinson, J., Gupta, M.K., McGlynn, P. (2011a) Interaction of Rep and DnaB on DNA. *Nucleic Acids Res.* 39(4): 1351-1359.
- Atkinson, J., Gupta, M.K., Rudolph, C.J., Bell, H., Lloyd, R.G., McGlynn, P. (2011b) Localization of an accessory helicase at the replisome is critical in sustaining efficient genome duplication. *Nucleic Acids Res.* 39(3):949-957.
- Baba, T., Ara, T., Hasegawa, M., Takai, Y., Okumura, Y., Baba, M., Datsenko, K.A., Tomita, M., Wanner, B.L., Mori, H. (2006) Construction of *Escherichia coli* K-12 in-frame, single-gene knockout mutants: The Keio collection. *Mol. Syst. Biol.* 2:2006.0008.
- Bachmann, B.J. (1990) Linkage map of *Escherichia coli* K12, Edn. 8. *Microbiol. Rev.* 54:130-197.
- Bavoux, C., Leopoldino, A.M., Bergoglio, V., O-Wang, J., Ogi, T., *et al.* (2005) Up-regulation of the erro-prone DNA polymerase κ promotes pleiotropic genetic alterations and tumorigenesis. *Cancer Res.* 65(1):325-330.
- Beacham, I.R. & Pritchard, R.H. (1971) The role of nucleoside phosphorylases in the degradation of deoxyribonucleosides by thymine-requiring mutants of *E. coli*. *Mol. Gen. Genet.* 110:289-298.
- Bell, J.C., Plank, J.L., Dombrowski, C.C., Kowalczykowski, S.C. (2012) Direct imaging of RecA nucleation and growth on single molecules of SSB-coated ssDNA. *Nature* 491(7423):274-280.
- Bensimon, A., Simon, A., Chiffaudel, A., Croquette, V., Heslot, F., Bensimon, D. (1994) Alignment and sensitive detection of DNA by a moving interface. *Science* 265(5181):2096-2098.
- Bipatnath, M., Dennis, P.P., Bremer, H. (1998) Initiation and velocity of chromosome replication in *Escherichia coli* B/r and K-12. *J. Bacteriol.* 180(2):265-273.
- Boubakri, H., de Septenville, A.L., Vigurea, E., Michel, B. (2010) The helicases DinG, Rep and UvrD cooperate to promote replication across transcription units *in vivo*. *EMBO J.* 29(1):145-157.

- Breier, A.M., Weier, H.U., Cozzarelli, N.R. (2005) Independence of replisomes in *Escherichia coli* chromosomal replication. *Proc. Natl. Acad. Sci. USA.* 102(11):2942-2947.
- Brent, R. & Ptashne, M. (1981) Mechanism of action of the *lexA* gene product. *Proc. Natl. Acad. Sci. USA.* 78(7):4204-4208.
- Bridges, B.A. (2005) Error-prone DNA repair and translesion DNA synthesis. II: The inducible SOS hypothesis. *DNA Repair.* 4(6):725-6, 739.
- Cairns, J. (1963) The chromosome of *Escherichia coli*. *Cold Spring Harb Symp Quant Biol* 28:43-46.
- Chandler, M., Bird, R.E., Caro, L. (1975) The replication time of the *Escherichia coli* K12 chromosome as a function of cell doubling time. *J. Mol. Biol.* 94(1):127-132.
- Cooper, S. & Helmstetter, C.E. (1968) Chromosome replication and the division cycle of *Escherichia coli* B/r. *J. Mol. Biol.* 31(3):519-540.
- Courcelle, J., Crowley, D.J., Hanawalt, P.C. (1999) Recovery of DNA replication in UV-irradiated *Escherichia coli* requires both excision repair and RecF protein function. *J. Bacteriol.* 181(3):916-922.
- Courcelle, J., Khodursky, A., Peter, B., Brown, P.O., Hanawalt, P.C. (2001) Comparative gene expression profiles following UV exposure in wild-type and SOS-deficient *Escherichia coli*. *Genetics* 158(1):41-64.
- Courcelle, J. & Hanawalt, P.C. (2003) RecA-dependent recovery of arrested DNA replication forks. *Annu. Rev. Genet.* 37:611-46.
- Courcelle, C.T., Chow, K.H., Casey, A., Courcelle, J. (2006) Nascent DNA processing by RecJ favors lesion repair over translesion synthesis at arrested replication forks in *Escherichia coli*. *Proc. Natl. Acad. Sci. USA.* 103(24):9154-9559.
- Cox, M.M. (2007) Motoring along with the bacterial RecA protein. *Mol. Cell. Biol. – Nature Rev.* 8(2):127-138.
- Dallmann, H.G., Kim, S., Pritchard, A.E., Mariani, K.J., McHenry, C.S. (2000) Characterization of the unique C terminus of the *Escherichia coli* τ DnaX protein. Monomeric C- τ binds α and DnaB and can partially replace τ in reconstituted replication forks. *J. Biol. Chem.* 275(20):15512-15519.
- Datsenko, K.A. & Wanner, B.L. (2000) One-step inactivation of chromosomal genes in *Escherichia coli* K-12 using PCR products. *Proc. Natl. Acad. Sci. USA.* 97(12):244-249.
- De Septenville, A.L., Duigou, S., Boubakri, H., Michel, B. (2012) Replication fork reversal after replication-transcription collision. *PLoS Genet.* 8(4):1-12.

- Doublet, B., Douard, G., Targant, H., Meunier, D., Madec, J.Y., Cloeckaert, A. (2008) Antibiotic marker modification of λ Red and FLP helper plasmids, pKD46 and pCP20, for inactivation of chromosomal genes using PCR products in multidrug-resistant strains. *J. Microbiol. Methods* 75(2):359-361.
- Drake, J.W. (1969) Spontaneous mutation: Genetic control of mutation rates in Bacteriophage T4. *Nature* 221:1128-1132.
- Fay, P.J., Johanson, K.O., McHenry, C.S., Bambara, R.A. (1981) Size classes of products synthesized processively by DNA polymerase III and DNA polymerase III holoenzyme of *Escherichia coli*. *J. Biol. Chem.* 256:976-983.
- Ferullo, D.J., Cooper, D.L., Moore, H.R., Lovett, S.T. (2009) Cell cycle synchronization of *Escherichia coli* using the stringent response, with fluorescence labelling assays for DNA content and replication. *Methods* 48(1):8-13.
- Fossum, S., Crooke, E., Skarstad, K. (2007) Organization of sister origins and replisomes during multifork DNA replication in *Escherichia coli*. *EMBO J.* 26(21): 4514-4522.
- Friedkin, M., Kornberg, A. (1957) The enzymatic conversion of deoxyuridylic acid to thymidylic acid and the participation of tetrahydrofolic acid. In *A Symposium on the Chemical Basis of Heredity*, ed. WD McElroy, B Glass, p. 609. Baltimore, MD: John Hopkins Univ. Press.
- Furukohri, A., Goodman, M.F., Maki, M. (2008) A dynamic polymerase exchange with *Escherichia coli* DNA polymerase IV replacing DNA polymerase III on the sliding clamp. *J. Biol. Chem.* 283(17):11260-11269.
- Fujii, S., Fuchs, R.P. (2004) Defining the position of the switches between replicative and bypass DNA polymerase. *EMBO J.* 23(21):4342-4352.
- Funnell, B.E., Baker, T.A., Kornberg, A. (1986) Complete enzymatic replication of plasmids containing the origin of the *Escherichia coli* chromosome. *J. Biol. Chem.* 261(12):5616-5624.
- Godoy, V.G., Jarosz, D.F., Walker, F.L., Simmons, L.A., Walker, G.C. (2006) Y-family DNA polymerases respond to DNA damage-independent inhibition of replication fork progression. *EMBO J.* 25(4):868-879.
- Godoy, V.G., Jarosz, D.F., Simon, S.M., Abyzov, A., Ilyin, V., Walker, G.C. (2007) UmuD and RecA directly modulate the mutagenic potential of the Y family DNA polymerase DinB. *Mol. Cell.* 28:1058-1070.
- Goodman, M.F. (2002) Error-prone repair DNA polymerase in prokaryotes and eukaryotes. *Annu. Rev. Biochem.* 71:17-50.

- Guyer, M.S., Reed, R.R., Steitz, J.A., Low, K.B. (1981) Identification of a sex-factor-affinity site in *E. coli* as $\gamma\delta$. *Cold Spring Harb Symp Quant Biol* 45 Pt 1:135-140.
- Herrick, J. & Bensimon, A. (1999) Single molecule analysis of DNA replication. *Biochimie* 81(8-9):859-871.
- Higuchi, K., Katayama, T., Iwai, S., Hidaka, M., Horiuchi, T., Maki, H. (2003) Fate of DNA replication fork encountering a single DNA lesion during oriC plasmid DNA replication *in vitro*. *Genes Cells* 8(5):437-449.
- Indiani, C., McInerney, P., Georgescu, R., Goodman, M.F., O'Donnell, M. (2005) A sliding-clamp toolbelt binds high- and low-fidelity DNA polymerases simultaneously. *Mol. Cell*. 19(6): 805-815.
- Indiani C, Lance D. Langston, Olga Yurieva, Myron F. Goodman, Mike O'Donnell (2009) Translesion DNA polymerases remodel the replisome and alter the speed of the replicative helicase. *Proc. Natl. Acad. Sci. USA*. 106(15): 6031-6038.
- Indiani, C., Patel, M., Goodman, M.F., O'Donnell, M.E. (2013) RecA acts as a switch to regulate polymerase occupancy in a moving replication fork. *Proc. Natl. Acad. Sci. USA*. 110(14):5410-5415.
- Katayama, T., Ozaki, S., Keyamura, K., Fujimitsu, K. (2010) Regulation of the replication cycle: conserved and diverse regulatory systems for DnaA and *oriC*. *Nat. Rev. Microbiol.* 8:163-170.
- Kelman, Z. & O'Donnell, M. (1995) DNA polymerase III holoenzyme: Structure and function of a chromosomal replicating machine. *Annu. Rev. Biochem.* 64:171-200.
- Khidhir, M.A., Casaregola, S., Holland, I.B. (1985) Mechanism of transient inhibition of DNA synthesis in ultraviolet-irradiated *E. coli*: Inhibition is independent of recA whilst recovery requires RecA protein itself and an additional, inducible SOS function. *Mol. Gen. Genet.* 199(1):133-140
- Khodursky, A.B., Peter, B.J., Schmid, M.B., DeRisi, J., Botstein, D., Brown, P.O., Cozzarelli, N.R. (2000) Analysis of topoisomerase function in bacterial replication fork movement: Use of DNA microarrays. *Proc. Natl. Acad. Sci. USA*. 97(17):9419-9424.
- Kim, S., Dallmann, H.G., McHenry, C.S., Marians, K.J. (1996) Coupling of a replicative polymerase and helicase: $\Delta\tau$ -DnaB interaction mediated rapid replication fork movement. *Cell* 84(4):643-650.

- Kogoma, T. (1997) Stable DNA replication: Interplay between DNA replication, homologous recombination, and Transcription. *Microbiol. Mol. Biol. Rev.* 61(2):212-238.
- Kong, X.P., Onrust, R., O'Donnell, M., Kuriyan, J. (1992) Three-dimensional structure of the β subunit of *E. coli* DNA polymerase III holoenzyme: a sliding DNA clamp. *Cell* 69(3):425-437.
- LaDuca, R.J., Crute, J.J., McHenry, C.S., Bambara, R.A. (1986) The β subunit of the *Escherichia coli* DNA polymerase III holoenzyme interacts functionally with the catalytic core in the absence of other subunits. *J. Biol. Chem.* 261(16):7550-7557.
- Lane, H.E. & Denhardt, D.T. (1974) The rep mutation. III. Altered structure of the replicating *Escherichia coli* chromosome. *J. Bacteriol.* 120(2):805-814.
- Lee, H.C., Kim, J.H., Kim, J.S., Jang, W., Kim, S.Y. (2009) Fermentative Production of Thymidine by a Metabolically Engineered *Escherichia coli* strain. *Appl. Environ. Microbiol.* 75(8):2423-2432.
- Lindahl, T., Ljungquist, L., Siegert, W., Nyberg, B., Sperens, B. (1977) DNA N-glycosidase: Properties of uracil-DNA glycosidase from *Escherichia coli*. *J. Biol. Chem.* 252(10):3286-3294.
- Lia, G., Rigato, A., Long, E., Chagneau, C., Masson, M.L., Allemand, J.F., Michel, B. (2013) RecA-promoted, RecFOR-independent progressive disassembly of replisomes stalled by helicase inactivation. *Mol. Cell.* 49(3):547-557.
- Link, A.J., Phillips, D., Church, G.M. (1997) Methods for generating precise deletions and insertions in the genome of wild-type *Escherichia coli*: Application to open reading frame characterization. *J. Bacteriol.* 179(20):6228-6237.
- Little, J.W., Edmiston, S.H., Pacelli, L.Z., Mount, D.W. (1980) Cleavage of the *Escherichia coli* *lexA* protein by the *recA* protease. *Proc. Natl. Acad. Sci. USA.* 77(6):3225-3229.
- Little, J.W., Mount, D.W., Yanishch-Perron, C.R. (1981) Purified *lexA* protein is a repressor of the *recA* and *lexA* genes. *Proc. Natl. Acad. Sci. USA.* 78(7):4199-4203.
- Lopes, M., Cotta-Ramusino, C., Pelliccioli, A., Liberi, G., Plevani, P., Muzi-Falconi, M., Newlon, C.S., Foiani, M. (2001) The DNA replication checkpoint response stabilizes stalled replication forks. *Nature* 413(6846):557-561.
- Lu, M., Campbell, J.L., Boye, E., Kleckner, N. (1994) SeqA: a negative modulator of replication initiation in *E. coli*. *Cell* 77(3):413-426.

- Maki, H., Horiuchi, T., Kornberg, A. (1985) The polymerase subunit of DNA polymerase III of *Escherichia coli*. I. Amplification of the *dnaE* gene product and polymerase activity of the α subunit. *J. Biol. Chem.* 260(24):12982-12986.
- Maki, H., Mo, J.Y., Sekiguchi, M. (1991) A strong mutator effect caused by an amino acid change in the α subunit of DNA polymerase III of *Escherichia coli*. *J. Biol. Chem.* 266(8):403-436.
- Maki, H., Maki, S., Kornberg, A. (1988) DNA polymerase III holoenzyme of *Escherichia coli*. IV. The holoenzyme is an asymmetric dimer with twin active sites. *J. Biol. Chem.* 263:6570-6578.
- Maki, M. (2004) DNA polymerase III, bacterial. In *Encyclopaedia of Biological chemistry*. Academic Press, Waltham, MA, Vol. 1, pp. 729-733.
- Maki, M., & Furukohri, A. (2013) DNA polymerase III, bacterial. In *Encyclopaedia of Biological chemistry*, Academic Press, MA, vol. 2, pp. 92-95.
- Makino, F. & Munakata, N. (1978) Deoxyuridine residue in DNA of thymine-requiring *Bacillus subtilis* strains with defective *N*-Glycosidase activity for Uracil-containing DNA. *J. Bacteriol.* 134(1):24-29.
- Masson, M.L., Baharoglu, Z., Michel, B. (2008) *ruvA* and *ruvB* mutants specifically impaired for replication fork reversal. *Mol. Microbiol.* 70(2):537-548.
- McGlynn, P., Savery, N.J., Dillingham, M.S. (2012) The conflict between DNA replication and transcription. *Mol. Microbiol.* 85(1):15-20.
- McHenry, C.S. (1988) DNA polymerase III holoenzyme of *Escherichia coli*. *Annu. Rev. Biochem.* 57:519-550.
- McHenry, C.S. (2011) DNA replicases from a bacterial perspective. *Annu. Rev. Biochem.* 80:403-436.
- McInerney, P. & O'Donnell, M. (2004) Functional uncoupling of twin polymerases: mechanism of polymerase dissociation from a lagging-strand block. *J. Biol. Chem.* 279(20):21543-21551.
- Miller, J.H. (1972) *Experiments in Molecular Genetics*. Cold Spring Harbor Laboratory Press, New York.
- Mirkin, E.V. and Mirkin, S.M. (2007) Replication fork stalling at natural impediments. *Microbiol. Mol. Biol. Rev.* 71(1):13-35.
- Mori, T., Nakamura, T., Okazaki, N., Furukohri, A., Maki, M., Akiyama, M.T. (2012) *Escherichia coli* DinB inhibits replication fork progression without significantly inducing the SOS response. *Genes. Genet. Syst.* 87(2):75-87.
- Odsbu, I., Morigen, Skarstad, K. (2009) A reduction in ribonucleotide reductase activity

- slows down the chromosome replication fork but does not change its localization. *PLoS One* 4(10): e7617.
- O'Donnell, M. (2006) Replisome architecture and dynamics in *Escherichia coli*. *J. Biol Chem.* 281(16):10653-10656.
- Ogura, Y., Imai, Y., Ogasawara, N., Moriya, S. (2001) Autoregulation of dnaA-dnaN operon and effects of DnaA protein levels on replication initiation in *Bacillus subtilis*. *J. Bacteriol.* 183(13):3833-3841.
- Pages, V. & Fuchs, R.P.P. (2002) How DNA lesions are turned into mutations within cells?. *Oncogene* 21(58):8957-8966.
- Patel, S.S., Pandey, M., Nandakumar, D. (2011) Dynamic coupling between the motors of DNA replication: hexameric helicase, DNA polymerase, and primase. *Curr. Opin. Chem. Biol.* 15(5):595-605.
- Pennington, J.M. & Rosenberg, S.M. (2007) Spontaneous DNA breakage in single living *Escherichia coli* cells. *Nat Genet.* 39(6):797-802.
- Petermann, E., Maya-mendoza, A., Zachos, G., Gillespie, D.A., Jackson, D.A., Caldecott, K.W. (2006) Chk1 requirement for high global rates of replication fork progression during normal vertebrate S phase. *Mol. Cell. Biol.* 26(8):3319-3326.
- Petermann, E., Woodcock, M., Helleday, T. (2010) Chk1 promotes replication fork progression by controlling replication initiation. *Proc. Natl. Acad. Sci. USA.* 107(37):16090-16095.
- Rayssiguier, C., Thaler, D.S., Radman, M. (1989) The barrier to recombination between *Escherichia coli* and *Salmonella typhimurium* is disrupted in mismatch-repair mutants. *Nature* 342(6248):296-401.
- Renzette, N., Gumlaw, N., Nordman, J.T., Krieger, M., Yeh, S.P., Long, E., Centore, R., Boonsombat, R., Sandler, S.J. (2005) Localization of RecA in *Escherichia coli* K-12 using RecA-GFP. *Mol. Microbiol.* 57(4):1074-1085.
- Rimsky, S. & Travers, A. (2011) Pervasive regulation of nucleoid structure and function by nucleoid-associated protein. *Curr. Opin. Microbiol.* 14(2):136-141.
- Roepke, R.R., Libby, R.L., Small, M.H. (1944) Mutation or variation of *Escherichia coli* with respect to growth requirements. *J. Bacteriol.* 48(4):401-412.
- Roth, A. & Messer, W. (1998) High-affinity binding sites for the initiator protein DnaA on the chromosome of *Escherichia coli*. *Mol. Microbiol.* 28(2):395-401.
- Rudolph, C.J., Upton, A.L., Lloyd, R.G. (2007) Replication fork stalling and cell cycle arrest in UV-irradiated *Escherichia coli*. *Genes. Dev.* 21(6):668-681.
- Saka, K., Tadenuma, M., Nakade, S., Tanaka, N., Sugawara, H., Nishikawa, K.,

- Ichiyoshi, N., Kitagawa, M., Mori, H., Ogasawara, N., Nishimura, A. (2005) A complete set of *Escherichia coli* open reading frames in mobile plasmids facilitating genetic studies. *DNA Res.* 12: 63-68.
- Sambrook, J. and Russel, D.W. (2001) *Molecular cloning, A Laboratory manual*. Cold Spring Harbor Laboratory Press, New York.
- Seigneur, M., Bidnenko, V., Ehrlich, S.D., Michel, B. (1998) RuvAB acts at arrested replication forks. *Cell* 95(3):419-430.
- Skarstad, K., Boye, E., Steen, H.B. (1986) Timing of initiation of chromosome replication in individual *Escherichia coli* cells. *EMBO J.* 5(7):1711-1717.
- Skarstad, K. & Katayama, T. (2013) Regulating DNA replication in bacteria. *Cold Spring Harb Perspect Biol* 5(4):a012922.
- Soultanas, P. (2011) The replication-transcription conflict. *Transcript* 2(3):140-144.
- Studwell, P.S. & O'Donnell, M. (1990) Processive replication is contingent on the exonuclease subunit of DNA polymerase III holoenzyme. *J. Biol. Chem.* 265(2):1171-1178.
- Sugimura, K., Takebayashi, S., Taguchi, H., Takeda, S., Okumura, K. (2008) PARP-1 ensures regulation of replication fork progression by homologous recombination on damaged DNA. *J. Cell. Biol.* 183(7):1203-1212.
- Sugaya, Y., Ihara, K., Masuda, Y., Ohtsubo, E., Maki, M. (2002) Hyper-processive and slower DNA chain elongation catalysed by DNA polymerase III holoenzyme purified from the *dnaE173* mutator mutant of *Escherichia coli*. *Genes Cells* 7(4):385-399.
- Syljuasen, R.G., Sorensen, C.S., Hansen, L.T., Fugger, K., Lundin, C., Johansson, F., Helleday, T., Sehested, M., Lukas, J., Bartek, J. (2005) Inhibition of human Chk1 causes increased initiation of DNA replication, phosphorylation of ATR targets, and DNA brakage. *Mol. Cell. Biol.* 25(9):3553-3562
- Tang, M., Pham, P., Shen, X., Taylor, J.S., O'Donnell, M., Woodgate, R., Goodman, M.F. (2000) Roles of *E. coli* DNA polymerase IV and V in lesion-targeted and untargeted SOS mutagenesis. *Nature* 404(6781):1014-1018.
- Tanner, N.A., Hamdan, S.M., Jergic, S., Loscha, K.V., Schaeffer, P.M., Dixon, N.E., van Oijen, A.M. (2008) Single-molecule studies of fork dynamics in *Escherichia coli* DNA replication. *Nat. Struct. Mol. Biol.* 15(2):170-176.
- Tanner, N.A., Loparo, J.J., Hamdan, S.M., Jergic, S., Dixon, N.E., van Oijen, A.M. (2009) Real-time single-molecule observation of rolling-circle DNA replication. *Nucleic Acids Res.* 37(4):e27.

- Tehranchi, A.K., Blankschien, M.D., Zhang, Y., Halliday, J.A., Srivatsan, A., Peng, J., Christophe, H., Wang, J.D. (2010) The transcription factor DksA prevents conflicts between DNA replication and transcription machinery. *Cell* 141(4): 595-605.
- Titz, B., Hauser, R., Engelbrecher, A., Uetz, P. (2007) The *Escherichia coli* protein YjjG is a house – cleaning nucleotidase in vivo. *FEMS Microbiol. Lett.* 270(1):49-57.
- Uchida, K., Furukohri, A., Shinozaki, Y., Mori, T., Ogasawara, D., Kanaya, S., Nohmi, T., Maki, M., Akiyama, M. (2008) Overproduction of *Escherichia coli* DNA polymerase DinB (Pol IV) inhibits replication fork progression and is lethal. *Mol. Microbiol.* 70(3):608-622.
- van Oijen, A. & Loparo, J.J. (2010) Single-Molecule studies of the replisome. *Annu. Rev. Biophys.* 39:429-448.
- Wagner, J., Gruz, P., Kim, S.R., Yamada, M., Matsui, K., Fuchs, R.P., Nohmi, T. (1999) The *dinB* gene encodes a novel *E. coli* DNA polymerase, DNA Pol IV, involved in mutagenesis. *Mol. Cell.* 4(2):281-286.
- Wagner, J., Fujii, S., Gruz, P., Nohmi, T., Fuchs, R.P. (2000) The β clamp targets DNA polymerase IV to DNA and strongly increases its processivity. *EMBO J.* 1(6):484-488.
- Waldminghaus, T., Weigel, C., Skarstad, K. (2012) Replication fork movement and methylation govern SeqA binding to the *Escherichia coli* chromosome. *Nucleic Acids Res.* 40(12):5465-5476.
- Wang, W., Li, G.W., Chen, C., Xie, X.S., Zhuang, X. (2011) Chromosome organization by a nucleoid-associated protein in live bacteria. *Science* 333(6048):1445-1449.
- Watson, J.D., Baker, T.A., Bell, S.P., Gann, A.A.F., Levine, M., Losick, R.M. (2008) *Molecular Biology of the gene.* 6th Edition. Cold Spring Harbour Laboratory Press, New York.
- Weiss, B. (2006) YjjG, a dUMP phosphatase, is critical for Thymine Utilization by *Escherichia coli* K-12. *J. Bacteriol.* 189(5):2186-2189.
- Willetts, N.S., Clark, A.J., Low, B. (1969) Genetic location of certain mutations conferring recombination deficiency in *Escherichia coli*. *J. Bacteriol.* 97(1):6640-6645.
- Witkin, E.M. (1967) The radiation sensitivity of *Escherichia coli* B: A hypothesis relating filament formation and prophage induction. *Proc. Natl. Acad. Sci.*

USA. 57(5):1275-1279.

- Wu, R. and Taylor, E. (1971) Nucleotide sequence analysis of DNA: II. Complete nucleotide sequence of the cohesive ends of bacteriophage λ DNA. *J. Mol. Biol.* 57(3):491-511.
- Wu, C.A., Zechner, E.L., Hughes, A.J.Jr., Franden, M.A., McHenry, C.S., Marians, K.J. (1992) Coordinated leading- and lagging-strand synthesis at the *Escherichia coli* DNA replication fork. IV. Reconstitution of an asymmetric, dimeric DNA polymerase III holoenzyme. *J. Biol. Chem.* 267(6):4064-4073.
- Yanagihara, F., Yoshida, S., Sugaya, Y., Maki, M. (2007) The *dnaE173* mutator mutation confers on the α subunit of *Escherichia coli* DNA polymerase III a capacity for highly processive DNA synthesis and stable binding to primer/template DNA. *Genes. Gent. Syst.* 82(4):273-280.
- Yao, N.Y., Georgescu, R.E., Finkelstein, J., O'Donnell, M.E. (2009) Single-molecule analysis reveals that the lagging strand increases replisome processivity but slow replication fork progression. *Proc. Natl. Acad. Sci. USA.* 106(32):13236-13241.
- Yuzhakove, A., Turner, J., O'Donnell, M. (1996) Replisome assembly reveals the basis for asymmetric function in leading and lagging strand replication. *Cell* 86(6):877-886.
- Zhao, J., Bacolla, A., Wang, G., Vasquez, K.M. (2010) Non-B DNA structure – induced genetic instability and evolution. *Cell. Mol. Life Sci.* 67:43-62.